Cell cycle-dependent localization of hexose transporter mRNA in *Saccharomyces cerevisiae*

Inauguraldissertation
zur
Erlangung der Würde eines Doktors der Philosophie
vorgelegt der
Philosophisch-Naturwissenschaftlichen Fakultät
der Universität Basel

von
Timo Stahl
aus Deutschland

Basel, 2018

Genehmigt von der Philosophisch-Naturwissenschaftlichen Fakultät
auf Antrag von

Prof. Dr. Anne Spang
Prof. Dr. Sabine Rospert

Basel, den 18. September 2018

Prof. Dr. Martin Spiess
Dekan der Philosophisch-Naturwissenschaftlichen Fakultät

For my wonderful wife and son,

Rahel and Aviel, you are the light of my life!

Summary 5

1. Introduction 6

1.1 The cell cycle of Saccharomyces cerevisiae 6

Spindle pole body segregation drives asymmetry 7

1.2 Multistage regulation of gene expression 9

Translation and localization of mRNAs are tightly controlled 11

1.3 The glucose responsiveness pathway 15

1.4 Hexose transporters 17

2. Aim of the study 21

3. Results 22

Abstract 24

Introduction 25

Results 26

Discussion 34

Experimental Procedures 37

Acknowledgements 47

References 47

Figure Legends 53

Figures 57

4. Additional Data 67

5. Further Discussion and Outlook 69

6. Appendix 74

6.1 Materials and Methods 74

Materials 74

Methods 80

6.2 Abbreviations 89

6.3 References 91

6.4 Acknowledgments 102

Summary

Unicellular organisms like yeast face constantly changing environmental conditions. Especially fluctuating concentrations of glucose affect growth of *S. cerevisiae.* Thus yeast evolved several hexose transporters with different affinities and expression patterns. We observed that the high-affinity transporter Hxt2 is differentially localized during the cell cycle. Analyzing the localization of its mRNA, by Fluorescent In Situ Hybridization (FISH), unveiled a comparable distribution pattern. Under glucose-rich conditions, the mRNA is retained in the mother cell early in the cell cycle and only later, after Metaphase to Anaphase Transition (MAT), *HXT2* mRNA is equally distributed. This is true for all four hexose transporters, we investigated.

Furthermore, we could show that the release from the mother cell to the bud after MAT, is dependent on active translation and that the binding of *HXT2* mRNA to polysomes confers its stability. Upon deleting the RNA-binding protein Scp160, which is associated with translational control and binds to ribosomes, we found that *HXT2* mRNA is enriched in the bud after MAT. Moreover, the deletion of *ASC1*, that mediates binding of Scp160/Bfr1 to ribosomes, also leads to the enrichment of *HXT2* mRNA.

Interestingly, Asc1 was also described as being involved in the glucose responsiveness pathway of *S. cerevisiae*. Here, Asc1 is thought to inhibit the adenylyl cyclase. In fact, we could show that activation of the adenylyl cyclase and subsequently activating the cAMP-dependent protein kinase A, phenocopies the deletion of *ASC1*. Intriguingly, when we activated the glucose responsiveness pathway by re-feeding starved cells with glucose, we found that especially *HXT2* mRNA is enriched in the bud after MAT. Moreover, this enrichment is transient and happens only during the first 1-2 cell divisions after coming from starvation. Next, we deleted the glucose receptor Gpr1 and its associated G-protein Gpa2 in order to investigate the involvement of upstream factors of the glucose responsiveness pathway. Whereas deletion of Gpr1/Gpa2 did not show an effect, a mutated version of Ras2, which does not elicits an increase of cAMP under glucose-shift conditions, inhibits the enrichment of *HXT2* mRNA in the bud.

Apart from establishing the involvement of the Ras2/cAMP/PKA pathway, we demonstrated that transcription as well as nuclear segregation are necessary, but not sufficient for the enrichment of *HXT2* mRNA in the bud. Furthermore, we identified Kar9, which is involved in the asymmetric spindle pole body segregation, as well as Mlp1, Mlp2 and Nup2, which are components of the nuclear basket, as important trans-acting factors for the asymmetric distribution of *HXT2* mRNA under glucose shift conditions. Finally, we were wondering, whether there is an advantage for the daughter cell to be provided with high levels of *HXT2* mRNA. We carried out growth tests and observed that cells that express *HXT2* as their sole hexose transporter grow faster than cells expressing other *HXTs*. Taken together, the results presented in this thesis suggest that *S. cerevisiae* enriches specifically *HXT2* mRNA in the daughter cell, when coming from quiescence or starvation. Expression of *HXT2* presumably enables the daughter cell to rapidly accumulate glucose, switch from respiration to fermentation and to start re-growth ahead of cells, that do not enrich *HXT2* mRNA.

1. Introduction

1.1 The cell cycle of *Saccharomyces cerevisiae*

Dividing cells have to coordinate processes such as DNA replication, mitosis and cytokinesis, collectively termed the cell cycle (Sullivan and Morgan, 2007). Progression through the cell cycle is highly regulated by periodic activation and inhibition of so-called Cyclin Dependent Kinases (CDKs). The CDK-associated cyclins function as regulatory subunits of CDKs and render them active (Sullivan and Morgan, 2007). Therefore, CDKs are only active when associated with a cyclin. There are at least 11 different cell cycle-specific cyclins in yeast known to form complexes with Cdc28, the yeast CDK (Beach, Durkacz, and Nurse, 1982). The cell cycle can be divided into four oscillatory phases: G1, S, G2 and mitosis (M phase). In G1, cells have to decide whether they irreversibly commit to a new cell cycle by passing START (Donjerkovic and Scott, 2000). In this phase, cells need to make sure that on the one hand, damaged DNA is repaired before mutations or fragmented chromosomes are passed on to the next generation (Bartkova et al., 1997). On the other hand, they have to grow until they reach a critical size which is dependent on the availability of nutrients (Hartwell & Unger, 1977; Johnston et al., 1977; Pringle & Hartwell, 1981). Thus, START coordinates cell cycle with cell growth. There are additional checkpoints, that arrest the cell cycle if the DNA replication is incomplete, chromosomes are not correctly aligned or spindle formation is improper (Lew and Reed, 1995). When START is passed, the level of G1 cyclins (Cln1, Cln2, and Cln3) dramatically increases and governs the transition from G1 to S phase. In yeast, there are six B-type cyclins (CLB) involved in the activation of the S, G2, and M phases of the cell cycle. Both Clb5 and Clb6 are most abundant during late G1 and promote progression into the S phase (Kuhne and Linder, 1993; Schwob and Nasmyth, 1993). Clb3p and Clb4p arise near the beginning of the S phase and remain high until late anaphase. They may be both involved in DNA replication and spindle assembly as well as in the G2/M-phase transition (Feldmann et al., 2011, Yeast: Molecular and Cell Biology, Second Edition). Clb1 and Clb2 peak shortly before anaphase and their transcription is repressed by the end of mitosis (Fitch et al., 1992).

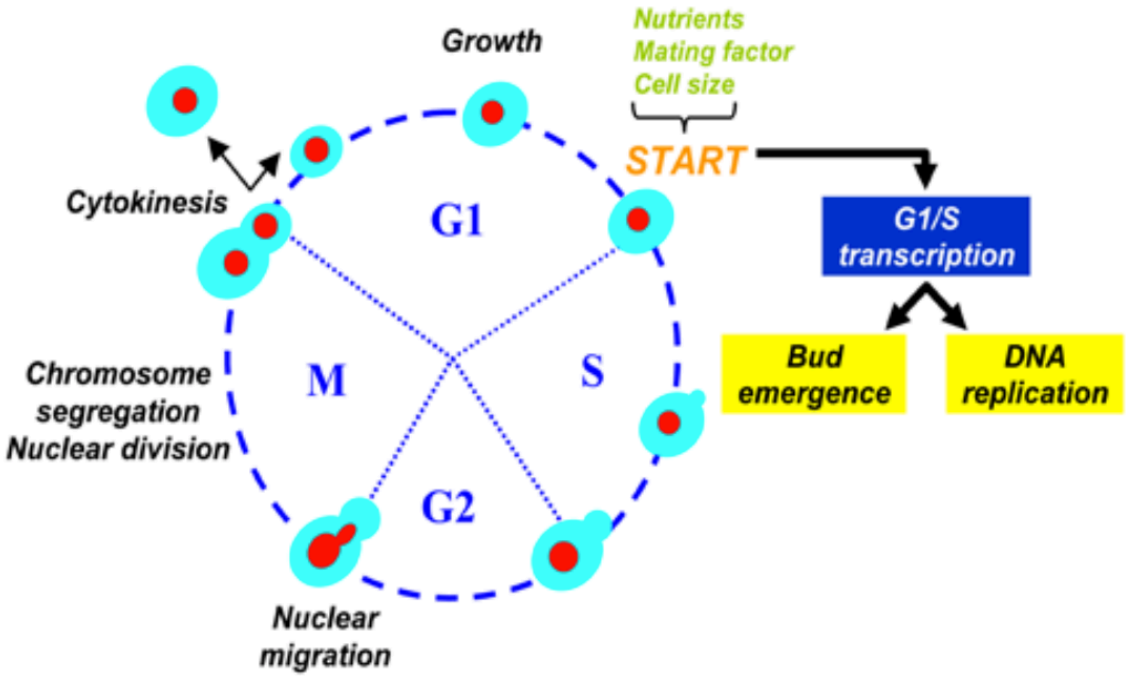

Fig. 1.1: The cell cycle of the budding yeast Saccharomyces cerevisiae. After cytokinesis the daughter cell, which has 2/3 of the size of its mother cell needs to grow before passing START and entering the cell cycle again (adapted from Busti et al., 2010).

Spindle pole body segregation drives asymmetry

S. cerevisiae divides in an asymmetric pattern (Fig.1.1). The daughter cell has only 2/3 the size of the mother cell and the Spindle Pole Body (SPB), the yeast equivalent of the centrosome, is distributed non-randomly between mother and daughter cell after duplication. During the closed mitosis of *S. cerevisiae*, the SPB that is inherited from the previous cell cycle and consists mainly of old proteins (Pereira et al., 2001; Rüthnick and Schiebel, 2018) is allocated to the bud, whereas the SPB that remains in the mother cell is assembled de novo. This results in two morphologically and functionally distinct SPBs (Adams and Kilmartin, 2000; Yoder et al., 2003) that allow for the asymmetric distribution of factors to only one of the two dividing cells (Siller and Doe, 2009; Barral and Liakopoulos, 2009).

In G1/S, the SPB duplicates via a template-based mechanism (Adams and Kilmartin 1999; Jaspersen and Winey 2004). Duplication starts with the expansion of the half-bridge and the formation of a precursor called satellite at the distal tip of the half-bridge. By addition of soluble, mainly cytoplasmic precursors, a duplication plaque is assembled which is then inserted into the Nuclear Envelope (NE), mediated by Ndc1, Mps2, Bbp1, and Nbp1 (Winey et al., 1991, 1993; Adams and Kilmartin 1999; Schramm et al., 2000; Araki et al., 2006). After insertion, the inner plaque is formed with nucleoplasmic components to create duplicated side-by-side SPBs (Byers and Goetsch 1974; Byers and Goetsch 1975; Adams and Kilmartin 1999; Jaspersen and Winey 2004; Winey and Bloom 2012). At the onset of S-phase, the bridge is cleaved and the SPBs are separated leaving one half bridge with each SPB.

The asymmetric distribution of the protein Kar9 governs the alignment of the spindle with the mother-bud axis and the segregation of the old SPB to the bud (Liakopoulos et al., 2003; Pereira et al., 2001). In mammalian cells, the presumed functional homolog to Kar9 is the Adenomatous Polyposis Coli (APC) tumor suppressor. APC has been shown to localize to kinetochores and its loss leads to chromosome segregation defects (Schweiggert et al., 2016). The localization of Kar9 in *S. cerevisiae* is dependent on its phosphorylation. At the new SPB, Kar9 becomes phosphorylated by Clb4/Cdc28, which inhibits efficient association with the microtubule-binding protein Bim1, the yeast homolog of EB1 (Miller et al., 1999; Lee et al., 2000; Korinek et al., 2000). At the old SPB on the other hand, Kar9 is not phosphorylated, binds to Bim1 and promotes together with Myo2, an actin-binding type V myosin (Yin et al., 2000) the movement of microtubule plus ends along actin cables towards the bud (Beach et al., 2000; Liakopoulos et al., 2003). Besides the Kar9-dependent pathway, cells can align their spindles with the polarity axis in a dynein-dependent manner (Adames and Cooper, 2000; Carminati and Stearns, 1997; Grava et al., 2006). Because each pathway can compensate for the absence of the other, only the simultaneous loss of both is lethal (Miller and Rose, 1998).

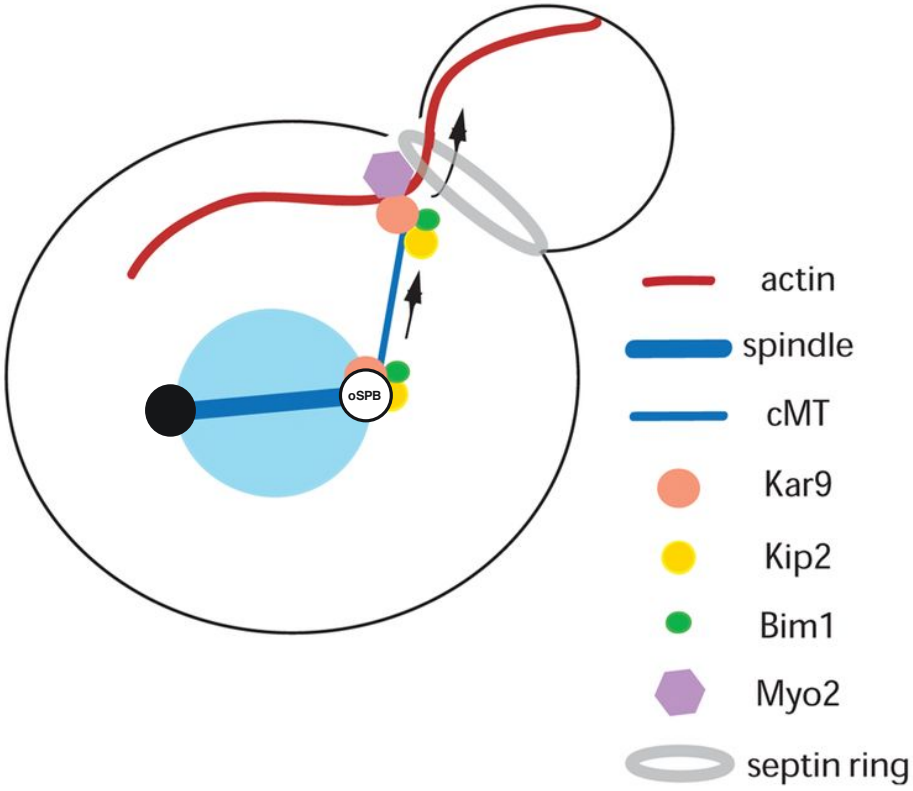

Fig. 1.2: Positioning of the spindle pole body and segregation of the nucleus depends on the cytoskeleton and, among others, the complex of Kar9, Bim1 and Myo2, which connects actin with microtubules (adapted from Hotz et al., 2012).

Besides its role in SPB duplication, Ndc1 has an additional role in the biogenesis of Nuclear Pore Complexes (NPC; Lau et al., 2004; Madrid et al., 2006; Stavru et al., 2006), where it interacts with the membrane proteins Pom34 and Pom152 (Alber et al., 2007a,b; Onischenko et al., 2009). NDC1 shows genetic interactions with EAP1 (Chial et al., 2000),

an eIF4E-binding protein that prevents formation of the eIF4E–eIF4G complex. As a result, the recruitment of the 5'-end of mRNAs to the 40S ribosomal subunit during initiation of translation is hampered (Gingras et al., 1999). Eap1 forms the SESA complex together with the GYF-domain protein Smy2, the mRNA-binding protein Scp160 and the RACK-ortholog Asc1. In response to failure of SPB insertion into the nuclear envelope, SESA inhibits the translation initiation of *POM34* mRNA which in turn leads to reduced levels of Pom34, restoring viability in cells defective in SPB duplication (Sezen et al., 2009). Interestingly, Scp160 is also required for proper assembly of processing bodies (P-bodies) that are involved in mRNA decapping, nonsense-mediated decay, translational repression and mRNA storage (Parker and Sheth, 2007; Weidner et al., 2014). They consist of the decapping enzymes Dcp1 and Dcp2, the helicase Dhh1, activators of decapping such as Pat1, Scd6, Edc3 and the Lsm1-7 complex and the 5'-3' exonuclease Xrn1 (Parker and Sheth, 2007). P-bodies are found in close proximity to the ER (Kilchert et al., 2010) and transcripts that are stored in P-bodies may either return to the pool of actively translated mRNAs or be degraded (Coller and Parker, 2005; Franks and Lykke-Andersen, 2008). P-bodies can contain both, common and stress-specific mRNAs. Translational control via the SESA network and localization of mRNA to P-bodies are only two examples for the cell's ability to temporally and spatially regulate gene expression.

1.2 Multistage regulation of gene expression

In general, the control of gene expression is carried out on several levels, starting in the nucleus. Here, either activating or repressing transcription factors bind to promotor regions that lie proximal to the genes they regulate. RNA polymerases are then recruited to synthesize messenger RNA (mRNA) which immediately will be covered by specific RNA-binding proteins (RBPs). Post-transcriptional regulation is mediated by these RBPs which initiate the first RNA processing reactions including 5'-end capping, splicing, 3'-end cleavage and polyadenylation. Nuclear mRNA quality control mediated by nuclear exosomes ensures degradation of unadenylated or 3'-extended mRNAs (Burkard and Butler, 2000; Torchet et al., 2002). Next, the export of messenger ribonucleoprotein complexes (mRNPs) from the nucleoplasm to the cytoplasm occurs.

The nucleocytoplasmic transport is controlled by Nuclear Pore Complexes (NPCs) within the nuclear envelope. In *S. cerevisiae* the central structure of NPCs is composed of multiple copies of around 30 different nucleoporins (Nups). Besides scaffolding and linker Nups, there are a dozen largely unfolded FG-repeat Nups which influence nucleocytoplasmic transport and can be regulated for example by phosphorylation. The Myosin-like proteins Mlp1 and Mlp2 are components of the nucleoplasmic part of the NPC, the nuclear basket. Studies implicate that they might be involved in positioning NPCs and may serve as a binding platform for mRNPs during nuclear export (Kölling et al., 1993; Strambio-de-Castillia et al., 1999; Niepel et al., 2013). After the export from the nucleus, mRNAs are either directly translated in the cytoplasm or they get localized to specific cellular compartments first, for example the ER. Translation and localization are

often connected and need to be tightly regulated to prevent unwanted or even deleterious effects.

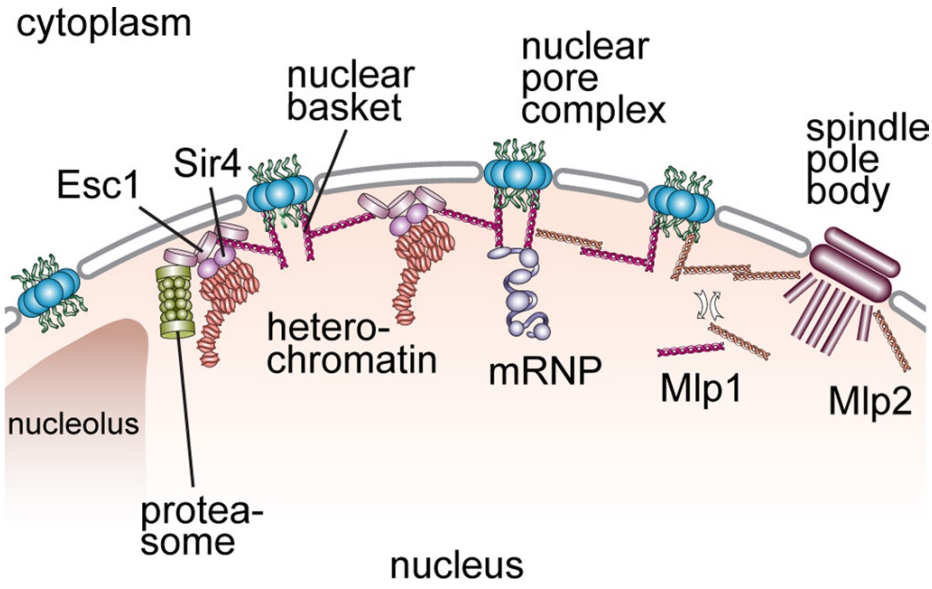

Fig. 1.3: Nuclear export of mRNAs is controlled by nuclear pore complexes, which are positioned and connected by a dynamic protein network, the nuclear basket. Mlp1 and Mlp2 are major components of the nuclear basket. Furthermore, Esc1 and Sir4 are involved in binding of heterochromatin and the proteasome to the nuclear basket, providing an additional level of gene expression regulation (adapted from Niepel et al., 2013).

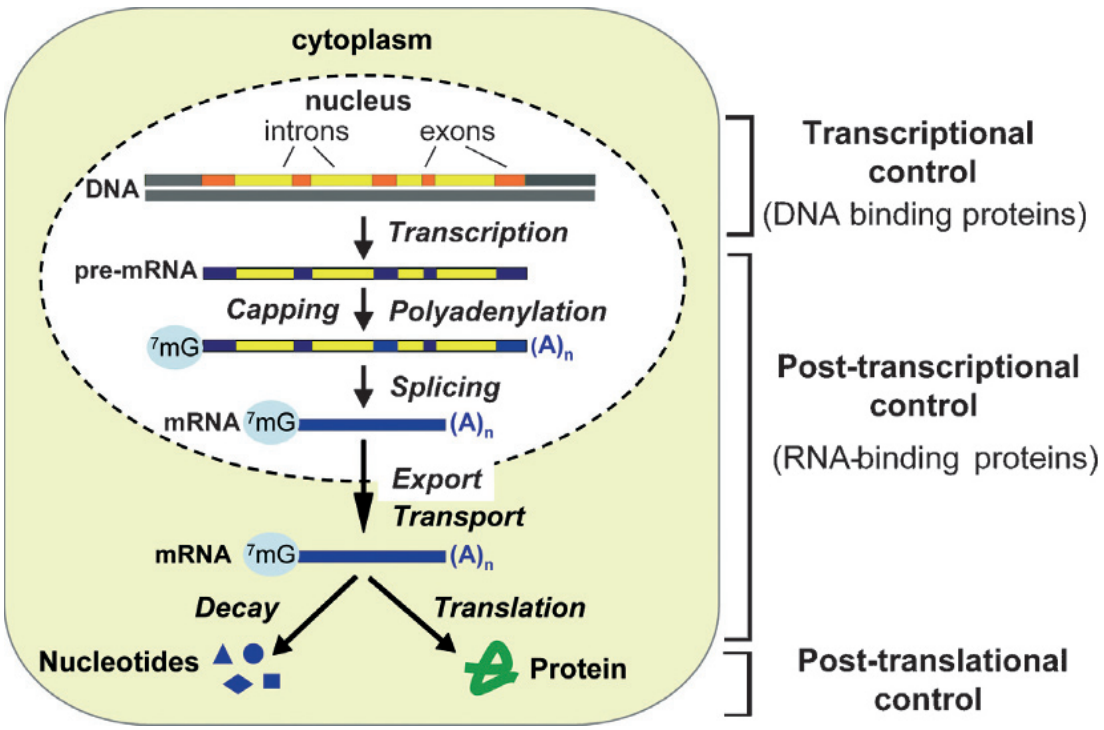

Fig. 1.4: Several different steps are involved in converting the information stored in the DNA via mRNA into a functional protein. Every step is tightly regulated by the cell to ensure the proper spatial and temporal function of the encoded protein. (adapted from Halbeisen et al., 2007).

Translation and localization of mRNAs are tightly controlled

Protein synthesis consists of three stages, initiation, elongation and termination. At every step regulation can occur, but initiation is thought to be the rate-limiting step (Pichon et al., 2012). Translation initiation requires canonical initiation factors (eIFs) and sequence elements within the 5' and 3' untranslated regions (UTRs) of the transcript, to which trans-acting proteins bind. As a first step, the 7-methyl-Guanosine cap structure is bound by a trimeric complex consisting of eIF4E, the cap-binding protein, eIF4A, a DEAD-box helicase and eIF4G which serves as a scaffold protein. After association of eIF2 that is loaded with initiator Met-tRNAi and the 40S small ribosome subunit, this complex then scans the transcript, directed by the anticodon–codon specificity of Met-tRNAi, until it finds the first AUG codon. Here the 60S large ribosome subunit joins to form the 80S monosome. eIF5 catalyzes the first peptide bond formation between the start methionine and the second amino acid (Asano et al., 2002). Thereafter, the initiation factors are released and the elongation step begins.

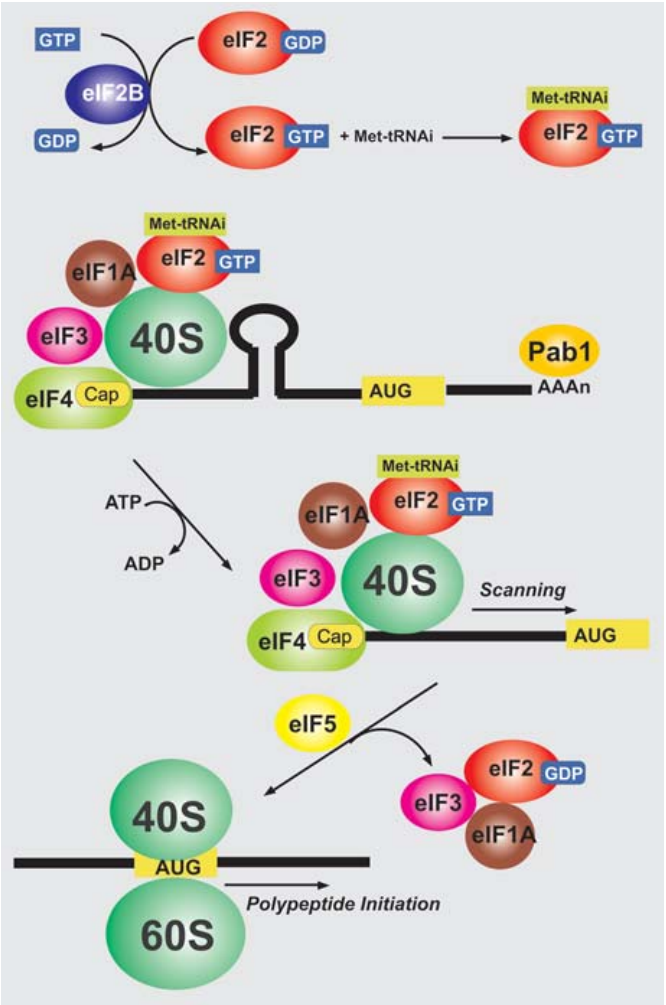

Fig. 1.5 : Translation initiation is mediated by subsequent binding and release of initiation factors and the ribosomal subunits. The multiprotein complex consisting of eIF1-4, Met-tRNAi and ribosomal subunit 40S scans the mRNA until the start codon. Thereafter, the complex dissociates, the 60S subunit binds to form the functional ribosome and the polypeptide elongation starts (adapted from Feldmann et al., Yeast: Molecular and Cell Biology, Second Edition).

Like initiation, translation elongation is mediated by specific components, called elongation factors (eEFs). The yeast elongation factor eEF1A promotes the binding of aminoacyl-tRNA to the ribosomal A site, while eEF1B catalyzes GDP/GTP exchange on eEF1A. eEF2 is assumed to be required for translocation of the peptidyl-tRNA to the P site. Moreover, eEF1A and eEF2 may be involved in intracellular mRNA transport by binding to cytoskeletal components (Liu et al., 2002; Perez and Kinzy, 2014). As soon as one of the stop codons UAA, UAG, or UGA is recognized by the release factor eRF1, translational termination is engaged and peptide release is mediated. The whole process of translation is dependent on energy which is provided by the hydrolization of either ATP to ADP or GTP to GDP by eIFs, eEFs and eRFs (Feldmann et al., 2011, Yeast: Molecular and Cell Biology, Second Edition).

Translation initiation is targeted by a plethora of regulatory pathways. Starvation for nutrients is known to cause a general inhibition of translation (Hinnebusch, 1984; Tzamarias et al., 1989). Depletion of amino acids for example leads to the phosphorylation of the translation initiation factor eIF2 through the protein kinase Gcn2. This phosphorylation causes a general inhibition of translation (Dever et al., 1992; Rolfes and Hinnebusch, 1993). In addition, a growing body of evidence suggests that also elongation is subject to regulatory mechanisms (Richter and Coller, 2015). Scp160 for instance influences elongation by binding to polysomes at the ER (Lang and Fridovich-Keil, 2000; Frey et al., 2001; Mendelsohn et al.., 2003; Baum et al., 2004; Sezen et al., 2009). Scp160 is a homologue of eukaryotic vigilins, a family of RNA binding proteins that contain multiple KH domains. Together with Bfr1 (Brefeldin A resistance), Scp160 associates to the 40S ribosomal subunit. Like Scp160, Bfr1 has been characterized as an RNA binding protein and it is known that its interaction with Scp160 relies on the presence of mRNA (Hogan et al.., 2008; Lang et al., 2001). Binding of the Scp160/Bfr1 complex to the ribosome on the other hand is mediated by Asc1, the ortholog of mammalian receptor of activated C-kinase (RACK1). It functions as a receptor for various inputs from different signaling pathways, including responses to different stresses (Nilsson et al., 2004).

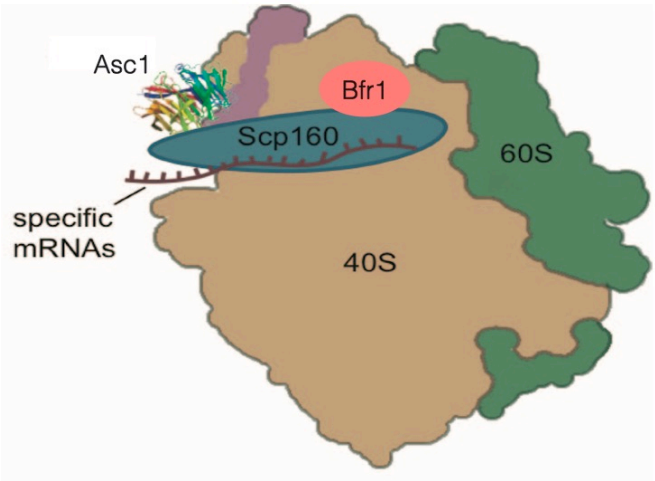

Fig.1.6: The complex of Scp160 and Bfr1 binds to the ribosome via Asc1. This interaction could deliver specific transcripts to the ribosome and regulate their translation (adapted from Coyle et al., 2009).

The mRNA of many secreted or membrane bound proteins is targeted in a translation-dependent way to the ER. In this case, ribosomes initiate translation in the cytoplasm and the amino terminus of the newly synthesized polypeptide, harboring a signal peptide, is recognized by the signal recognition particle (SRP). The SRP then binds to its receptor on the ER membrane and protein elongation across the membrane is continued (Schwartz, 2007). In comparison, the targeting of ABP140 mRNA in *S. cerevisiae* to the distal pole of the mother cell is an example for translation-dependent, but SRP-independent localization (Kilchert and Spang, 2011). Here, the translated N-terminal actin-binding domain (ABD) binds to cytoplasmic actin cables and ABP140 mRNA is transported in a complex consisting of ribosome, mRNA and nascent protein by retrograde flow of actin.

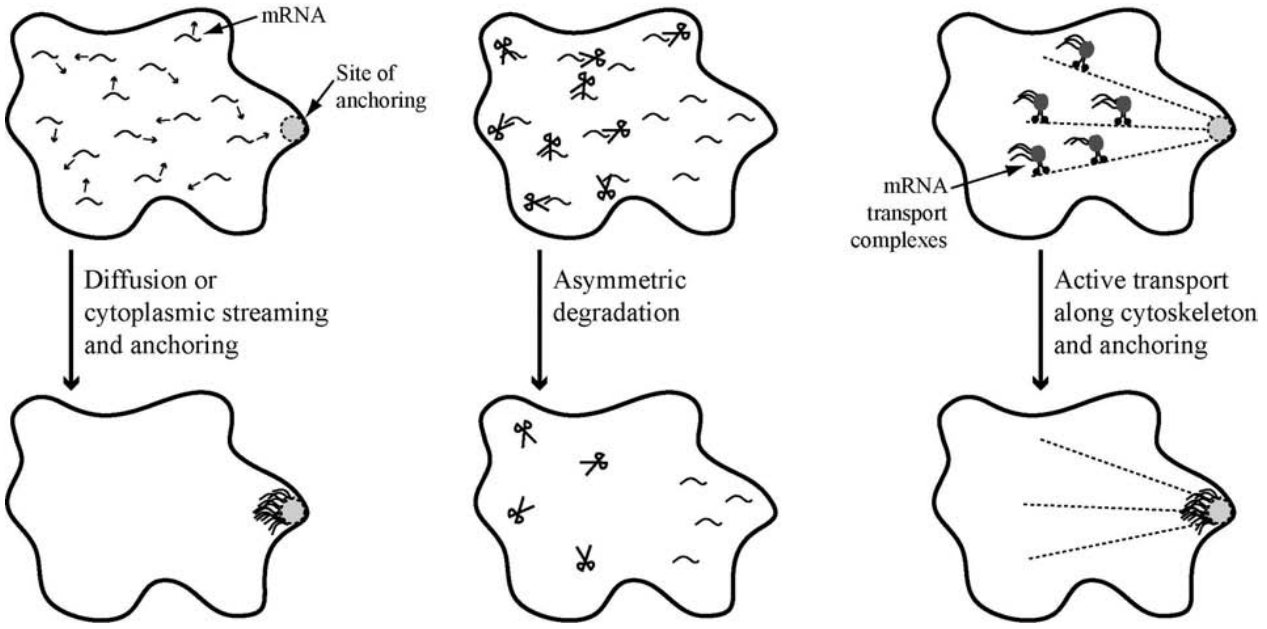

Fig. 1.7: Mechanisms of asymmetric mRNA localization. Left: Diffusion with subsequent anchoring at specific compartments. Middle: Degradation coupled with local protection of a particular mRNA can lead to its asymmetric distribution. Right: Directed transport along the cytoskeleton via mRNPs consisting of RNA-binding, adaptor and motor proteins (adapted from Jansen and Niessing, 2012).

It was long assumed that mRNA localization is only relevant for specific transcripts (Holt and Bullock, 2009; Meignin and Davis, 2010). But more and more studies implicate that a large number of mRNAs have distinct cellular localization and that this is a way of gene expression regulation conserved from yeast to mammals (Takizawa et al., 1997; Marc et al., 2002; Shepard et al., 2003; Lécuyer et al., 2007; Blower et al., 2007; Aronov et al., 2007; Mili et al., 2008; Saint-Georges et al., 2008; Zipor et al., 2009). For many different processes such as embryonic development, cell motility or synaptic plasticity, establishing and maintaining cell polarity through mRNA localization is crucial (Pratt and Mowry, 2013). The underlaying mechanisms are quite diverse. One can distinguish between selective degradation, diffusion coupled with entrapment or active transport of the localized transcript (Fig. 1.7; Jansen, 2001; Holt and Bullock, 2009). In order to

become localized, transcripts need to contain so-called cis-regulatory elements or 'zip codes', which are still largely unknown. These can be specific sequences found within the 3'- or 5'-untranslated region (UTR), the coding sequence (CDS) or any combination of the three. Additionally, secondary structures like hairpin loops can also serve as cis-regulatory elements (Jansen, 2001).

Trans-acting factors on the other hand denote proteins that either bind directly or indirectly to cis-regulatory elements of the mRNA. In Drosophila embryos for example, the unlocalized maternal mRNA is bound by the RNA-binding protein Smaug that mediates its deadenylation and destabilization by recruiting the CCR4/POP2/NOT-deadenylation complex. In comparison, *hsp83* mRNA localizes to the pole plasm and is protected from degradation. Smaug is also involved in the deadenylation and degradation of numerous other maternal transcripts in Drosophila (Carine Meignin and Ilan Davis, 2010). *nanos* mRNA in Drosophila is another example for this mechanism. However, studies argue that some *nanos* mRNAs also localize by diffusion in the oocyte with subsequent entrapment at the pole plasm in an actin-dependent manner (Forrest and Gavis, 2003).

In *S. cerevisiae, ASH1* mRNA is actively transported and the involved cis-regulatory elements and trans-acting factors have been unveiled. Ash1 (asymmetric synthesis of HO) is a transcriptional repressor of the HO endonuclease that mediates mating type switching (Besse and Ephrussi, 2008). After transcription, the trans-acting factor She2 binds to *ASH1* mRNA in the nucleus and together they are exported to the cytoplasm. There, Khd1, pumilio-homology domain family-6 (Puf6) and Myo4 associate to form a ribonucleoprotein particle (RNP). Khd1 and Puf6 inhibit premature translation, while the motor protein Myo4 mediates the active transport to the bud tip along actin cables. At the bud tip, Khd1 and Puf6 are phosphorylated by the membrane-associated kinases Yck1 (yeast type I casein kinase) and casein kinase-II (CK2), respectively. This leads to their dissociation which allows the active translation of the *ASH1* mRNA (Paquin et al., 2007). Ash1 enters the daughter-cell nucleus, where it represses the transcription of the HO endonuclease, thereby inhibiting mating type switching in the daughter cell (Paquin and Chartrand, 2008). This type of active transport, where translation is inhibited, is contrary to the mRNA localization of many secreted or membrane proteins which is carried out co-translational (see above).

There are a lot of advantages in transporting mRNA prior to translating them to protein (Medioni et al., 2012; Cody et al., 2013; Di Liegro et al., 2013). A cell can save energy by transporting only a few transcripts and translate them several times where they are needed, rather than bringing each individual protein to its site of action. Additionally, facilitates a high concentration of the same protein in close proximity the assembly of multi-protein complexes (Mingle et al., 2005). The mRNA of β-actin for instance is localized to the leading edge of lamellipodia, where it is translated repeatedly. The high amount of β-actin leads to the formation of nucleation complexes in order to promote actin polymerization, generating forward protrusions (Shestakova et al., 2001). Besides this, local protein synthesis can provide a fast and specific response to incoming signals, which is crucial in modulating synaptic plasticity in neurons (Steward and Schuman, 2003). Furthermore, localization of mRNAs and spatially restricted translation prevents the

cell from potentially unwanted or even deleterious effects of proteins at the wrong place. In this regard, oligodendrocytes in the central nervous system need to restrict the distribution of the myelin basic protein (MBP), a major component of the axon-wrapping myelin sheet, to zones of myelin formation. Otherwise, this sticky protein could cause aberrant membrane aggregation, if falsely targeted (Di Liegro et al., 2013).

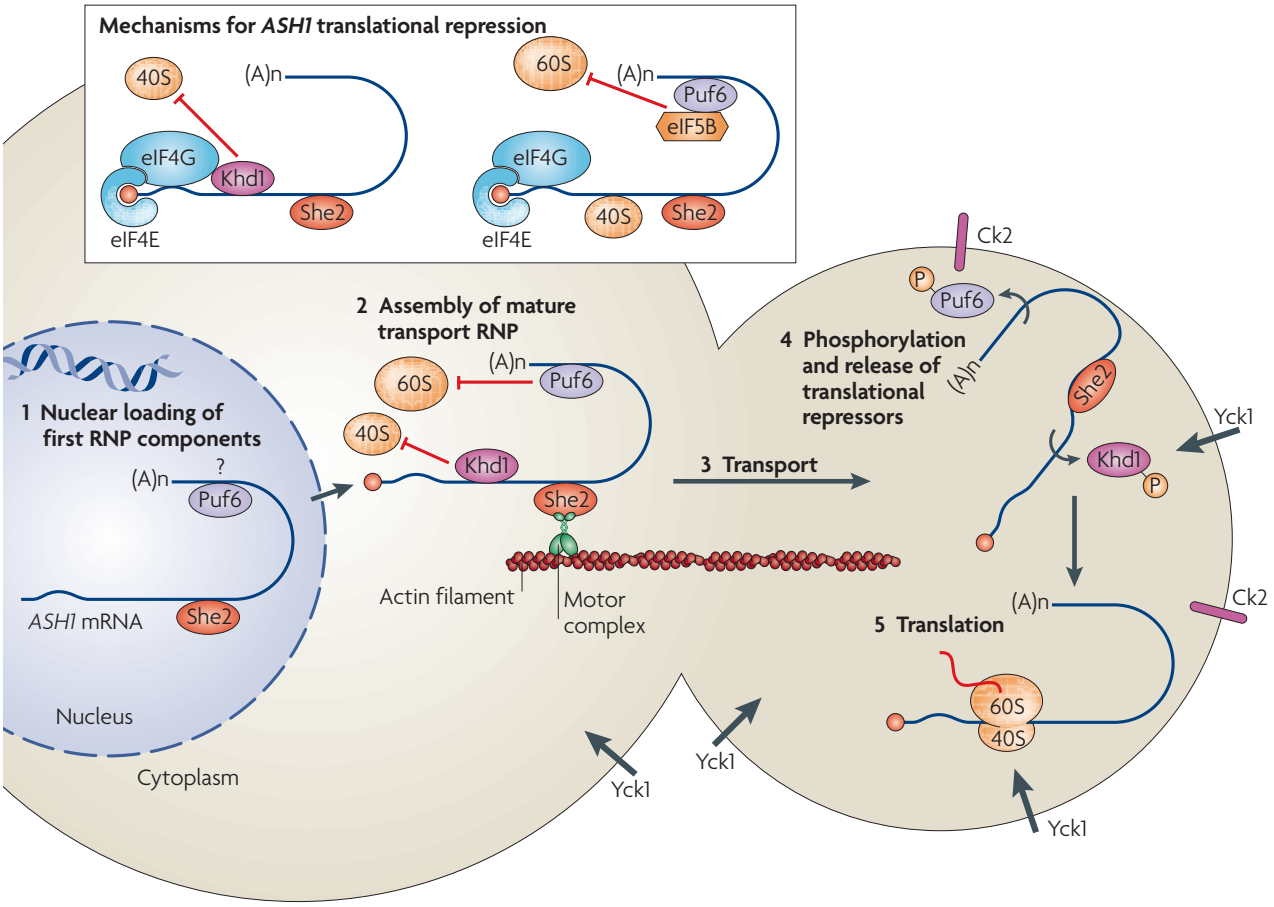

Fig. 1.8: The active transport of the *ASH1* mRNA depends on actin cables. The motor protein Myo4 binds the mRNA via She2 and transports the *ASH1* mRNP to the bud tip. To prevent premature translation during transport, Khd1 and Puf6 are also part of the complex. At the bud tip, translation is activated by phosphorylation of Khd1 and Puf6, causing their dissociation from the mRNA. The Ash1 protein is then imported into the nucleus of the daughter cell (adapted from Besse and Ephrussi, 2008).

1.3 The glucose responsiveness pathway

The cell cycle machinery is sensitive to nutrient depletion and its progression depends on energy consuming processes such as transcription, translation and protein degradation (Buchakjian and Kornbluth, 2010). When cells are deprived of essential nutrients, their smaller daughter cells cannot reach the critical size in order to pass START and will not enter the cell cycle (Broach, 2012; Johnson and Skotheim, 2013; Wang and Proud, 2009; Zaman et al., 2008). For S. cerevisiae, glucose is the most important carbon source and several studies suggest a link between glycogen and trehalose storage and the cell cycle. The length of G1 for example correlates with the amount of carbohydrates stored (Silljé et

al., 1997; Paalman et al., 2003; Brauer et al., 2008) and when cells in G1 decide to further progress to START, they change from carbohydrate accumulation to glucose and trehalose utilization (Silljé et al., 1997; Müller et al., 2003). When recovering from starvation or stationary phase/quiescence, the glucose responsiveness pathway is activated in order to switch from respiration to fermentation. This induction can accelerate cell cycle entry (Peeters et al., 2017). Extracellular glucose activates the pathway by either binding to the G-protein coupled membrane receptor Gpr1 or via the GTP-binding protein Ras2. Heterotrimeric G-proteins consist of α, β and γ subunits. In case of Gpr1, the associated Gα subunit is Gpa2. When glucose binds to Gpr1, a conformational change in Gpa2 exchanges GDP with GTP which causes the disassociation from G$\beta\gamma$. Each subunit is able to influence downstream targets. The Gα and G$\beta\gamma$ re-associate when the Gα subunit hydrolyzes GTP to GDP and the signaling ceases.

The downstream target of both, Gpr1 and Ras2, is the adenylyl cyclase (Cyr1) which synthesizes cyclic AMP from ATP. cAMP in turn activates the cAMP-dependent ProteinKinase A (PKA) or Tpk in *S. cerevisiae.* Tpk is a hetero tetramer with two identical regulatory subunits, encoded by *BCY1* and two catalytic subunits, encoded by three related genes, *TPK1*, *TPK2*, and *TPK3* (Broach, 2012; Toda et al., 1987). The catalytic subunits show redundancy but are also linked to different specific functions (Ptacek et al., 2005). Loss of all three catalytic subunits is lethal, while keeping either one maintains viability (Broach, 2012). Binding of cAMP to Bcy1 eliminates its inhibitory activity on the catalytic subunits, rendering the PKA active which subsequently leads to changes of transcription, translation and metabolism (Broach, 2012).

Apart from the glucose responsiveness pathway, the pheromone response pathway in *S. cerevisiae* is another G-protein signaling pathway, that has been well studied and is exemplary for this type of stimulus-response pathway (Zeller et al., 2007). Intriguingly, Asc1 and Scp160 that were mentioned before in connection with translational control and stress response mechanisms, are involved in both. Scp160 for instance forwards the signal from the Gα subunit Gpa1 of the pheromone sensing receptor during mating of haploid a and α cells (Guo et al., 2003). Asc1 on the other hand harbors a classical WD40 structure that is typical for Gβ subunits which can negatively regulate Cyr1. Indeed, it was shown that deletion of Asc1 results in a higher adenylyl cyclase activity after glucose stimulation in vivo (Zeller et al., 2007).

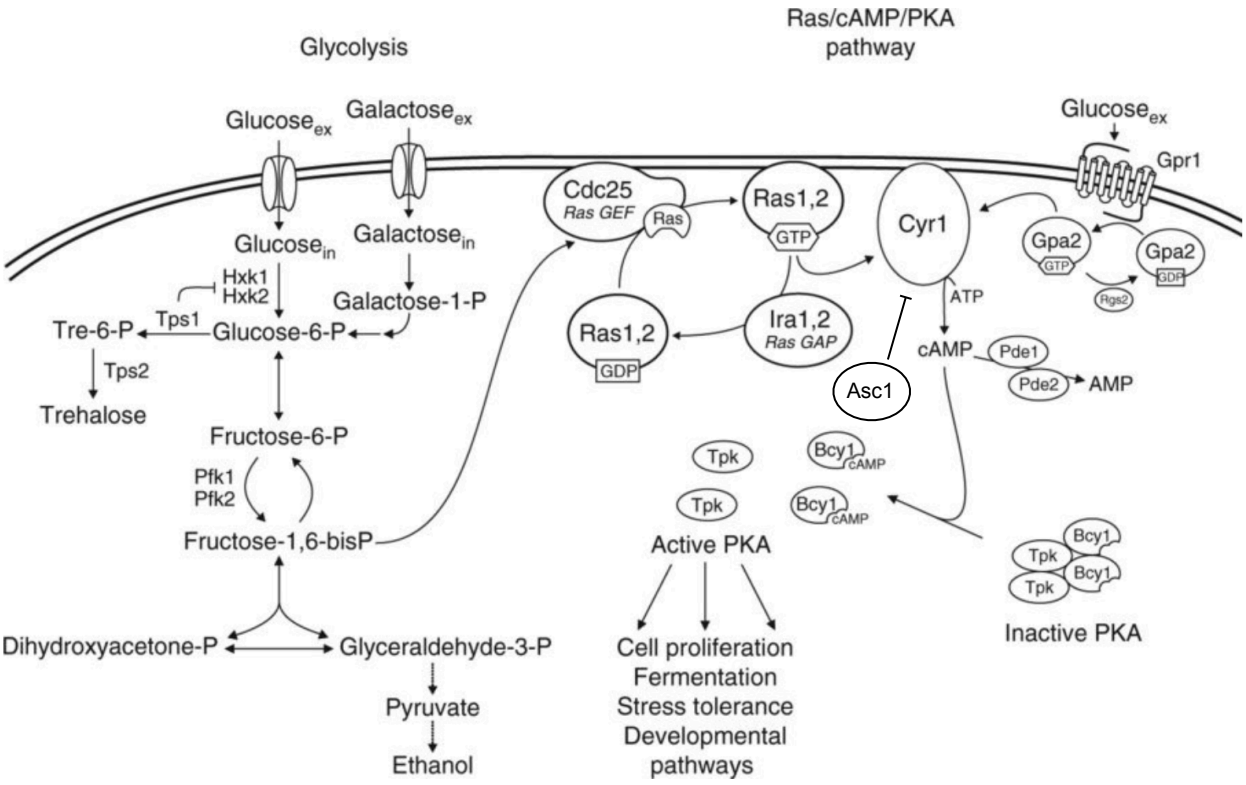

Fig. 1.8: In the glucose responsiveness pathway, two pathways converge on the adenylyl cyclase Cyr1. This leads to increased cAMP concentrations, which in turn renders the PKA (Tpk) active, thus influencing gene expression, metabolism and growth (adapted from Peeters et al., 2017)

1.4 Hexose transporters

S. cerevisiae prefers glucose as its main carbon source. The first step in glucose utilization is the transport across the plasma membrane. This process is mediated by hexose transporters that import hexoses via facilitated diffusion (Busti et al., 2010).

The HeXose Transporter (HXT) family is a subfamily of the major facilitator superfamily (MFS). The MFS consists of a large variety of transporters for a large range of metabolites in eukaryotes and prokaryotes (Marger and Saier, 1993). Sequence alignments showed conservation especially in the sequence that encodes 12 putative transmembrane helices (Kruckeberg, 1996). The N- and C-terminal regions are very variable but they are all predicted to be located in the cytoplasm (Fig. 1.9).

The genome of S. cerevisiae comprises 17 hexose transporters encoded by *HXT1-17* and *GAL2.* In addition to importing glucose, budding yeast also senses extracellular glucose concentrations through two hexose sensors Snf3 and Rgt2 (Boles and Hollenberg, 1997; Özcan and Johnston, 1999). However, under physiological conditions the most important hexose transporters seem to be Hxt1-4 and Hxt6/7 (Maier et al., 2002). The various hexose transporters differ considerably in their substrate affinities as well as their expression patterns. Hxt1 and Hxt3 are low-affinity carriers (Km-values between 29 and 107 mM) and are expressed mainly at high glucose concentrations (Özcan and Johnston, 1995). Hxt2 and Hxt4, in comparison, are high-

affinity transporters (Km-value between 1.5 and 6.2 mM) and are expressed at low glucose concentrations (Maier et al., 2002; Özcan and Johnston, 1995).

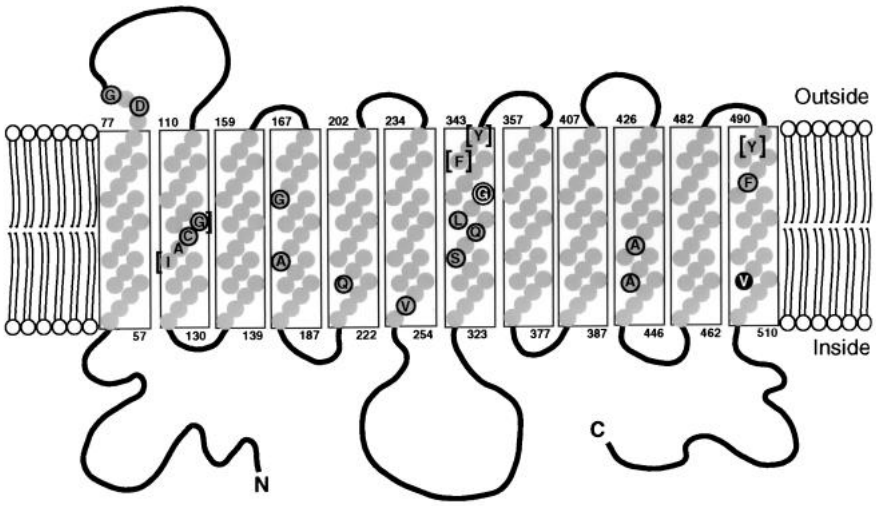

Fig. 1.9: Transmembrane domain model of Hxt3. Each of the 12 transmembrane domains that form α helices and traverse the membrane, are represented by shaded circles (adapted from Liang et al., 1998).

Interestingly, it has been observed that yeast cells expressing Hxt2 at low glucose concentration display both, a high-affinity (1.5 mM) and a low-affinity (60 mM) component (Perez et al., 2005) which could hint at a special role for this transporter.

Hexose transporter	Vm	Glucose affinity
Hxt1	107 mM	low
Hxt2	1.5/60 mM	high/moderate
Hxt3	29 mM	moderate
Hxt4	6.2 mM	high

Fig. 1.10: Different hexose transporters have different affinities for glucose. This provides an opportunity to fine-tune glucose transport over a wide range of concentrations.

Snf3 and Rgt2 mediate both, transcriptional repression and derepression of the genes that encode hexose transporters (*HXTs*). In general, Snf3 is required for the induction of mainly high-affinity HXT genes under low glucose conditions, whereas Rgt2 is required for the high-glucose induction of low-affinity *HXT* genes (Fig.1.11). They exercise their regulatory function via Rgt1, a DNA-binding protein that represses *HXT* gene as well as hexokinase gene (*HXK2*) expression (Lakshmanan et al., 2003; Mosley et al., 2003). After glucose activation, the two corepressors of Rgt1, Mth1 and Std1, bind to the C-terminal tails of Snf3 and Rgt2 at the plasma membrane, where they are phosphorylated by casein kinases Yck1 and Yck2. Upon phosphorylation, Mth1 and Std1 are targeted for degradation by the proteosome via the SCF^{Grr1} ubiquitin-protein ligase (Spielewoy et al., 2004). Lack of these co-repressors exposes Rgt1 to phosphorylation by PKA and alleviates its repressive activity on *HXT* genes (Palomino et al., 2006; Busti et al., 2010).

Depletion of glucose renders Mth1 and Std1 available for Rgt1 interaction, which conceals PKA phosphorylation sites on Rgt1. As a result, the repressor remains bound to promoters, suppressing expression of low-affinity *HXT* genes (Flick et al., 2003). Mth1 and Std1 play partially redundant roles in regulation, because they bind to a common site on Rgt1 in order to block access to PKA (Palomino et al., 2006).

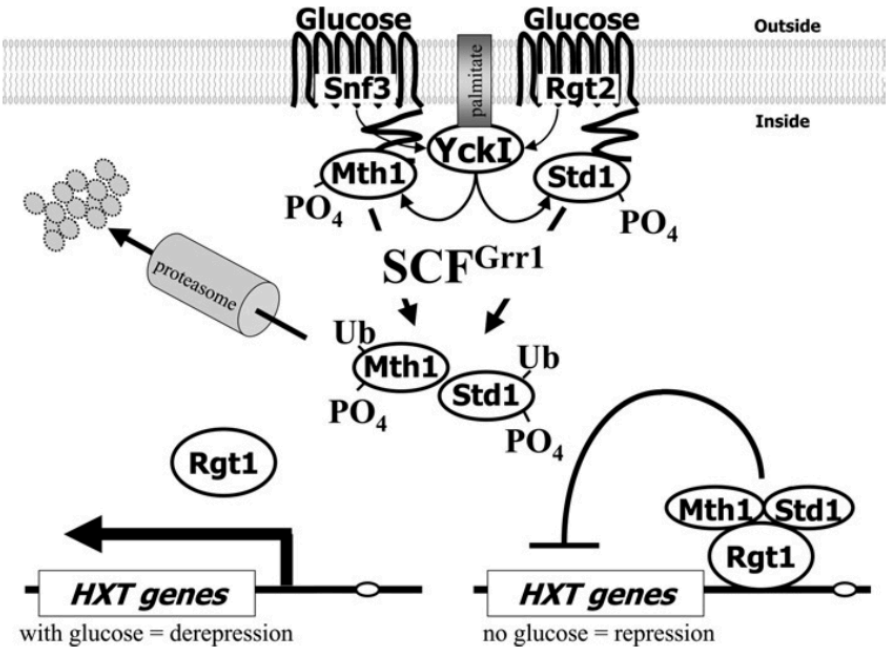

Fig.1.11: Depending on the glucose levels, Snf3 and Rgt2 mediate either repression or derepression of *HXT* genes via the stabilization or the degradation of the Rgt1 co-repressors Mth1 and Std1. At high glucose concentrations, Mth1 and Std1 get degraded via the proteasome. Low glucose concentrations lead to the binding of Mth1 and Std1 to Rgt1 and thus to the repression of low-affinity *HXT* genes (adapted from Johnston and Kim 2005).

The kinase Snf1 plays a critical role in glucose responsiveness. Snf1 is activated at low glucose levels (Busti et al., 2010). Under these conditions, it acts to repress low affinity transporters and at the same time derepresses transcription of high-affintiy transporters such as Hxt2. Repression is achieved by stimulating Rgt1, while for derepression, the repressor Mig1 is inactivated (Kaniak et al., 2004; Palomino et al., 2006). This leads to decreased repression of high-affinity hexose transporters at low glucose concentrations (van Oevelen et al., 2006).

The complex interaction between Rgt1 and Snf1/Mig1 is critical for a graded derepression of different HXTs and is important for the response to variable glucose levels, allowing for expression of only those transporters that have the appropriate affinity (Johnston and Kim 2005).

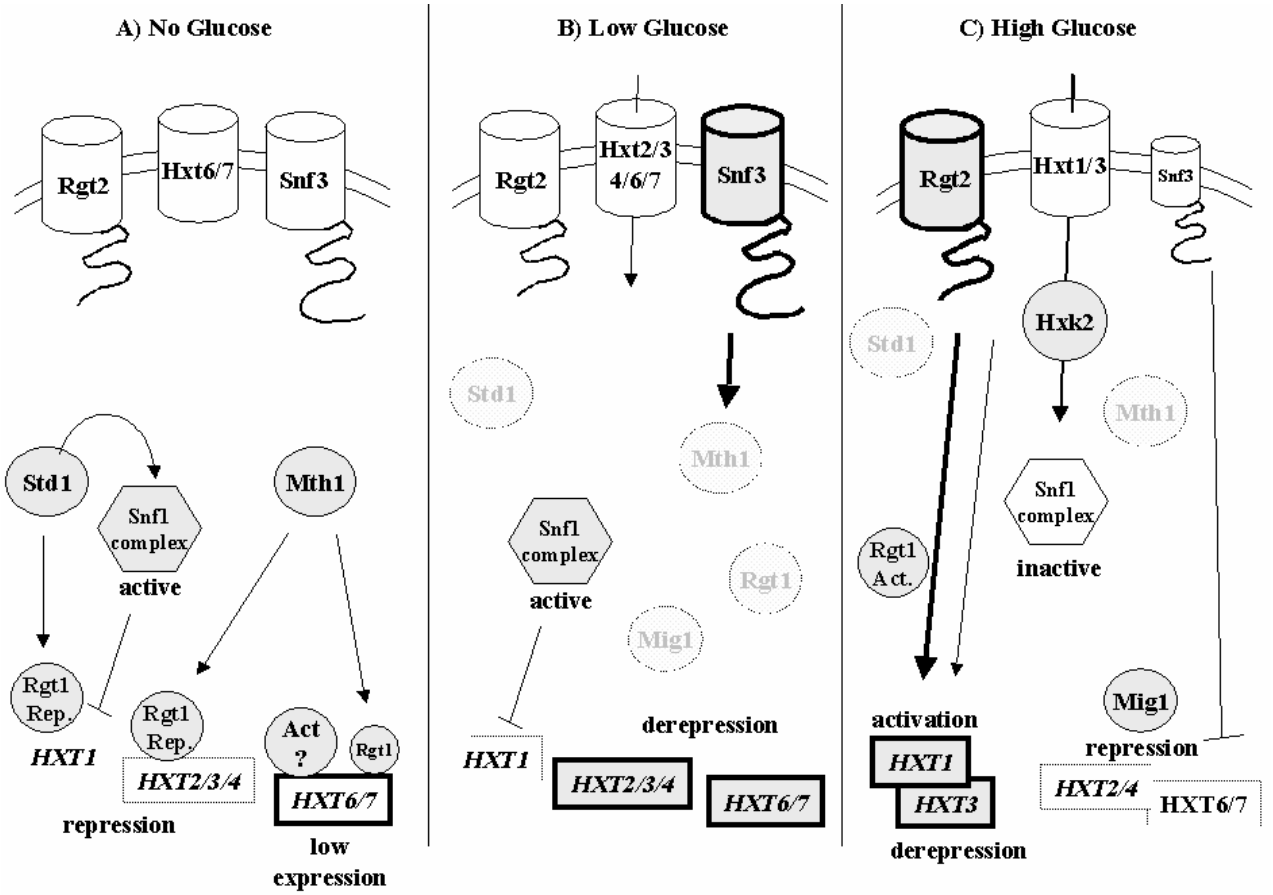

Fig.1.12: The expression of hexose transporters with different affinities is precisely adapted to variable glucose levels. This ensures expression of only those glucose transporters, that provide the most efficient import of available glucose (adapted from Rolland et al., 2002).

2. Aim of the study

More and more studies show that specific localization of mRNAs is a very important, highly conserved mechanism that allows cells to spatially and temporally regulate gene expression. During cell division, certain transcripts are often distributed asymmetrically between mother and daughter cell. This increases heterogeneity within a cell population and provides a way to adapt to changing environments. Especially nutrient availability markedly influences cell growth. *S. cerevisiae* preferentially uses glucose as its main carbon source and thus it is important to ensure proper glucose uptake at any given extracellular glucose concentration.
In this study, we analyzed the cell cycle dependent mRNA localization of the four most physiological relevant HeXose Transporters (HXT). Under glucose-rich conditions, the transcripts of all four investigated HXTs were first retained in the mother cell early in the cell cycle and only later, the mRNA was released to the bud. However, under conditions where cells were re-fed with glucose after starvation, we observed a strong enrichment of *HXT2* mRNA in the bud late in the cell cycle, whereas other HXT transcripts were not enriched.
Therefore, we addressed the following questions:

- What is the mechanism underlaying retention and subsequent release of HXT mRNA under glucose-rich conditions?
- How is *HXT2* mRNA enriched in the bud under glucose-shift conditions?
- What are the cis- and trans-acting elements involved in retention, equal distribution and enrichment of *HXT* mRNA?
- What is the biological significance of *HXT2* mRNA enrichment?

3. Results

The following manuscript was uploaded to the bioRxiv pre-print server and submitted to EMBO Journal on July 30th, 2018.

Statement of contributions:

Timo Stahl: all experimental work presented in this study, including the creation and assembly of all figures unless otherwise stated. He provided critical comments on the manuscript.

Stefan Hümmer: started the project, created strains and plasmids used in this study and provided critical comments on the manuscript.

Nikolaus Ehrenfeuchter: wrote the macro used to quantify FISH signals, provided help on image handling and critical comments on the manuscript.

Geoffrey Fucile: Identification of PKA targets at the ER and the nuclear envelope.

Anne Spang: supervised the study and wrote the manuscript.

Asymmetric Distribution of Glucose Transporter mRNA Provides Growth Advantage

Timo Stahl[1], Stefan Hümmer[1,2], Nikolaus Ehrenfeuchter[1], Geoffrey Fucile[3], and Anne Spang[1]

[1]Biozentrum, University of Basel, 4056 Basel, Switzerland

[2]current affiliation: Translational Molecular Pathology, Vall d'Hebron Research Institute, Universitat Autònoma de Barcelona, Barcelona and Spanish Biomedical Research Network Centre in Oncology (CIBERONC), Spain

[3]SIB Swiss Institute of Bioinformatics, sciCORE Computing Center, University of Basel, 4056 Basel, Switzerland

Address of Correspondence:

Anne Spang

Biozentrum

University of Basel

Klingelbergstrasse 70

CH-4056 Basel

Switzerland

Email: anne.spang@unibas.ch

Phone: +41 61 207 2380

Running title: PKA asymmetrically localizes HXT2 mRNA

Abstract

Asymmetric localization of mRNA is important for cell fate decisions in eukaryotes and provides the means for localized protein synthesis in a variety of cell types. Here we show that hexose transporter mRNAs are retained in the mother cell of *S. cerevisiae* until metaphase-anaphase transition (MAT) and then are released into the bud. The retained mRNA was translationally inactive but bound to ribosomes before MAT. Importantly, when cells were shifted from starvation to glucose-rich conditions, *HXT2* mRNA, but none of the other *HXT* mRNAs, was enriched in the bud after MAT. This enrichment was dependent on the Ras/cAMP/PKA pathway, the APC ortholog Kar9 and nuclear segregation into the bud. Competition experiments between strains that only expressed one hexose transporter at a time revealed that *HXT2* only cells grow faster than their counterparts when released from starvation. Therefore, asymmetric distribution of *HXT2* mRNA provides a growth advantage for young daughters, who are better prepared for nutritional changes in the environment. Our data provide evidence that asymmetric mRNA localization is an important factor in determining cellular fitness.

Keywords

Cellular fitness/mRNA/signaling/stress response/glucose transport/PKA/Ras/cAMP

Introduction

Cells have to respond to an ever-changing environment. This is true not only for single cell organisms like the yeast *Saccharomyces cerevisiae* but also for multicellular organisms, including humans. Variations in the availability of nutrients, in particular glucose, is one of the major challenges and cells have evolved a number of strategies to counteract glucose depletion. For example, under glucose-rich conditions insulin promotes the plasma membrane expression of the glucose transporter GLUT4 in adipocytes allowing glucose storage (Karnieli, Zarnowski et al., 1981, Martin, Millar et al., 2000). In contrast, another glucose transporter, GLUT1, is stabilized at the plasma membrane under energy stress conditions (Wu, Haynes et al., 2013). Alterations in glucose transporter expression have been observed in numerous diseases, including a variety of cancers. For example, GLUT1 and GLUT3 are overexpressed in solid tumors, and their expression levels are used as prognostic and predictive markers. Overexpression has been associated with poor survival (Barron, Bilan et al., 2016) as it may help to increase biomass production and tumor progression (Calvo, Figueroa et al., 2010, Yun, Rago et al., 2009).

The yeast *Saccharomyces cerevisiae* is sensitive to alterations of nutrient availability in the environment. Because of its inability to actively move towards a food source it has developed strategies to adapt quickly to local changes. Depending on the accessibility of glucose for example, yeast expresses a suitable set of its 17 hexose transporters to ensure an optimal growth pattern (Bisson, Fan et al., 2016). It has been well established that the transcription of the hexose transporters is modulated by glucose concentrations. In addition, the abundance of glucose transporters at the plasma membrane is regulated by endocytosis and subsequent degradation, if they are no longer needed (Hovsepian, Defenouillere et al., 2017, Llopis-Torregrosa, Ferri-Blazquez et al., 2016, O'Donnell, McCartney et al., 2015, Roy, Kim et al., 2014, Snowdon & van der Merwe, 2012). Even though these processes were initially studied mostly in yeast, they are conserved up to humans, indicating that *S. cerevisiae* is an excellent model organism for these types of studies.

Responses to changes in the environment can occur on both the transcriptional as well as the post-transcriptional level. Whereas our understanding of global transcriptional responses to environmental dynamics has vastly expanded from the deluge of next generation sequencing data, much less is known about post-transcriptional processes. This is partly due to the complexity of regulatory processes occurring at the levels of both RNA and protein. In the case of mRNA, a multitude of factors determines its stability, whether it is translated or stored, and how and where it is localized. All these mechanisms contribute to regulate protein expression and can be modulated in response to specific stresses (Wang, Schmich et al., 2018).

In this regard, subcellular localization of mRNA has been established as one important mechanism to control the timing and extent of protein expression (Parton, Davidson et al., 2014). During development and stem cell division for example, asymmetric localization of mRNA determines cell fate. Additionally, for neurotransmission, axonal mRNA localization and localized translation are essential. Yet, mRNA localization is

not only limited to specialized cells. Localized mRNAs have been detected in a wide range of organisms including bacteria, yeast, plants and animals (Medioni, Mowry et al., 2012). Moreover, mRNA can be localized to a variety of intracellular organelles. In fact, there are thousands of mRNAs that exhibit specific subcellular localization patterns in mammals and Drosophila (Lecuyer, Yoshida et al., 2007, Mili, Moissoglu et al., 2008). It is generally assumed that mRNA localization correlates with regulated translation, suggesting that this highly conserved process is very efficient.

Here, we investigated the mRNA localization of the hexose transporter Hxt2. Hxt2 mRNA is asymmetrically localized during the cell-cycle, showing a strong retention in the mother cell until mitosis at which point equal portioning between mother and future daughter cell is achieved. The retained mRNA is presumably translational inactive during early phases of the cell-cycle and only becomes translated upon entry into mitosis. Importantly, refeeding of starved cells with glucose, shifted the equal distribution of HXT2 mRNA to an enrichment in the bud. This process was dependent on the Ras/cAMP/PKA signaling pathway, spindle positioning and the nuclear pore components Nup2 and Mlp1/2, which were reported to be involved in nuclear pore complex inheritance. The asymmetric enrichment of HXT2 mRNA during mitosis may contribute to a growth advantage of those daughters over cells that are unable to mount a similar response.

Results

Hxt2 protein is asymmetrically localized in yeast cells.

We and others have used Hxt2 protein as a marker of the plasma membrane (Bagnat & Simons, 2002, Estrada, Muruganandam et al., 2015, Walther, Brickner et al., 2006, Zanolari, Rockenbauch et al., 2011). We observe, however, that in small and medium sized buds Hxt2 levels were always rather low but increased as the cell cycle progressed until at cytokinesis equal levels of Hxt2 were present in the mother and the daughter cells (Fig. 1A). These differences in protein levels might have been brought about by transcriptional and/or translational control. Indeed, several high throughput studies indicate that HXT2 mRNA expression occurs at restricted times in the cell cycle (Cho, Campbell et al., 1998, Pramila, Wu et al., 2006, Spellman, Sherlock et al., 1998). However, HXT2 mRNA was reported to be expressed at the mitosis to G1 boundary, an expression pattern that does not match well with the observed protein expression pattern.

HXT2 mRNA is asymmetrically localized early and equally distributed late in the cell cycle.

As pointed out above, mRNA localization is a potential mechanism to regulate protein expression. Therefore, we determined HXT2 mRNA cellular distribution by FISH (*F*luorescence *I*n *S*itu *H*ybridization) (Fig. 1B). In small and medium budded cells, HXT2 mRNA was restricted to the mother cell (Fig. 1B, white arrowheads), but in large budded

cells (Fig. 1B, yellow arrowhead) HXT2 mRNA became equally distributed between mother and daughter cells. One explanation for this observation is that the mRNA distribution was connected to DNA segregation onto the two poles or in other words to the metaphase-anaphase transition (MAT). To investigate whether HXT2 mRNA localization is indeed correlated to cell cycle progression, we abrogated mitosis by treatment with nocodazole. Under these conditions, HXT2 mRNA remained restricted to the mother cell, suggesting a link between HXT2 mRNA localization and cell-cycle stage (Fig. S1A). For a more quantitative measure as readout from the FISH experiments, we determined the fluorescence intensity in the mother and the bud. The quotient of the mean fluorescence intensity of the mother cell over the bud/daughter cell reflects the relative mRNA distribution. A quotient of >1 indicates enrichment in the mother, and <1 in the bud (Fig. 1C). We scored cells with a bud and containing either one (before metaphase-anaphase transition (MAT)) or two nuclei (after MAT). We conclude that HXT2 mRNA localization changes over the cell cycle and that this change in localization is very robust and reproducible.

We wondered whether the HXT2 mRNA was transported to the bud through an active transport pathway, which would involve the cytoskeleton or through passive diffusion. We depolymerized actin cables with latrunculin A (LatA) (Fig. S1B) and microtubules (MTs) with benomyl (Fig. S1C), and assessed the localization of HXT2 mRNA. A benomyl concentration was chosen such that the number of cytoplasmic MTs was strongly reduced but cells could still undergo mitosis (Fig. S1C). However, neither mother cell retention nor release after MAT of HXT2 mRNA were affected when the cytoskeletal drugs were applied (Fig 1D and E). Our data suggest that under these conditions HXT2 mRNA diffuses into the bud after MAT.

HXT2 mRNA localization in the bud is independent of de novo transcription

Even though Hxt2 mRNA was reported to be expressed at the M/G1 boundary, we cannot exclude that the change in distribution is due to transcriptional activity. To distinguish between mRNA movement in the cytoplasm from the mother to the bud and transcriptional increase of HXT2 mRNA concentration, we blocked transcription with 1,10-phenanthroline. Under these conditions the overall HXT2 mRNA signal was weaker, consistent with a decrease in transcriptional activity. Nevertheless, we still observed equal distribution of the mRNA after anaphase (Fig. S2A and B). Therefore, the change in HXT2 mRNA localization is largely independent of *de novo* mRNA synthesis. To corroborate our findings, we replaced the HXT2 promoter by the constitutive ADH and GPD promoters, which vary in their strength and led to a slight to moderate overexpression of HXT2 mRNA (Fig. S2C). Interestingly, under those conditions, HXT2 mRNA was still retained in the mother (Fig. S2D and E), indicating an active retention mechanism. In contrast, after mitosis, most of the HXT2 mRNA was still present in the mother cell, suggesting that the mRNA signal in the daughter is independent of increased mRNA levels. Taken together, these results suggest that transcription is not major contributor to HXT2 mRNA localization changes in logarithmically growing cells.

HXT2 mRNA is associated with stalled ribosomes in the mother cell.

Next, we asked whether these changes in mRNA localization were connected to translation. To this end, we treated cells with two translational inhibitors. Cycloheximide inhibits the elongation cycle during translation and therefore the mRNA is covered with stalled ribosomes ('polysomes'), while verrucarin A is a translation initiation inhibitor, leading to accumulation of monosomes and 'free' RNA. In both cases, we observed a FISH signal reduction in the bud after MAT (Fig. 2A). In addition, we noticed that the overall FISH signal was stronger in cycloheximide-treated cells and somewhat weaker in the presence of verrucarin A, when compared to control (Fig. 2B), indicating that HXT2 mRNA is stabilized by binding to ribosomes. To test this hypothesis, we performed qPCR. Indeed, the HXT2 mRNA levels were slightly increased in the presence of cycloheximide (Fig. 2C). Conversely HXT2 mRNA levels were reduced when translation initiation was attenuated using the temperature-sensitive initiation factor *prt1-1* mutant (Fig. 2C). Our data imply that HXT2 mRNA requires ribosome association for protection from decay and suggest that HXT2 mRNA is ribosome-associated in the mother cell early in the cell-cycle. Since we detected Hxt2 protein only much later in the cell-cycle, we infer that the ribosomes on HXT2 mRNA would be stalled early in the cell cycle and that this block would be released at a later time point.

An HXT2 mRNA-ribosome complex is retained in the mother cell in an SRP-independent manner

Our data suggest that HXT2 mRNA is part of a translationally inactive ribosomal complex that is present in the mother cell before entry in mitosis. Since HXT2 mRNA is apparently synthesized in M/G1, one possible explanation for the mother cell localization is that HXT2 mRNA becomes ribosome-associated and translation is initiated in G1. The Hxt2 protein contains twelve transmembrane domains (Kasahara, Ishiguro et al., 2006) and hence must be co-translationally translocated into the ER. The transfer of a translating ribosome from the cytoplasm to the ER membrane is mediated by the signal recognition particle (SRP) (Hann & Walter, 1991). Thus, it is conceivable that during HXT2 mRNA translation, when the nascent polypeptide chain emerges from the ribosome, the HXT2 RNP is transferred to the ER by SRP, where the translation might be stalled. To test this possibility, we examined the HXT2 mRNA localization in a *Δsrp54* mutant, in which SRP function and translocation into the ER are strongly impaired (Hann & Walter, 1991). We did not observe any difference in the distribution of HXT2 mRNA between wild-type and *Δsrp54* cells (Fig. 2D), making it unlikely that SRP is actively involved in restricting HXT2 mRNA localization in the mother cell.

Loss of the mRNA binding protein Scp160 causes enrichment of Hxt2 mRNA in the bud after mitosis

The results presented above imply that translation efficiency might be key to the retention of HXT2 mRNA in the mother cell. The polysome-associated mRNA binding protein

Scp160 is ER-localized and is involved in translational efficiency (Hirschmann, Westendorf et al., 2014, Sezen, Seedorf et al., 2009, Weidner, Wang et al., 2014). Therefore, we tested whether *SCP160* deletion would affect HXT2 mRNA localization. While the localization was not altered early in the cell-cycle, HXT2 mRNA unexpectedly was enriched in the bud after MAT (Fig. 3A). *Δscp160* cells rapidly become polyploid (Wintersberger, Kuhne et al., 1995). To ensure that ploidy had no effect on the mRNA localization, we used a strain in which Scp160 expression is dependent on doxycycline (Hirschmann et al., 2014). Acute depletion of Scp160 also promoted HXT2 mRNA enrichment in the bud (Fig. 3B + Doxy, Fig S3A). Likewise deleting 2 or 4 of the C-terminal KH domains of Scp160 (Baum, Bittins et al., 2004) was sufficient for HXT2 mRNA bud enrichment (Fig. 3B). Thus, loss of Scp160 function promotes enrichment of HXT2 mRNA in the bud after anaphase. Yet, Scp160 does not appear to play a role in the initial retention of HXT2 mRNA in the mother cell.

The association of Scp160 with polysomes depends on Bfr1 and Asc1 (Baum et al., 2004, Lang, Li et al., 2001). Deletion of either *BFR1* or *ASC1* showed a phenotype indistinguishable from *scp160* mutants or depletion (Fig. 3A). The phenotype was specific because deletion of two other RNA binding proteins involved in mRNA localization, Khd1 and Vts1, did not show HXT2 mRNA accumulation in the bud (Fig. 3A).

Scp160 and Asc1 are part of the SESA complex, which functions in translational control of a subset of mRNAs (Sezen et al., 2009). Yet, deletion of another component of this complex, Eap1, had no effect on HXT2 mRNA localization, indicating that Scp160, Bfr1, and Asc1 act independently of the SESA complex in this process (Fig. S3B). Taken together, our results demonstrate that lack of Scp160, Bfr1 and Asc1 causes asymmetric HXT2 mRNA distribution after MAT.

The HXT2 mRNA enrichment in the bud in *scp160*, *bfr1* and *asc1* mutants was rather unexpected and very surprising. Therefore, we decided to further explore the mechanism and function of HXT2 mRNA enrichment in the bud after MAT.

Increase of cAMP levels and PKA activity promote asymmetric distribution of HXT2 mRNA after metaphase/anaphase transition

Asc1 is the functional orthologue of mammalian RACK1 and was reported to function as a G-protein β-subunit coupled to glucose responsiveness (Zeller, Parnell et al., 2007) (Fig. 3C). Since Hxt2 is a glucose transporter, it is conceivable that Asc1's function in repressing adenylate cyclase to keep cAMP levels low, would prevent HXT2 mRNA accumulation in the bud. Conversely, in this scenario, raising cAMP levels should drive HXT2 mRNA accumulation in the bud. To test this idea, we treated cells with forskolin, an activator of adenylate cyclase. As expected, forskolin did not affect HXT2 mRNA localization early in the cell cycle (Fig. 3D). However, we observed an increase in HXT2 mRNA signal in the bud comparable with that observed in the *Δasc1*, *Δbfr1* and *scp160* mutants. High cAMP levels cause the activation of PKA by binding to the inhibitory subunit Bcy1, which dissociates from PKA in the cAMP-bound form (Fig. 3C). We tested whether PKA signaling was involved in the HXT2 mRNA bud enrichment by deleting

BCY1. In fact, HXT2 mRNA enrichment was even more pronounced in *Δbcy1* cells (Fig. 3D), indicating that indeed activation of PKA was responsible for HXT2 mRNA enrichment in the bud after mitosis.

Rather than using mutants to up-regulate cAMP/PKA signaling constitutively, we sought an approach to recapitulate transient cAMP production and hence transiently activate PKA. When starved cells are fed with glucose, they transiently increase cAMP levels (Jiang, Davis et al., 1998). We decided to use this regime to explore the changes in HXT2 mRNA localization upon transient PKA activation. We starved cells for 2 h and then shifted them to glucose-rich medium for 30 min prior to FISH analysis. HXT2 mRNA was enriched in the bud after MAT (Fig. 3E), demonstrating that indeed the cAMP/PKA pathway is responsible for the enrichment of HXT2 mRNA in the bud. This enrichment was also confirmed by single molecule FISH (smFISH) (Fig. S3C). The cAMP/PKA pathway can be activated through G-protein coupled receptor activation or Ras (Jiang et al., 1998, Xue, Batlle et al., 1998). To determine the upstream component of the adenylate cyclase, we deleted the receptor, *GPR1*, and the α-subunit *GPA2,* and used a strain carrying the *ras2^{318S}* mutation (Jiang et al., 1998). While loss of the G-protein-coupled receptor branch did not interfere with HXT2 mRNA localization after refeeding, the *ras2^{318S}* mutant was defective in HXT2 mRNA enrichment in the bud after MAT (Fig. 3E). We conclude that HXT2 mRNA enrichment in the bud after MAT is dependent on the Ras/cAMP/PKA signaling pathway. Since PKA is also involved in *HXT2* transcriptional activation (Kim & Johnston, 2006), we wondered whether transcription could contribute to the asymmetric HXT2 mRNA localization. When we blocked transcription with 1,10 phenanthroline after glucose shift, we did not observe an HXT2 mRNA enrichment in the bud after MAT (Fig. S2A and B), indicating that *de novo* synthesis is required for the asymmetric mRNA distribution under these conditions.

Hexose transporter mRNAs are retained in the mother but not all of them are enriched in the bud when released from starvation

Seventeen *HXT* genes are encoded in the *S. cerevisiae* genome. We aimed to determine whether changes in mRNA localization are a common feature among HXTs. We concentrated on the 3 most important Hxts besides Hxt2: the low affinity transporters Hxt1 and Hxt3 and the high affinity transporter Hxt4 (Fig. 4A). Hxt2 can adopt at least two conformations that have been proposed to reflect high affinity and low affinity transporter states (Perez, Luyten et al., 2005, Reifenberger, Boles et al., 1997). Therefore, Hxt2 is special in that it cannot be clearly assigned to the low or high affinity transporter group. HXT1, HXT3 and HXT4 mRNAs were each retained in the mother early in the cell cycle and equally distributed after mitosis (Fig. 4B and C). However, HXT1, HXT3 and HXT4 mRNA were less responsive than HXT2 mRNA to high PKA levels in *Δbcy1* cells. HXT3 mRNA did not show any enrichment in the daughter cell (Fig. 4D). In a *Δbcy1* strain, PKA is constitutively hyperactive. To investigate HXT mRNA localization in a more physiologically relevant context, we again shifted cells from starvation to glucose to induce a short cAMP peak, which in turn is sufficient to activate PKA. Under those

conditions, HXT1, HXT3 and HXT4 mRNA did not show any enrichment in the daughter cell after mitosis, while HXT2 mRNA was still enriched (Fig. 4E).

To corroborate our findings, we separated young, newborn daughters from mother cells through elutriation during which we switched from no glucose to glucose-rich medium. We then extracted the total mRNA from the different cell populations and performed qPCR for HXTs. As a control, we used ASH1 mRNA, which is known to be enriched in daughter cells. ASH1 mRNA was about 2.3-fold enriched in daughter cells, a value which is in good agreement with the 2-2.2-fold increase reported previously (Takizawa, DeRisi et al., 2000). Among the HXT mRNAs, HXT2 was the only mRNA that accumulated in daughter cells (Fig. 4F). Taken together, retention in the mother prior to entering mitosis appears to be a general feature among the most important hexose transporter mRNAs, while the enrichment in the bud late in the cell cycle after release from starvation is specific for HXT2 mRNA.

The spindle positioning protein Kar9 and nuclear segregation are essential for HXT2 mRNA bud enrichment under glucose shift conditions

Even though *de novo* HXT2 mRNA synthesis is required for bud enrichment (Fig. S2A and B), overexpression of HXT2 mRNA by itself was not sufficient to promote asymmetric mRNA distribution (Fig. S2C and D). Therefore, an additional layer of regulation must be required. It is conceivable that the enrichment of HXT2 mRNA in the bud late in the cell-cycle could be dependent on three not mutually exclusive mechanisms: active transport of the mRNA into the bud, diffusion and retention, and selective degradation in the mother cell. P-bodies are the primary site of mRNA decay in yeast, and the exonuclease Xrn1 is responsible for the degradation of most mRNAs (Muhlrad, Decker et al., 1994). Therefore, we determined HXT2 mRNA localization after shift from starvation to glucose containing medium in *Δxrn1* cells. We could not detect a significant difference in mRNA localization when compared to wild-type cells (Fig. 5A). Thus, localized mRNA decay is an unlikely mechanism for the asymmetric HXT2 mRNA localization. To distinguish between active and passive transport, we repeated the treatment of cells with benomyl and LatA under the glucose shift conditions. Both benomyl and LatA treatment abrogated the HXT2 mRNA enrichment. (Fig. 5B). In addition, inhibition of the Arp2/3 complex by CK-666 inhibited HXT2 mRNA accumulation (Fig. 5B). Our data suggest that actin and MTs both contribute to the asymmetric distribution of HXT2 mRNA. Accordingly, we sought a cellular process involving both MTs and actin. Spindle positioning and spindle pole body (SPB) movement to the bud is such a process (Miller, Matheos et al., 1999). A key component in this process is the APC ortholog Kar9. Deleting *KAR9* reduced HXT2 mRNA asymmetric localization to the bud after MAT upon refeeding (Fig. 5C and D). In a *Δkar9* mutant, the old SPB is no longer preferentially segregated to the bud/daughter cell, and oftentimes both nuclei are retained in the mother cell after mitosis (Miller & Rose, 1998, Pereira, Tanaka et al., 2001). In large budded-cells after MAT, we observed equal HXT2 mRNA distribution when mother and daughter received a nucleus. In contrast, in cells in which both nuclei remained in the mother, HXT2 mRNA was likewise retained (Fig.

5C and D). Thus, Kar9 and potentially nuclear segregation into the bud play an essential role in asymmetric HXT2 mRNA distribution.

Kar9 is required for asymmetric distribution of HXT2 mRNA on the nuclear envelope

To corroborate our results, we deleted another component of the spindle positioning pathway, the EB1 homolog Bim1 (Lee, Tirnauer et al., 2000). In *Δbim1* cells, in which one of the nuclei reached the bud, HXT2 mRNA asymmetric distribution was largely unaffected (Fig. 5C and D). However, when both nuclei were retained in the mother, HXT2 mRNA was likewise retained. Our results are consistent with HXT2 mRNA requiring nuclear segregation into the bud for its asymmetric enrichment after glucose shift. Moreover, this process appears to be dependent on the spindle positioning pathway. Yet, the effect of *Δkar9* and *Δbim1* on HXT2 mRNA localization in mothers containing two nuclei was different. While in *Δbim1* cells HXT2 mRNA was preferentially localized to one of two nuclei, in *Δkar9* cells, the mRNA was not closely associated with a particular nucleus, and often not even recruited to the nuclear envelope (Fig. 5C and E). These results suggest that Kar9 is required for asymmetric loading of HXT2 mRNA on the nuclear envelope.

The nuclear pore components Nup2 and Mlp1/2 are involved the asymmetric localization of HXT2 mRNA

We have shown above that PKA activation and nuclear segregation in the bud are prerequisites for the asymmetric distribution of HXT2 mRNA upon refeeding. Even though Kar9 is phosphorylated, this phosphorylation event has not been attributed to PKA action. We consequently hypothesized that PKA might phosphorylate a protein at the nuclear envelope or the endoplasmic reticulum, which in its phosphorylated form might contribute to asymmetric HXT2 mRNA localization. To test this hypothesis, we searched databases for ER/nuclear envelope localized PKA substrates (Table S1). Within this list, we found two components of the nuclear pore complex (NPC), which were promising candidates for asymmetric localization of mRNA - Nup2, which is involved in NPC inheritance (Suresh, Markossian et al., 2017) and the FG-repeat containing central core component Nup53. Indeed, when we deleted *NUP2*, the asymmetric localization of HXT2 mRNA to the bud was dampened (Fig. 6A and B). In contrast, a deletion mutant of *NUP53* and its paralog *NUP59*, did not affect the asymmetric HXT2 mRNA distribution (Fig. 6A and B). The *S. cerevisiae* NPC components Mlp1/2 were shown to be enriched at NPC insertion sites during anaphase at the old SPB that enters the bud (Ruthnick, Neuner et al., 2017). Deletion of *MLP1/2* resulted in a similar defect on HXT2 mRNA enrichment to *Δnup2* (Fig. 6A and B). Our data suggest a contribution by NPCs to the enrichment of HXT2 mRNA in anaphase in the bud upon refeeding, presumably through the NPC inheritance pathway. If our assumption was correct, we should be able to detect HXT2 mRNA on the nuclear envelope. To this end, we marked the nuclear envelope with Nup84-HA and performed FISH-IF. HXT2 mRNA was detected on the nuclear envelope in the bud (Fig. 6C).

To further corroborate our findings, we aimed to image movement of HXT2 mRNA during mitosis using an improved MS2-GFP based system (Tutucci, Vera et al., 2018). HXT2 mRNA was associated with the nucleus as it entered the bud in mitosis after refeeding (Fig. 6D, Movie S1). Such a movement was not observed in cells that did not experience glucose withdrawal (Fig. 6D, Movie S2). Taken together, our data provide strong evidence for an involvement of the nuclear envelope in the asymmetric HXT2 mRNA distribution during mitosis.

HXT2 expression provides a growth advantage.

Why would the yeast cell specifically enrich HXT2 mRNA into the bud following starvation? To gain insights into the biological function of this process, we used yeast strains in which all seventeen *HXT* genes had been deleted and which were kept alive by the expression of a single *HXT* gene under its endogenous promoter (Wieczorke, Krampe et al., 1999, Youk & van Oudenaarden, 2009). Those strains were either grown to stationary phase or cells were scraped off directly from a plate on which they were in a quiescent state. Serial dilutions were dropped on rich media plates. Growth of cells was assessed 2-3 days later. Cells expressing only *HXT2* grew better than cells expressing either only *HXT1*, *HXT3* or *HXT4* on a wide range of glucose concentrations (Fig. 7A and B, Fig. S4). Next, we tested whether HXT2 only strains would also do better when they were directly competing with the other HXT only strains in culture. To this end, we mixed stationary cultures of the 4 HXT only strains, collected a sample for the starting point and let them grow over night. Then we collected another sample and performed qPCR on the DNA. Under direct competition for resources, the HXT2 only strain grew faster and outcompeted the other strains (Fig. 7C and D). Collectively, our data suggest that asymmetric HXT2 mRNA distribution provides a growth advantage.

The cell does not retain a long-lasting memory for HXT2 mRNA localization

We envisage that the increase in HXT2 mRNA in newborn daughters, will allow those daughters to take up more glucose and therefore grow faster than their counterparts that do not increase HXT2 expression. In this scenario, the daughters with high HXT2 will also reach the critical size earlier to enter the cell cycle and become a mother. We wondered, whether asymmetric HXT2 mRNA distribution would be retained in future generations in order not lose the competitive edge. In other words, we asked whether high HXT2 daughters remember that they received more HXT2 and will therefore also asymmetrically distribute the HXT2 mRNA during the next cell division, even though the daughters have not experienced nutrient limiting conditions themselves? Alternatively, there is no memory of the previous events transmitted to the daughters because entering the cell cycle faster comes at an expense in that errors that occurred during previous cell cycle may not be corrected. To distinguish between the two possibilities, we performed a glucose shift experiment and took samples at different time-points after the shift. FISH revealed that a significant enrichment in the daughter was observed only up to 2 h after shift (Fig. 7E). Considering the lag phase upon resuming the cell division cycle, these results indicate

that a newborn daughter does not retain a memory in terms of HXT2 mRNA localization of its mother's starvation experience, when it becomes a mother itself.

Discussion

We have identified a mechanism in *S. cerevisiae* by which the mRNA of the glucose transporter Hxt2 is specifically enriched in the daughter cell when cells are coming out of quiescence or starvation. We assume that this enrichment provides a growth advantage to these young daughters as they are potentially able to take up more glucose and thus increase in size faster than daughters with less Hxt2. This mechanism allows those daughters to outcompete cells that cannot mount a similar response and provides an ecological advantage. This partitioning is not shared by other major glucose transporters, underscoring a unique role of Hxt2. Hxt2 differs from the other glucose transporters in that it can act as both high affinity and low affinity transporter (Perez et al., 2005), rendering it particularly suitable for such a regulation. We demonstrate that accumulation of HXT2 mRNA is dependent on the Ras/cAMP/PKA pathway and the nuclear envelope. We speculate that the short cAMP peak upon refeeding provides sufficient PKA activity to phosphorylate targets on the nuclear envelope such as Nup2 (Figure 7F). Our data are consistent with a model in which PKA phosphorylates the NPC component Nup2. This would then in turn allow the piggy-back of HXT2 mRNA into the daughter cell. Whether this piggy-back is through the NPC inheritance pathway, direct interaction with Nup2 or correlates to NPC function remains to be determined. However, we favor at this point the involvement of the NPC inheritance pathway rather than NPC function or direct binding to Nup2 based on the observation that deletion of another NPC PKA target, the FG repeat protein Nup53 and its paralog Nup59, did not affect HXT2 mRNA localization. These data argue against NPC function per se being essential for the asymmetric mRNA localization. In contrast, Mlp1/2, which are NPC components that are enriched in the daughter cell during mitosis are likewise contributing to the accumulation of HXT2 mRNA in the daughter cell (Ruthnick et al., 2017). Importantly, NPCs have been shown to accumulate around the yeast centrosome (SPB) presumably through a mechanism involving Mlp2 and Nup2 (Niepel, Strambio-de-Castillia et al., 2005, Suresh et al., 2017, Winey, Yarar et al., 1997).

Our data provide strong evidence that movement of the nucleus into the bud is critical for asymmetric enrichment of HXT mRNA. Both actin and microtubules as well as the yeast EB1 and APC homologs, Bim1 and Kar9, respectively, are essential for this process. Yet, it appears that Kar9 has an additional role in that it may help to generate the asymmetry on the nuclear envelope. While in a *Δbim1* background HXT2 mRNA was present preferentially only on one of two nuclei that were retained in the mother, in *Δkar9* this asymmetry was abolished. During spindle formation early in the cell-cycle Kar9 becomes enriched on the old SPB, which will move into the bud during mitosis in a process dependent on both actin and microtubules (Cepeda-Garcia, Delgehyr et al., 2010, Liakopoulos, Kusch et al., 2003, Maekawa & Schiebel, 2004). During this process, Kar9 translocates from the SPB to the MT (+) ends in the bud by binding to Bim1 (Huls,

Storchova et al., 2012). Therefore, it is likely that Kar9 asymmetry is instructive for HXT2 mRNA localization. However, the underlying mechanism that controls Kar9 asymmetry remains unclear and highly controversial (Juanes, Twyman et al., 2013).

We also found that *HXT2* transcription contributed to the asymmetric enrichment in the bud upon refeeding. However, transcription per se was not sufficient because *HXT2* overexpression did not influence mRNA localization. The *HXT2* transcription during mitosis in the glucose shift experiments might be driven by the same Ras and cAMP-dependent peak of PKA activity (Kim & Johnston, 2006) that drives asymmetric mRNA localization. This scenario would elegantly couple gene transcription to asymmetric distribution of its mRNA.

We generally observed that HXT mRNA was retained in the mother cell before MAT. We assume that the mRNAs are engaged with ribosomes and membrane bound. This retention was also coupled, at least for HXT2, with translational stalling. The mechanism by which this is achieved remains unclear but does not appear to involve SRP. We suppose that at least a part of the stalling of the ribosomes is due to some cis-elements on the mRNA itself. However, since this is a regulated process, trans-acting factors are likely to play a role as well. How these stalled ribosomes would escape ribosome quality control needs also be investigated. Further studies are needed to elucidate the retention mechanism of HXT2 retention.

We propose a model in which the asymmetric HXT2 mRNA distribution upon refeeding allows the daughters to uptake more glucose and therefore grow faster than daughters with less HXT2 mRNA. Since cell size is one of the hallmarks for entering a new cell cycle, the faster growing daughters will start a new division cycle before the others. The faster entry into the cell cycle appears to be sufficient to out compete the slower growing cells. Yet, the faster growing daughters do not retain an obvious memory of the glucose limitation and refeeding because they do not provide more HXT2 mRNA for their daughters. This finding is consistent with the observation that a temporal cAMP/PKA activity peak is sufficient to drive the mRNA enrichment, and hence a memory may not be needed. Moreover, it may not be advantageous for the cells to always enter the cell division cycle as fast as possible. Before passing START, the cells usually check whether the last cell division was successful on multiple levels and aim to repair defects that may have occurred. Therefore, the time between two cell division cycles needs to be balanced between speed and fidelity.

Maintaining such a balance is in contrast to what likely happens in cancer cells. In numerous cancer types, glucose transporters (GLUTs), in particular GLUT1 and GLUT3, are upregulated and often linked to oncogenic RAS (Adekola, Rosen et al., 2012). Like HXTs in yeast, GLUTs are localized in polarized fashion in epithelial cells. Moreover, GLUT3 expression is up-regulated by cAMP in a breast cancer cell line (Meneses, Medina et al., 2008) and increased GLUT1 level have been correlated with poor prognosis in colorectal carcinomas (Sakashita, Aoyama et al., 2001). Thus, cancer cells may employ a similar strategy in terms of accelerating growth, but lack check points to monitor damage that occurred in the previous cell cycle. This may be different in cancer stem cells (CSCs), which are metabolically more similar to stem cells in that they can use glycolysis over

OXPHOS and are often in hypoxic environments (Wong, Che et al., 2017). At least in embryonic stem cells GLUT1 and GLUT3 expression levels are correlated to maintaining pluripotency (Wu, Song et al., 2017, Zhang, Skamagki et al., 2017). Moreover, GLUT1 is asymmetrically localized in dividing lymphocytes and becomes enriched in the differentiating daughter (Chen, Kratchmarov et al., 2018). Therefore, the controlled expression of specific glucose transporter at the plasma membrane, is an important and conserved cellular feature to maintain competitiveness in difficult environments.

Experimental Procedures

Yeast strains and growth conditions

Standard genetic techniques were employed throughout (Sherman, 1991). Unless otherwise noted, all genetic modifications were carried out chromosomally. Chromosomal tagging and deletions were performed as described (Gueldener, Heinisch et al., 2002, Janke, Magiera et al., 2004, Knop, Siegers et al., 1999). For amplification of C-terminal tagging by chromosomal integration pYM (Knop et al., 1999) and for deletions pUG plasmids (Gueldener et al., 2002) were used. For N-terminal tagging or promoter exchange by chromosomal integration pYM-N plasmids were used (Janke et al., 2004). Primers, strains and plasmids used in this study are listed in Supplementary Tables S2-4. The plasmids pMS449 and pMS450 carrying the ΔC2 and ΔC4 truncation of Scp160 were a kind gift from M. Seedorf (ZMBH Heidelberg, Germany). The plasmid pRJ1463 bearing Scp160 under the control of a Tet-off promoter was a kind gift from Ralf-Peter Jansen (Jansen, Niessing et al., 2014). For glucose rich conditions, yeast cells were grown in either YPD (1% w/v Bacto yeast extract, 2% w/v Bacto-peptone, 2% w/v dextrose) or selective medium (prepared as described (Kaiser, 1994)) at 30°C, 200 rpm. For glucose shift conditions, cultures were first grown over night in YPD, then washed two times in YP media without glucose diluted to an OD_{600} of 0.3 and further grown for 2 h in YP media without glucose. After this incubation, glucose was added to a final concentration of 2%. Generally, yeast cells were harvested at mid-log phase with an OD_{600} of 0.4-0.8. OD_{600} as determined with a UltroSpec 3100 pro Spectrophotometer (GE healthcare).

Life cell imaging

Yeast cells were grown in YPD or HC-Leu (2% dextrose, 1x adenine) to early log phase and either analyzed directly or first starved without dextrose for 2 h then supplemented with 2 % dextrose. The cells were taken up in HC-complete or HC-Leu medium and immobilized on 1% agar pads. Fluorescence was monitored with an Orca Flash 4.0 camera (Hamamatsu) mounted on an Axio M2 imager (Carl Zeiss) using a Plan Apochromat 63x/NA1.40 objective and filters for mCherry and GFP. ZEN software version 2.3 (blue edition) was used to acquire images (Carl Zeiss). Further Image processing was performed using Fiji (Schindelin, Arganda-Carreras et al., 2012). All pictures from the same experiment were treated equally.

Fluorescence in situ hybridization (FISH) and FISH combined with immunofluorescence (FISH-IF)

FISH and FISH-IF were performed as described previously (Kilchert & Spang, 2011, Takizawa, Sil et al., 1997). For IF, we used as primary antibodies anti-GFP (Torrey Pines, rabbit, polyclonal, 1:400), anti-HA (Covance, mouse, monoclonal, 1:400) and as secondary antibodies Alexa Fluor 488 goat-anti-rabbit or anti-mouse, respectively (Invitrogen, polyclonal, 1:400). Images were acquired with an Axiocam MRm camera

mounted on an Axioplan2 fluorescence microscope using a Plan Apochromat 63x/NA1.40 objective and filters for eqFP611, DAPI and GFP. AxioVision software 3.1 to 4.8 was used to process images (Carl Zeiss).

FISH quantification - Image Processing and Analysis

Images were acquired on a Zeiss Axioplan2 microscope as described above. Segmentation and analysis were performed using a custom macro for Fiji (available upon request) carrying out the following steps: Based on the red (FISH) channel, the CLAHE (Zuiderveld, 1994) filter was executed to increase the local contrast with the goal of revealing enough contrast for being able to distinguish all cell bodies from the background. Parameters for the CLAHE filter were used with their defaults as provided by the plugin with a block size of 127, a default slope of 2 and 256 histogram bins. After filtering, the local thresholding method as described by (Phansalkar, 2011) was used to create a binary image marking the cell bodies (thresholding radius: 50, object size minimum: 50). To reduce artifacts in the segmentation the binary image was then processed with Fiji's binary "Fill Holes" operation, followed by a "Close" operation. The resulting binary mask was then split into individual masks per cell by using the classical "Watershed" separation. As a last step for the segmentation individual ROIs (regions of interest) were created from this binary mask. After creating the ROIs, they were used to quantify intensities in the red (FISH) channel by measuring the mean gray value per round cell shape. With those results, fluorescence intensities for mothers and their buds were determined separately and finally the ratio of fluorescence intensity in the mother over bud was calculated. At least 50 mother cells and their corresponding buds from at least three biologically independent experiments were counted per condition.

Elutriation

Elutriation was performed in a Beckman elutriation system (Avanti J-26 XP centrifuge combined with a JE-5.0 elutriator rotor and a 200 ml elutriation chamber, as well as standard elutriation accessories) according to (Marbouty, Ermont et al., 2014) with modifications. For glucose shift experiments, first a colony was inoculated in 500 ml YPD medium and incubated overnight at 30°C. The next day, the cells were washed 2x with YP medium without glucose, then diluted to an OD_{600} ~1 in 2 x 1 l fresh YP medium without dextrose and further grown for 2 h. Dextrose was added to a final concentration of 2 % and the cultures were incubated for another 30 min at 30°C. The elutriation chamber was filled with the cell culture at a flow rate of ~25ml/min and a rotor speed of 3,000 rpm at 4°C. The flow rate was gradually increased until the cells reached the top of the chamber. Equilibrium was allowed to settle in the chamber for 1 h while switching medium to PBS. The flow through was checked for escaping cells by OD_{600} measurement. The flow rate was carefully increased by increments of 2 ml/min until the OD_{600} raised above 0.05, at which point cells were collected. The budding index of the recovered cells was checked by microscopy and only daughter cell fractions with less than 5 % budded cells were used. After collection of the daughter cells, the centrifuge

was stopped and the remaining cells were collected, providing the mother cell fraction. The fractions were spun down. The pellets were frozen in liquid nitrogen and stored at -80°C.

Total RNA isolation

Total RNA was isolated from yeast essentially as described (Schmitt, Brown et al., 1990). Briefly, 10 OD_{600} of yeast cells were harvested after different treatments. Cells were resuspended in 1 ml AE buffer (50 mM NaOAc pH 5.2, 10 mM EDTA), 100 µl 20 % SDS and 1 ml PCI (125:24:1, pH 4.4) were added and the tube vortexed for 10 s. After incubation for 10 min at 65°C, tubes were chilled in liquid nitrogen for 30 s, thawed and then centrifuged (2 min, 16,000 x g, RT). The upper aqueous phase was transferred to a fresh tube and 1 ml PCI was added and vortexed 10 s. After phase separation by centrifugation, the upper aqueous phase was transferred to a fresh tube and 1/10 vol. of 3 M NaCl (pH 5.2) was added. The RNA was precipitated with 1 vol. 100 % EtOH at -80°C for at least 1 h. The precipitate was collected (30 min, 16,000 x g, 4°C), washed with 70 % EtOH and again centrifuged. The pellet was resuspended in 200 µl RNase-free water.

Quantitative RT-PCR

0.5-1 µg of total RNA was reversely transcribed with the Transcriptor reverse transcriptase kit (Roche, Cat# 03531287001), oligo-dTs and random hexamers. The mRNA levels were analyzed by SYBR green incorporation using the ABI StepOne Plus real-time PCR system (Applied Biosystems). Primers used in qRT-PCR are listed in Table S3.

Drop assays

Colonies were either directly taken from plate or grown overnight in liquid YP medium supplemented with 2% dextrose to stationary phase ($OD_{600} \geq 9$). After adjusting to equal cell concentrations ($OD_{600} \sim 0.3$), five serial dilutions (1:5) were dropped onto YP plates supplemented with either 0.1, 0.5, 2, or 4 % glucose using a “frogger” stamp (custom-built). Plates were incubated for 2-3 days at 30°C and photographed for documentation.

Actin staining

Actin cytoskeleton staining was performed essentially as described previously (Adams & Pringle, 1991). Cells were grown over night and fixed with 4% formaldehyde for 30 min at RT under gentle agitation. Cells were washed twice with PBS containing 1 mg/ml BSA (3 min, 1,000 g, RT). The cell pellet was resuspended in 25 µl PBS containing 1 mg/ml BSA and 5 µl of rhodamine-phalloidin (Molecular Probes, 300 U/1.5 ml MeOH). After incubation for 1 h at RT in the dark, cells were washed three times and resuspended in 500 µl PBS containing 1 mg/ml BSA. An aliquot was allowed to settle for 30 min on polyethyleneimine-treated multi-well slides. The slides were washed briefly in PBS,

Citifluor AF1 was added and the coverslips were sealed with nail-polish. Slides were stored at -20°C. Rhodamine fluorescence was observed by epifluorescence microscopy using the Cy3 channel on an Axioplan 2 fluorescence microscope from Zeiss. Pictures were taken with an Axiocam MRm camera using AxioVision software. Image processing was performed with Fiji.

Western Blotting

Nine ml of a mid-log grown culture were taken, immediately treated with cold trichloroacetic acid (10% final concentration) and incubated on ice for at least 5 min. Yeast extracts were prepared as described (Stracka, Jozefczuk et al., 2014). The protein concentration was determined using the DC Protein Assay (Bio-Rad) and the total lysate was analyzed by SDS-PAGE. The first antibody was rabbit anti-Scp160 (Weidner et al 2014, 1:1,000), secondary antibody was goat-anti-rabbit, HRP-conjugated (Pierce, polyclonal, 1:15,000). Enhanced Chemiluminescence solution (ECL; GE Healthcare) was used for detection.

PKA target prediction

To identify potential PKA targets, we intersected subcellular localization annotations and known phosphopeptides from yeast. The localization set of interest includes all UniProt entries for *S. cerevisiae* with at least one localization annotation of "endoplasmic reticulum", "nucleus outer membrane", or "nucleus envelope" (The UniProt, 2017). Yeast phosphopeptides were identified from the ISB Library of the PeptideAtlas Project (Desiere, Deutsch et al., 2006) "The PeptideAtlas Project", Nucleic Acids Research 34, D655-D658]. Custom Python scripts were used to identify exact matches between phosphopeptides of the yeast PeptideAtlas and the protein sequences of the UniProt entries filtered by localization.

Table S1: PKA substrate on the nuclear envelop/endoplasmic reticulum

Name	Systematic Name	Proposed Function
ARE2	YNR019W	Acyl-coenzyme A: cholesterol acyl transferase-Related Enzyme
ECM3	YOR092W	ExtraCellular Mutant
ESBP6	YNL125C	Protein with similarity to monocarboxylate permeases
FLC3	YGL139W	FLavin Carrier
MPS2	YGL075C	MonoPolar Spindle
NUP2	YLR335W	NUclear Pore
NUP53	YMR153W	NUclear Pore
ORM1	YGR038W	Protein that mediates sphingolipid homeostasis
ORM2	YLR350W	Protein that mediates sphingolipid homeostasis
PAH1	YMR165C	Phosphatidic Acid phosphor Hydrolase
PEX19	YDL065C	PEroXisome related
PGA2	YNL149C	Processing of Gas1p and ALP
SEC63	YOR254C	SECretory
SHE3	YBR130C	Swi5p-dependent HO Expression
TRM1	YDR120C	tRNA Methyltransferase
UBX2	YML013W	UBiquitin regulatory X
YSP2	YDR326C	Yeast Suicide Protein
ZRG17	YNR039C	Zinc Regulated Gene

Table S2: Strains used in this study

Strain	**Designation**	**Genotype**	**Source**
YAS2086	Δ*bcy1*	*MAT a ade2-101oc his3-Δ200 leu2-Δ1 lys2-801am trp-Δ63 ura3-52 BCY1::LEU2 (K. lactis)*	this study
YAS4178	Δ*eap1*	*MAT a ade2-101oc his3-Δ200 leu2-Δ1 lys2-801am trp-Δ63 ura3-52 EAP1::LEU2 (K. lactis)*	this study
YAS2597	Δ*khd1*	*MAT a ade2-101oc his3-Δ200 leu2-Δ1 lys2-801am trp-Δ63 ura3-52 KHD1::URA3*	this study
YAS4194	Δ*scp160*	*MAT a ade2-101oc his3-Δ200 leu2-Δ1 lys2-801am trp-Δ63 ura3-52 SCP160::LEU2 (K. lactis)*	this study
YAS4188	Δ*vts1*	*MAT a ade2-101oc his3-Δ200 leu2-Δ1 lys2-801am trp-Δ63 ura3-52 VTS1::HIS3*	this study
YAS4197	Δ*xrn1*	*MAT a ade2-101oc his3-Δ200 leu2-Δ1 lys2-801am trp-Δ63 ura3-52 XRN1::LEU2 (K. lactis)*	this study

YAS4295	*ADH-HXT2*	*MAT a ade2-101oc his3-Δ200 leu2-Δ1 lys2-801am trp-Δ63 ura3-52 HXT2::natNT2-pADH1-HXT2*	this study
YAS4267	*GPD-HXT2*	*MAT a ade2-101oc his3-Δ200 leu2-Δ1 lys2-801am trp-Δ63 ura3-52 HXT2::natNT2-pGPD1-HXT2*	this study
YPH499	WT	*MAT a ade2-101oc his3-Δ200 leu2-Δ1 lys2-801am trp-Δ63 ura3-52*	Sikorski and Hieter, 1989
YAS5481	Δ*kar9*	*MAT a ade2-101oc his3-Δ200 leu2-Δ1 lys2-801am trp-Δ63 ura3-52 KAR9::LEU2*	this study
YAS5479	Δ*bim1*	*MAT a ade2-101oc his3-Δ200 leu2-Δ1 lys2-801am trp-Δ63 ura3-52 BIM1::URA3*	this study
YAS5482	Δ*gpr1*Δ*gpa2*	*MAT a ade2-101oc his3-Δ200 leu2-Δ1 lys2-801am trp-Δ63 ura3-52 GPR1::LEU2 GPA2::URA3*	this study
YAS5476	Δ*nup2*	*MAT a ade2-101oc his3-Δ200 leu2-Δ1 lys2-801am trp-Δ63 ura3-52 NUP2::URA3*	this study
YAS5480	Δ*mlp1*Δ*mlp2*	*MAT a ade2-101oc his3-Δ200 leu2-Δ1 lys2-801am trp-Δ63 ura3-52 MLP1::LEU2 MLP2::URA3*	this study
YAS5457	Δ*asc1*	*MAT a ade2-101oc his3-Δ200 leu2-Δ1 lys2-801am trp-Δ63 ura3-52 ASC1::LEU2*	this study
YAS5459	Δ*bfr1*	*MAT a ade2-101oc his3-Δ200 leu2-Δ1 lys2-801am trp-Δ63 ura3-52 BFR1::URA3*	this study
YAS5228	Δ*nup53*Δ*nup59*	*MAT a ade2-101oc his3-Δ200 leu2-Δ1 lys2-801am trp-Δ63 ura3-52 NUP53::URA3 NUP59::LEU2 (K. lactis)*	this study
Y1426	WT	*MAT a ade2 his3-Δ1 leu2,3,-112 trp-289 ura3-52 cyh2*	Jiang et al, 1998
Y1857	ras2^{318S}	*MAT a ade2 his3-Δ1 leu2,3,-112 trp-289 ura3-52 cyh2 RAS1::HIS3 RAS2::ras2^{318S}*	Jiang et al, 1998
EBY.VW1000	HXT-null	*MAT α leu2-3,112 ura3-52 trp1-289 his3-v1 MAL2-8c SUC2 hxt17Δ hxt13Δ::loxP hxt15Δ::loxP hxt16Δ::loxP hxt14Δ::loxP hxt12Δ::loxP hxt9Δ::loxP hxt11Δ::loxP hxt10Δ::loxP hxt8Δ::loxP hxt514Δ::loxP hxt2Δ::loxP hxt367Δ::loxP gal2Δ*	Wieczorke et al, 1999
YAS5236	HXT2-only	*MAT α leu2-3,112 ura3-52 trp1-289 his3-v1 MAL2-8c SUC2 hxt17Δ hxt13Δ::loxP hxt15Δ::loxP hxt16Δ::loxP hxt14Δ::loxP hxt12Δ::loxP hxt9Δ::loxP hxt11Δ::loxP hxt10Δ::loxP hxt8Δ::loxP hxt514Δ::loxP hxt2Δ::loxP hxt367Δ::loxP gal2Δ* with plasmid #1736	this study

YAS5237	HXT1-only	*MAT α leu2-3,112 ura3-52 trp1-289 his3-v1 MAL2-8c SUC2 hxt17Δ hxt13Δ::loxP hxt15Δ::loxP hxt16Δ::loxP hxt14Δ::loxP hxt12Δ::loxP hxt9Δ::loxP hxt11Δ::loxP hxt10Δ::loxP hxt8Δ::loxP hxt514Δ::loxP hxt2Δ::loxP hxt367Δ::loxP gal2Δ* with plasmid #2012	this study
YAS5238	HXT3-only	*MAT α leu2-3,112 ura3-52 trp1-289 his3-v1 MAL2-8c SUC2 hxt17Δ hxt13Δ::loxP hxt15Δ::loxP hxt16Δ::loxP hxt14Δ::loxP hxt12Δ::loxP hxt9Δ::loxP hxt11Δ::loxP hxt10Δ::loxP hxt8Δ::loxP hxt514Δ::loxP hxt2Δ::loxP hxt367Δ::loxP gal2Δ* with plasmid #2013	this study
YAS5239	HXT4-only	*MAT α leu2-3,112 ura3-52 trp1-289 his3-v1 MAL2-8c SUC2 hxt17Δ hxt13Δ::loxP hxt15Δ::loxP hxt16Δ::loxP hxt14Δ::loxP hxt12Δ::loxP hxt9Δ::loxP hxt11Δ::loxP hxt10Δ::loxP hxt8Δ::loxP hxt514Δ::loxP hxt2Δ::loxP hxt367Δ::loxP gal2Δ* with plasmid #2014	this study
BHY116	Δ*srp54*	*MAT α ade2 his3 lys2 trp1 ura3 SRP54::LYS2*	Gift from S. Rospert
YAS5235	HXT2-MS2/ Nup84-3xmCherry	*MAT a ade2-101oc his3-Δ200 leu2-Δ1 lys2-801am trp-Δ63 ura3-52 HXT2::HXT2-24xMS2 NUP84::NUP84-3xmCherry* with plasmid pET296-YcpLac111 CYC1p-MCP-NLS-2xyeGFP	this study
YAS5234	NUP84-HA	*MAT a ade2-101oc his3-Δ200 leu2-Δ1 lys2-801am trp-Δ63 ura3-52 NUP84::NUP84-3xHA*	this study
YAS5231	HXT2-3xyeGFP	*MAT a ade2-101oc his3-Δ200 leu2-Δ1 lys2-801am trp-Δ63 ura3-52 HXT2::HXT2-3xGFP*	this study
YAS5230	Scp160 Tet-Off	*MAT a ade2-101oc his3-Δ200 leu2-Δ1 lys2-801am trp-Δ63 ura3-52 SCP160::URA3* with plasmid pCM182-SCP160 (Hirschmann et al, 2014)	this study
YAS5240	SCP160-ΔC2	*MAT a ade2-101oc his3-Δ200 leu2-Δ1 lys2-801am trp-Δ63 ura3-52 SCP160::SCP160-ΔC2*	this study
YAS5241	SCP160-ΔC4	*MAT a ade2-101oc his3-Δ200 leu2-Δ1 lys2-801am trp-Δ63 ura3-52 SCP160::SCP160-ΔC4*	this study

Table S3: Primers used in this study

Primer	Designation	Sequence	Purpose
TS004	BIM1 delta test	CTGAATGAACTTGAAGACCA	Deletion
TS005	BIM1 S1	GACTCAAAAGCAAGGATAATATTCCACCAAATCAG GGACGAAGCAcagctgaagcttcgtacgc	Deletion
TS006	BIM1 S2	AAAATAATACATATTCGAAAACAATACTGCTTTTTAGT TCTCAACgcataggccactagtggatctg	Deletion
TS027	GPA2 delta test	ATGAAGTCCGCCAATTCAGT	Deletion
TS028	GPA2 S1	CCTTATTGTTACAGCACAAATCACGCGTATTTTCAA GCAAATATCcagctgaagcttcgtacgc	Deletion
TS029	GPA2 S2	AGGGGAGAAGAGGCATGCAGTTTTGTCTCTGTTTT AGCTGTGCATgcataggccactagtggatctg	Deletion
TS030	GPR1 delta test	TCTACATCCCTTTCTCTACG	Deletion
TS031	GPR1 S1	AAGTGATCCGAAGTGTGACGAATAAAGCAAACTCT CCAACTCAAAcagctgaagcttcgtacgc	Deletion
TS032	GPR1 S2	TTACGTTCCTTACTTTCCATTTTCAAACATCGCGATA CAAAAACTgcataggccactagtggatctg	Deletion
TS038	HXT1 Seq P1	ATTCCATCTGGGGTCTCATG	Sequencing
TS039	HXT1 Seq P2	GGTGAAGGTCAAGAACTAGC	Sequencing
TS040	HXT1 XbaI rev	ggtggtTCTAGATCTTTACTGCTTCACCTCTTATCAA	Plasmid cloning
TS041	HXT1 XmaI fwd	ggtggtCCCGGGGCATTGAGTCAAAAGTTTTTCCGA A	Plasmid cloning
TS042	HXT2 3xGFP pYM fwd	AAATCTGGTAGCTGGATCTCAAAAGAAAAAAGAGT TTCCGAGGAACGTACGCTGCAGGTCGAC	C-terminal tagging
TS043	HXT2 3xGFP pYM fwd w stop	TCTGGTAGCTGGATCTCAAAAGAAAAAAGAGTTTC CGAGGAATAACGTACGCTGCAGGTCGAC	C-terminal tagging
TS044	HXT2 3xGFP pYM rev	AGCCATTAGCCTTAAAAAAATCAGTGCTAGTTTAAG TATAATCTCgcataggccactagtggatctg	C-terminal tagging
TS052	HXT2 MS2 tag fwd	TCTGGTAGCTGGATCTCAAAAGAAAAAAGAGTTTC CGAGGAATAACGCTCTAGAACTAGTGGAT	C-terminal tagging
TS053	HXT2 MS2 tag rev	AGCCATTAGCCTTAAAAAAATCAGTGCTAGTTTAAG TATAATCTCCATAGGCCACTAGTGGATCTG	C-terminal tagging
TS058	HXT3 Seq P1	CGCTTGGGGGTTGCATAT	Sequencing
TS059	HXT3 Seq P2	CTCGCCGATGGTATGAAGTT	Sequencing
TS060	HXT3 XbaI rev	ggtggtTCTAGAGTAAAGAAACCTGCTTAGAGATTCT	Plasmid cloning
TS061	HXT3 XmaI fwd	ggtggtCCCGGGTCTTAGCTATATTCTTCCAGCTTCG	Plasmid cloning
TS064	HXT4 XhoI fwd	ggtggtCTCGAGCCCCCCGGTTTTTTTTCCATGGGG C	Plasmid cloning
TS065	HXT4 XmaI rev	ggtggtCCCGGGCGGGTTGGTCAGTATATTTTGTATT	Plasmid cloning
TS069	KAR9 delta test	AAGATCACACCACAACCGTG	Deletion
TS070	KAR9 S1	CGAATCTTTGTCTGTAACAGCCTTAAAGATTTCAGT AGCACTGCCcagctgaagcttcgtacgc	Deletion
TS071	KAR9 S2	GGGAGGATATATAAAAATGTATAAGTATACAGTTTTAG GTTAGTAgcataggccactagtggatctg	Deletion
TS077	MLP1 delta test	CTTGACATGACAACAAGAGT	Deletion
TS078	MLP1 S1	TCGCCGAAGCTACACAAATAGTCAGTAACGCCACG TTTTAGGATAcagctgaagcttcgtacgc	Deletion
TS079	MLP1 S2	GAAAAAGGTTTAGTTTGTATTGATCCCTTGTTTTTAC TATCTCCTgcataggccactagtggatctg	Deletion

TS080	MLP2 delta test	GTACGGATGTAATAAACTCA	Deletion
TS081	MLP2 S1	AAAGAAATTTAAGGCGAAAGAACACTGGGCGGAA GCAAACCGGCAcagctgaagcttcgtacgc	Deletion
TS082	MLP2 S2	ATGTAGATGTTTCATATTTATATAATTACATTGTTTAATA TTACAgcataggccactagtggatctg	Deletion
TS083	MLP2 S3	AAAAAGGTTAAAGAGAGTCCAGCAAATGATCAAGC TTCCAACGAGCGTACGCTGCAGGTCGAC	Deletion
TS096	NUP2 delta test	ATTTGGTAAGGTATGAAATA	Deletion
TS097	NUP2 S1	TTCATACAAGTCCTTGTTAAGTAACTCAAAAAAATCA TTAACGAGcagctgaagcttcgtacgc	Deletion
TS098	NUP2 S2	ATATGAGGGTTCTATTCTATTTAAAATTGTTAACTGTA TTTACTCgcataggccactagtggatctg	Deletion
TS099	NUP53 delta test	TGATCAATATAAAGAAGCTA	Deletion
TS100	NUP53 S1	CTAGCCCAAATTCTCTCTGCACTCTCAATAACATAG CTTTTTAAAcagctgaagcttcgtacgc	Deletion
TS101	NUP53 S2	GCTGGAATCGCACCAAAGCACTACATTTGGGGGTA AGGTTTTTCAgcataggccactagtggatctg	Deletion
TS102	NUP59 delta test	TCATCTGGGATATGTCAAGA	Deletion
TS103	NUP59 S1	TTTTTTTTTTCTCTGTAACCTGAAAACAAGGAACGG CAAATTAAAcagctgaagcttcgtacgc	Deletion
TS104	NUP59 S2	TGAAGTATTGTAAATGTTCATGAATAATTAGCTGGAC GATTTCTGgcataggccactagtggatctg	Deletion
TS105	NUP84 S2	GCTGTTTACTTAAAATATAAACTTATTCTGCAATACAT TAATTGAgcataggccactagtggatctg	C-terminal tagging
TS106	NUP84 S3	AAAGAGTATCTGGATCTCGTTGCTCGCACAGCAAC CCTTTCGAACCGTACGCTGCAGGTCGAC	C-terminal tagging
TS107	NUP84 tag test	GCGGATTCGGCAGATTATGA	C-terminal tagging
SH_38	Scp160_P1	GCTCATTTTCGCGAATTGTT	delta test forward
SH_238	HXT4_P1	GTTGCTTTCGGTGGTTTTGT	FISH-forward
SH_239	HXT4_P2	TAATACGACTCACTATAGGGAGCGACAGCAGTGAA AACG	FISH-reverse_T7 (850bp)
SH_240	HXT2_P1	GAGAGTGCCTTTGGGTTTGA	FISH-forward
SH_241	HXT2_P2	TAATACGACTCACTATAGGGAGCAGCAATAGCCATA GCA	FISH-reverse_T7 (701bp)
SH_384	Scp160_P2	GCTTAAAATATACTTCCCACACCCCCTCCTTCCATT ATAACTGCAcagctgaagcttcgtacgc	S1 primer
SH_385	Scp160_P3	AAAGCCAAAATCTATATTGAAAAAAATTGGTTTCAAA GAGCTTGTgcataggccactagtggatctg	S2 primer
SH_571	Hxt1_P1	GTTGCTTTCGGTGGTTTCAT	FISH-forward
SH_572	Hxt1_P2	TAATACGACTCACTATAGGGAGTACCAGCGGCTCT CATT	FISH-reverse_T7 (850bp)
SH_577	Hxt3_P1	TTAACAAGGTTGCCCCAGAC	FISH-forward
SH_578	Hxt3_P2	TAATACGACTCACTATAGGGAGTGAGATGTTGGAAC CCA	FISH-reverse_T7 (850bp)
SH_695	Hxt1_RT_P1	ACTTCTTCTCCACTTGTTGTTCT	qPCR
SH_696	Hxt1_RT_P2	CAGCAGACCATACCGACAG	qPCR
SH_699	Hxt2_RT_P1	TAGGTATAGTCAACTTCGCATCCA	qPCR
SH_700	Hxt2_RT_P2	ACACCGACAGTAGAGAAGATAACA	qPCR
SH_793	Hxt3_RT_P1	GGTAATGAACATGCCTGAAGA	qPCR

SH_794	Hxt3_RT_P2	CCTGTATTTGGGTTGGTAAGT	qPCR
SH_795	Hxt4_RT_P1	TCAAGAGGATACAGCAGTC	qPCR
SH_796	Hxt4_RT_P2	CGTAGTTATTAGATTCTTCGTGAT	qPCR

Table S4: Plasmids used in this study

Plasmid	Description	Source
pUG72	loxP-URA3 cassette	J. Hegemann
pUG73	loxP-LEU2 cassette	J. Hegemann
pSH63	Cre-recombinase, *TRP1*	J. Hegemann
pYM12	yeGFP-kanMX4-cassette	E. Schiebel
pYM1	3HA-hphNT1-cassette	M. Knop
pYM26	yeGFP-kanMX4-cassette	M. Knop
pMS449	Scp160 ΔC2, *TRP1*	M.Seedorf
pMS450	Scp160 ΔC4, *TRP1*	M.Seedorf
pRS416/H1	HXT1 gene under native promotor, *URA3*	This study
pRS416/H3	HXT3 gene under native promotor, *URA3*	This study
pRS416/H4	HXT4 gene under native promotor, *URA3*	This study
02+1	HXT2 gene under native promotor, *URA3*	This study
pCM79	pFA6a-3mCherry-hnhNTI	M. Knop
RJP1463	pCM182-Scp160 Tet-off	R.P. Jansen

Acknowledgements

We thank J. Broach, E. Boles, S. Rospert, R.P. Jansen, M. Seedorf, R. Singer, and E. Schiebel for strains and reagents. We are grateful to E. Schiebel for discussions, and to I.G. Macara and K. Weis for critical comments on the manuscript. This work was supported by the Human Frontiers Science Program (RG0031/2009), the Swiss National Science Foundation (310030B-163480) and the University of Basel to AS and an EMBO longterm-fellowship (ALTF 289-2010) to SH.

The authors declare no competing financial interests.

References

Adams AE, Pringle JR (1991) Staining of actin with fluorochrome-conjugated phalloidin. *Methods Enzymol* 194: 729-31

Adekola K, Rosen ST, Shanmugam M (2012) Glucose transporters in cancer metabolism. *Curr Opin Oncol* 24: 650-4

Bagnat M, Simons K (2002) Cell surface polarization during yeast mating. *Proc Natl Acad Sci U S A* 99: 14183-8

Barron CC, Bilan PJ, Tsakiridis T, Tsiani E (2016) Facilitative glucose transporters: Implications for cancer detection, prognosis and treatment. *Metabolism* 65: 124-39

Baum S, Bittins M, Frey S, Seedorf M (2004) Asc1p, a WD40-domain containing adaptor protein, is required for the interaction of the RNA-binding protein Scp160p with polysomes. *Biochem J* 380: 823-30

Bisson LF, Fan Q, Walker GA (2016) Sugar and Glycerol Transport in Saccharomyces cerevisiae. *Adv Exp Med Biol* 892: 125-168

Calvo MB, Figueroa A, Pulido EG, Campelo RG, Aparicio LA (2010) Potential role of sugar transporters in cancer and their relationship with anticancer therapy. *Int J Endocrinol* 2010

Cepeda-Garcia C, Delgehyr N, Juanes Ortiz MA, ten Hoopen R, Zhiteneva A, Segal M (2010) Actin-mediated delivery of astral microtubules instructs Kar9p asymmetric loading to the bud-ward spindle pole. *Mol Biol Cell* 21: 2685-95

Chen YH, Kratchmarov R, Lin WW, Rothman NJ, Yen B, Adams WC, Nish SA, Rathmell JC, Reiner SL (2018) Asymmetric PI3K Activity in Lymphocytes Organized by a PI3K-Mediated Polarity Pathway. *Cell Rep* 22: 860-868

Cho RJ, Campbell MJ, Winzeler EA, Steinmetz L, Conway A, Wodicka L, Wolfsberg TG, Gabrielian AE, Landsman D, Lockhart DJ, Davis RW (1998) A genome-wide transcriptional analysis of the mitotic cell cycle. *Mol Cell* 2: 65-73

Desiere F, Deutsch EW, King NL, Nesvizhskii AI, Mallick P, Eng J, Chen S, Eddes J, Loevenich SN, Aebersold R (2006) The PeptideAtlas project. *Nucleic Acids Res* 34: D655-8

Estrada AF, Muruganandam G, Prescianotto-Baschong C, Spang A (2015) The ArfGAP2/3 Glo3 and ergosterol collaborate in transport of a subset of cargoes. *Biol Open* 4: 792-802

Gueldener U, Heinisch J, Koehler GJ, Voss D, Hegemann JH (2002) A second set of loxP marker cassettes for Cre-mediated multiple gene knockouts in budding yeast. *Nucleic Acids Res* 30: e23

Hann BC, Walter P (1991) The signal recognition particle in S. cerevisiae. *Cell* 67: 131-44

Hirschmann WD, Westendorf H, Mayer A, Cannarozzi G, Cramer P, Jansen RP (2014) Scp160p is required for translational efficiency of codon-optimized mRNAs in yeast. *Nucleic Acids Res* 42: 4043-55

Hovsepian J, Defenouillere Q, Albanese V, Vachova L, Garcia C, Palkova Z, Leon S (2017) Multilevel regulation of an alpha-arrestin by glucose depletion controls hexose transporter endocytosis. *J Cell Biol* 216: 1811-1831

Huls D, Storchova Z, Niessing D (2012) Post-translational modifications regulate assembly of early spindle orientation complex in yeast. *J Biol Chem* 287: 16238-45

Janke C, Magiera MM, Rathfelder N, Taxis C, Reber S, Maekawa H, Moreno-Borchart A, Doenges G, Schwob E, Schiebel E, Knop M (2004) A versatile toolbox for PCR-based tagging of yeast genes: new fluorescent proteins, more markers and promoter substitution cassettes. *Yeast* 21: 947-62

Jansen RP, Niessing D, Baumann S, Feldbrugge M (2014) mRNA transport meets membrane traffic. *Trends Genet* 30: 408-17

Jiang Y, Davis C, Broach JR (1998) Efficient transition to growth on fermentable carbon sources in Saccharomyces cerevisiae requires signaling through the Ras pathway. *EMBO J* 17: 6942-51

Juanes MA, Twyman H, Tunnacliffe E, Guo Z, ten Hoopen R, Segal M (2013) Spindle pole body history intrinsically links pole identity with asymmetric fate in budding yeast. *Curr Biol* 23: 1310-9

Kaiser CM, S; Mitchell, A. (1994) *Methods in yeast genetics: A Cold Spring Harbor Laboratory Course Manual*. Cold Spring Harbor Laboratory Press,

Karnieli E, Zarnowski MJ, Hissin PJ, Simpson IA, Salans LB, Cushman SW (1981) Insulin-stimulated translocation of glucose transport systems in the isolated rat adipose cell. Time course, reversal, insulin concentration dependency, and relationship to glucose transport activity. *J Biol Chem* 256: 4772-7

Kasahara T, Ishiguro M, Kasahara M (2006) Eight amino acid residues in transmembrane segments of yeast glucose transporter Hxt2 are required for high affinity transport. *J Biol Chem* 281: 18532-8

Kilchert C, Spang A (2011) Cotranslational transport of ABP140 mRNA to the distal pole of S. cerevisiae. *EMBO J* 30: 3567-80

Kim JH, Johnston M (2006) Two glucose-sensing pathways converge on Rgt1 to regulate expression of glucose transporter genes in Saccharomyces cerevisiae. *J Biol Chem* 281: 26144-9

Knop M, Siegers K, Pereira G, Zachariae W, Winsor B, Nasmyth K, Schiebel E (1999) *Epitope tagging of yeast genes using a PCR-based strategy: more tags and improved practical routines*.

Lang BD, Li A, Black-Brewster HD, Fridovich-Keil JL (2001) The brefeldin A resistance protein Bfr1p is a component of polyribosome-associated mRNP complexes in yeast. *Nucleic Acids Res* 29: 2567-74

Lecuyer E, Yoshida H, Parthasarathy N, Alm C, Babak T, Cerovina T, Hughes TR, Tomancak P, Krause HM (2007) Global analysis of mRNA localization reveals a prominent role in organizing cellular architecture and function. *Cell* 131: 174-87

Lee L, Tirnauer JS, Li J, Schuyler SC, Liu JY, Pellman D (2000) Positioning of the mitotic spindle by a cortical-microtubule capture mechanism. *Science* 287: 2260-2

Liakopoulos D, Kusch J, Grava S, Vogel J, Barral Y (2003) Asymmetric loading of Kar9 onto spindle poles and microtubules ensures proper spindle alignment. *Cell* 112: 561-74

Llopis-Torregrosa V, Ferri-Blazquez A, Adam-Artigues A, Deffontaines E, van Heusden GP, Yenush L (2016) Regulation of the Yeast Hxt6 Hexose Transporter by the Rod1 alpha-Arrestin, the Snf1 Protein Kinase, and the Bmh2 14-3-3 Protein. *J Biol Chem* 291: 14973-85

Maekawa H, Schiebel E (2004) Cdk1-Clb4 controls the interaction of astral microtubule plus ends with subdomains of the daughter cell cortex. *Genes Dev* 18: 1709-24

Marbouty M, Ermont C, Dujon B, Richard GF, Koszul R (2014) Purification of G1 daughter cells from different Saccharomycetes species through an optimized centrifugal elutriation procedure. *Yeast* 31: 159-66

Martin S, Millar CA, Lyttle CT, Meerloo T, Marsh BJ, Gould GW, James DE (2000) Effects of insulin on intracellular GLUT4 vesicles in adipocytes: evidence for a secretory mode of regulation. *J Cell Sci* 113 Pt 19: 3427-38

Medioni C, Mowry K, Besse F (2012) Principles and roles of mRNA localization in animal development. *Development* 139: 3263-76

Meneses AM, Medina RA, Kato S, Pinto M, Jaque MP, Lizama I, Garcia Mde L, Nualart F, Owen GI (2008) Regulation of GLUT3 and glucose uptake by the cAMP signalling pathway in the breast cancer cell line ZR-75. *J Cell Physiol* 214: 110-6

Mili S, Moissoglu K, Macara IG (2008) Genome-wide screen reveals APC-associated RNAs enriched in cell protrusions. *Nature* 453: 115-9

Miller RK, Matheos D, Rose MD (1999) The cortical localization of the microtubule orientation protein, Kar9p, is dependent upon actin and proteins required for polarization. *J Cell Biol* 144: 963-75

Miller RK, Rose MD (1998) Kar9p is a novel cortical protein required for cytoplasmic microtubule orientation in yeast. *J Cell Biol* 140: 377-90

Muhlrad D, Decker CJ, Parker R (1994) Deadenylation of the unstable mRNA encoded by the yeast MFA2 gene leads to decapping followed by 5'-->3' digestion of the transcript. *Genes Dev* 8: 855-66

Niepel M, Strambio-de-Castillia C, Fasolo J, Chait BT, Rout MP (2005) The nuclear pore complex-associated protein, Mlp2p, binds to the yeast spindle pole body and promotes its efficient assembly. *J Cell Biol* 170: 225-35

O'Donnell AF, McCartney RR, Chandrashekarappa DG, Zhang BB, Thorner J, Schmidt MC (2015) 2-Deoxyglucose impairs Saccharomyces cerevisiae growth by stimulating Snf1-regulated and alpha-arrestin-mediated trafficking of hexose transporters 1 and 3. *Mol Cell Biol* 35: 939-55

Parton RM, Davidson A, Davis I, Weil TT (2014) Subcellular mRNA localisation at a glance. *J Cell Sci* 127: 2127-33

Pereira G, Tanaka TU, Nasmyth K, Schiebel E (2001) Modes of spindle pole body inheritance and segregation of the Bfa1p-Bub2p checkpoint protein complex. *EMBO J* 20: 6359-70

Perez M, Luyten K, Michel R, Riou C, Blondin B (2005) Analysis of Saccharomyces cerevisiae hexose carrier expression during wine fermentation: both low- and high-affinity Hxt transporters are expressed. *FEMS Yeast Res* 5: 351-61

Phansalkar NM, Sumit; Sabale A.; Joshi, M. (2011) Adaptive Local Thresholding for Detection of Nuclei in Diversely Stained Cytology Images. In IEEE International Conference on Cummunications and Signal Processing (ICCSP), pp 218-222. Calicut, India: IEEE

Pramila T, Wu W, Miles S, Noble WS, Breeden LL (2006) The Forkhead transcription factor Hcm1 regulates chromosome segregation genes and fills the S-phase gap in the transcriptional circuitry of the cell cycle. *Genes Dev* 20: 2266-78

Reifenberger E, Boles E, Ciriacy M (1997) Kinetic characterization of individual hexose transporters of Saccharomyces cerevisiae and their relation to the triggering mechanisms of glucose repression. *Eur J Biochem* 245: 324-33

Roy A, Kim YB, Cho KH, Kim JH (2014) Glucose starvation-induced turnover of the yeast glucose transporter Hxt1. *Biochim Biophys Acta* 1840: 2878-85

Ruthnick D, Neuner A, Dietrich F, Kirrmaier D, Engel U, Knop M, Schiebel E (2017) Characterization of spindle pole body duplication reveals a regulatory role for nuclear pore complexes. *J Cell Biol* 216: 2425-2442

Sakashita M, Aoyama N, Minami R, Maekawa S, Kuroda K, Shirasaka D, Ichihara T, Kuroda Y, Maeda S, Kasuga M (2001) Glut1 expression in T1 and T2 stage colorectal carcinomas: its relationship to clinicopathological features. *Eur J Cancer* 37: 204-9

Schindelin J, Arganda-Carreras I, Frise E, Kaynig V, Longair M, Pietzsch T, Preibisch S, Rueden C, Saalfeld S, Schmid B, Tinevez JY, White DJ, Hartenstein V, Eliceiri K, Tomancak P, Cardona A (2012) Fiji: an open-source platform for biological-image analysis. *Nat Methods* 9: 676-82

Schmitt ME, Brown TA, Trumpower BL (1990) A rapid and simple method for preparation of RNA from Saccharomyces cerevisiae. *Nucleic Acids Res* 18: 3091-2

Sezen B, Seedorf M, Schiebel E (2009) The SESA network links duplication of the yeast centrosome with the protein translation machinery. *Genes Dev* 23: 1559-70

Sherman F (1991) Getting started with yeast. *Methods Enzymol* 194: 3-21

Snowdon C, van der Merwe G (2012) Regulation of Hxt3 and Hxt7 turnover converges on the Vid30 complex and requires inactivation of the Ras/cAMP/PKA pathway in Saccharomyces cerevisiae. *PLoS One* 7: e50458

Spellman PT, Sherlock G, Zhang MQ, Iyer VR, Anders K, Eisen MB, Brown PO, Botstein D, Futcher B (1998) Comprehensive identification of cell cycle-regulated genes of the yeast Saccharomyces cerevisiae by microarray hybridization. *Mol Biol Cell* 9: 3273-97

Stracka D, Jozefczuk S, Rudroff F, Sauer U, Hall MN (2014) Nitrogen source activates TOR (target of rapamycin) complex 1 via glutamine and independently of Gtr/Rag proteins. *J Biol Chem* 289: 25010-20

Suresh S, Markossian S, Osmani AH, Osmani SA (2017) Mitotic nuclear pore complex segregation involves Nup2 in Aspergillus nidulans. *J Cell Biol* 216: 2813-2826

Takizawa PA, DeRisi JL, Wilhelm JE, Vale RD (2000) Plasma membrane compartmentalization in yeast by messenger RNA transport and a septin diffusion barrier. *Science* 290: 341-4

Takizawa PA, Sil A, Swedlow JR, Herskowitz I, Vale RD (1997) Actin-dependent localization of an RNA encoding a cell-fate determinant in yeast. *Nature* 389: 90-3

The UniProt C (2017) UniProt: the universal protein knowledgebase. *Nucleic Acids Res* 45: D158-D169

Tutucci E, Vera M, Biswas J, Garcia J, Parker R, Singer RH (2018) An improved MS2 system for accurate reporting of the mRNA life cycle. *Nat Methods* 15: 81-89

Walther TC, Brickner JH, Aguilar PS, Bernales S, Pantoja C, Walter P (2006) Eisosomes mark static sites of endocytosis. *Nature* 439: 998-1003

Wang C, Schmich F, Srivatsa S, Weidner J, Beerenwinkel N, Spang A (2018) Context-dependent deposition and regulation of mRNAs in P-bodies. *Elife* 7

Weidner J, Wang C, Prescianotto-Baschong C, Estrada AF, Spang A (2014) The polysome-associated proteins Scp160 and Bfr1 prevent P body formation under normal growth conditions. *J Cell Sci* 127: 1992-2004

Wieczorke R, Krampe S, Weierstall T, Freidel K, Hollenberg CP, Boles E (1999) Concurrent knock-out of at least 20 transporter genes is required to block uptake of hexoses in Saccharomyces cerevisiae. *FEBS Lett* 464: 123-8

Winey M, Yarar D, Giddings TH, Jr., Mastronarde DN (1997) Nuclear pore complex number and distribution throughout the Saccharomyces cerevisiae cell cycle by three-dimensional reconstruction from electron micrographs of nuclear envelopes. *Mol Biol Cell* 8: 2119-32

Wintersberger U, Kuhne C, Karwan A (1995) Scp160p, a new yeast protein associated with the nuclear membrane and the endoplasmic reticulum, is necessary for maintenance of exact ploidy. *Yeast* 11: 929-44

Wong TL, Che N, Ma S (2017) Reprogramming of central carbon metabolism in cancer stem cells. *Biochim Biophys Acta* 1863: 1728-1738

Wu C, Haynes EM, Asokan SB, Simon JM, Sharpless NE, Baldwin AS, Davis IJ, Johnson GL, Bear JE (2013) Loss of Arp2/3 induces an NF-kappaB-dependent, nonautonomous effect on chemotactic signaling. *J Cell Biol* 203: 907-16

Wu H, Song C, Zhang J, Zhao J, Fu B, Mao T, Zhang Y (2017) Melatonin-mediated upregulation of GLUT1 blocks exit from pluripotency by increasing the uptake of oxidized vitamin C in mouse embryonic stem cells. *FASEB J* 31: 1731-1743

Xue Y, Batlle M, Hirsch JP (1998) GPR1 encodes a putative G protein-coupled receptor that associates with the Gpa2p Galpha subunit and functions in a Ras-independent pathway. *EMBO J* 17: 1996-2007

Youk H, van Oudenaarden A (2009) Growth landscape formed by perception and import of glucose in yeast. *Nature* 462: 875-9

Yun J, Rago C, Cheong I, Pagliarini R, Angenendt P, Rajagopalan H, Schmidt K, Willson JK, Markowitz S, Zhou S, Diaz LA, Jr., Velculescu VE, Lengauer C, Kinzler KW, Vogelstein B, Papadopoulos N (2009) Glucose deprivation contributes to the development of KRAS pathway mutations in tumor cells. *Science* 325: 1555-9

Zanolari B, Rockenbauch U, Trautwein M, Clay L, Barral Y, Spang A (2011) Transport to the plasma membrane is regulated differently early and late in the cell cycle in Saccharomyces cerevisiae. *J Cell Sci* 124: 1055-66

Zeller CE, Parnell SC, Dohlman HG (2007) The RACK1 ortholog Asc1 functions as a G-protein beta subunit coupled to glucose responsiveness in yeast. *J Biol Chem* 282: 25168-76

Zhang C, Skamagki M, Liu Z, Ananthanarayanan A, Zhao R, Li H, Kim K (2017) Biological Significance of the Suppression of Oxidative Phosphorylation in Induced Pluripotent Stem Cells. *Cell Rep* 21: 2058-2065

Zuiderveld K (1994) VII.5. - Contrast Limited Adaptive Histogram Equalization. In *Graphics Gems IV*, Heckbert PS (ed) pp 474-485. Academic Press Inc.

Figure Legends

Figure 1: The localization of both HXT2 mRNA and Hxt2 protein is cell-cycle dependent. (**A**) The distribution of the GFP-tagged Hxt2 changes during the cell division. In small and medium budded cells (white arrowhead), Hxt2 is mainly present in the membrane of the mother cell. In large budded cells, Hxt2 is distributed over the entire plasma membrane (yellow arrowhead). (**B**) *HXT2* mRNA localization correlate with that of the protein. FISH with an HXT2-specific probe. Early in the cell cycle the mRNA is predominantly found in the mother cell while it is equally distributed after MAT (**C**) Quantification of (**B**). The fluorescence intensities from mother and bud were independently measured and the ratio of the signal from the mother over the signal from the bud was calculated. Values > 1 indicate a stronger signal in the mother, < 1 a stronger signal in the bud and around 1 equal distribution. Three independent experiments with 50 mother cells and 50 buds were analyzed. Boxes represent the interquartile range from the 25th to the 75th percentile with the median. Whiskers represent the 10th and 90th percentile, respectively. (**D**) Changes of HXT2 mRNA localization appear to be independent of the cytoskeleton. Cells were either treated for 15 min with 30 mg/ml latrunculin A or with 30 mg/ml benomyl. (**E**) Quantification of (**D**) of three in dependent experiments with at least 50 cells each. Scale bars in (**A, B** and **D**) correspond to 10 µm.

Figure 2: Active Translation is important for *HXT2* mRNA release to the bud. (**A** and **B**) Inhibiting translation by either applying Cycloheximide (CHX) or Verrucarin A (VerruA) leads to the retention of *HXT2* mRNA in the mother cell after MAT. FISH of CHX or VerruA-treated cells. Chloro: chloroform; solvent control for VerruA; NT: not treated; control for CHX (**C**) CHX treatment leads to increased transcript stability. Quantitative PCR of *HXT2* mRNA in CHX-treated cells in comparison to *prt1-1* mutant cells. (**D**) The localization of *HXT2* mRNA is independent of the Signal Recognition Particle (SRP). Deletion of *SRP54* does not affect the retention in the mother cell or the equal distribution of *HXT2* mRNA. Quantification of the FISH experiments in (**A**) and (**D**) was performed as in Fig. 1C. ****: P < 0.0001 in a two-tailed, unpaired t-Test. Scale bars in (**B**) correspond to 5 µm.

Figure 3: Loss of the Scp160/Bfr1/Asc1 complex and PKA cause enrichment of HXT2 mRNA in the bud after MAT. (**A**) Deletion of *SCP160*, *ASC1*, or *BFR1* increases HXT2 mRNA signal in the bud. FISH experiment with deletions in various RNA binding proteins. (**B**) The effect of *Δscp160* on HXT2 mRNA localization is independent of its increased ploidy. Scp160 truncations that lack either the last two (ΔC2) or the last four (ΔC4) KH domains or a Tet-off *SCP160* construct, in which expression is blocked by the addition of doxycycline (Doxy) confirm the phenotype observed in (**A**). (**C**) Schematic depiction of the glucose responsiveness pathway. (**D**) Hyperactivation of PKA drives accumulation of HXT2 mRNA in the bud. Treatment of cells with forskolin (+Forsko) or using a *Δbcy1* strain, causes HXT2 mRNA to be bud-enriched. (**E**) HXT2 mRNA enrichment upon

refeeding is Ras2-dependent. Quantification of FISH experiments in (**A**, **B**, **D** and **E**) was performed as in Fig. 1C. ****: P < 0.0001; ***: P < 0.0005 in a two-tailed, unpaired t-Test.

Figure 4: HXT mRNAs are retained in the mother before MAT, but only HXT2 mRNA is enriched in the bud after MAT upon refeeding. (**A**) Table of the glucose affinity of the four most important hexose transporters. (**B**) FISH of HXT1, 3 and 4 under glucose rich conditions. White arrowheads depict cells before, yellow arrowheads cells after MAT. (**C**) Quantification of (**B**). (**D**) Hyperactive PKA promotes enrichment of all HXTs after MAT. (**E**) HXT2 mRNA is the only HXT mRNA showing enrichment in the bud after MAT upon transient PKA activation. (**C-E**) Quantification of FISH experiments performed as described in Fig. 1C. **** P < 0.0001 in a two-tailed, unpaired t-Test. (**F**) Elutriation confirms enrichment of HXT2 mRNA in daughter cells upon refeeding. Daughters and mothers were separated through elutriation. qPCR was performed to determine the relative levels of different HXTs and ASH1 mRNA in both fractions. The mean of three independent experiments is plotted; bars represent standard deviation. *: P < 0.05 in a two-tailed, unpaired t-Test. Scale bar in (**B**); 5 µm.

Figure 5: HXT2 mRNA enrichment in the bud depends on Kar9 and nuclear segregation. (**A**) RNA degradation is not essential for asymmetric HXT2 mRNA localization. FISH of wild-type and *Δxrn1* cells. (**B**) The cytoskeleton contributes to HXT2 mRNA enrichment in the bud. Cells were treated upon glucose addition with either 120 mg/ml benomyl for 15 min, 30 mg/ml latrunculin A for 30 min or 200 µM CK-666 for 30 min. HXT2 mRNA was detect by FISH. (**C**) Asymmetric loading of HXT2 mRNA onto the nuclear envelope and enrichment in the bud requires Kar9 but not Bim1 function. HXT2 mRNA FISH with Δ*bim1* and Δ*kar9* strains. Arrows point to a nucleus with HXT2 signal. (**D**) Quantification of the daughter cell enrichment from data displayed in (**C**). (**E**) Quantification of the HXT2 mRNA signal in cells with two nuclei in the mother cell from the experiment depicted in (**C**). Percentage of cells with asymmetric HXT2 mRNA staining is displayed. *: P < 0.05 in a two-tailed, unpaired t-Test. Quantification of the FISH experiments in (**A**, **B** and **D**) was performed as in Fig. 1C. ****: P < 0.0001 in a two-tailed, unpaired t-Test. Scale bars in (**C**) correspond to 5 µm.

Figure 6: NPC components aid the enrichment of HXT2 mRNA in the bud upon refeeding. (**A**) Deletion of *NUP2* and *MLP1/2* reduced HXT2 mRNA enrichment in the bud. FISH under glucose shift conditions with strains in which different NPC components were deleted. (**B**) Quantification of (**A**). Quantification was performed as in Fig. 1C. ****: P < 0.0001 in a two-tailed, unpaired t-Test. (**C**) HXT2 mRNA is on the nuclear envelope after MAT upon glucose shift. FISH-IF experiment with a probe against HXT2 mRNA and an antibody against the HA tag of the nuclear pore complex component Nup84-HA. White arrows point to HXT2 mRNA signals on the nuclear envelope. (**D**) HXT2 mRNA travels on the nuclear envelope into the bud during mitosis after glucose shift. Stills of time lapse movies. *HXT2* mRNA was visualized using the MS2-GFP system. Under glucose shift

conditions *HXT2* mRNA is mostly localized to the bud together with the nucleus. Under glucose rich conditions *HXT2* mRNA moves mostly independent of the nucleus. Cyan: Nup84-mCherry; white arrowhead: *HXT2* mRNA-MS2 + MCP-GFP. Scale bars in (**A**, **C** and **D**) correspond to 5 µm.

Figure 7: HXT2 mRNA enrichment in the bud under glucose shift conditions provides a growth advantage to daughter cells. (**A**) Schematic depiction of the growth assays. Cells expressing only one hexose transporter at a time were picked from a plate, serially diluted and plated on fresh YPD plates. (**B**) HXT2 only strains grow faster than the other HXT only strain. Growth was assessed 2-3 days after incubation at 30°C. (**C**) Workflow for the competition assay presented in (**D**). O/N cultures of HXT-only strains were diluted to the same OD_{600} and pooled. A sample was taken ('start'), the rest of the culture incubated O/N at 30°C. Cells were harvested ('end'), DNA was isolated from both samples, and the amount of *HXT* DNA was determined by qPCR. (**D**) Quantification of competition assay. qPCR with primers against either *HXT1, 2, 3* or *4* was performed. *HXT* gene abundance was normalized against actin. The results of three independent experiments are shown. Error bars represent standard deviation. Comparison of HXT-levels at the beginning and the end of growth shows that cells expressing only HXT2 outgrow other HXT-only cells in the range of 2 to 5-fold. *: $P < 0.05$ in a two-tailed, unpaired t-Test. (**E**) Daughter cells do not retain a memory of the previous stress situation encountered by their mothers. Cells were re-fed after starvation and analyzed for enrichment of HXT2 mRNA via FISH at different time points. Quantification was performed as in Fig. 1C. ****: $P < 0.0001$ in a two-tailed, unpaired t-Test. (**F**) Proposed model for the regulation of the asymmetric HXT2 mRNA distribution when cells come out of starvation or leave the quiescent state. For details, please see text.

Figure S1: (**A**) *HXT2* mRNA release from the mother cell is coupled to cell cycle progression and nuclear segregation respectively. Cells arrested in G2/M phase with nocodazole show still retention of *HXT2* mRNA in the mother even in large budded cells (arrows). Cells were treated with 15 µg/ml for 3h, subsequently fixed and mRNA was visualized by FISH. (**B**) Rhodamin-phalloidin staining. Cells were either treated with 30 µg/ml Latrunculin A (LatA) or as a solvent control with DMSO for 30 min. After fixation, actin was stained with Rhodamin-phalloidin. LatA treated cells show no actin cables or patches anymore. (**C**) Benomyl treatment leads to the depolymerization of cytoplasmic microtubules but cells are still able to segregate the nuclei. Immunofluorescence of microtubules with an antibody against α-tubulin.

Figure S2: Inhibition of transcription with 1,10-phenanthroline (1,10-Phen) hampers the enrichment of *HXT2* mRNA in the bud under glucose shift conditions but not the equal distribution under glucose rich conditions. (**A**) Cells were treated with 100 µM 1,10-phenanthroline or the solvent control ethanol (EtOH) for 1h. (**B**) Quantification of (A). (C-E) Increased transcription of *HXT2* per se does not lead to its enrichment in the bud. ****: $P < 0.0001$ in a two-tailed, unpaired t-Test (**C**) Exchanging the 5'-UTR with either the ADH- or GPD-promotor leads to the overexpression of *HXT2. Q*uantification of *HXT2* expression compared to WT with qPCR. (**D**) FISH experiments revealed that *HXT2* mRNA is still retained in the mother cell after MAT under glucose rich conditions when the native 5'-UTR is swapped for the ADH- or GPD-promotor. (**E**) Quantification of (D). ****: $P < 0.0001$ in a two-tailed, unpaired t-Test. **: $P < 0.05$ in a two-tailed, unpaired t-Test.

Figure S3: (**A**) Protein levels of Scp160 under the control of a Tet-off promotor markedly decrease when treated with 2 µg/ml Doxycycline (+Doxy) for 6h. PGK1 serves as loading control. (**B**) Deleting another component of the SESA complex does not have an influence on the localization of *HXT2* mRNA as compared to Scp160 or Asc1. (**C**) Single molecule FISH (smFISH) shows the same distribution pattern for *HXT2* mRNA under both, glucose rich and glucose shift conditions.

Figure S4: At different glucose concentrations HXT2 only cells still grow faster compared to other HXT only cells. Growth assay as described in 7A on plates with indicated glucose concentrations.

Figures

Figure 1, Stahl et al.

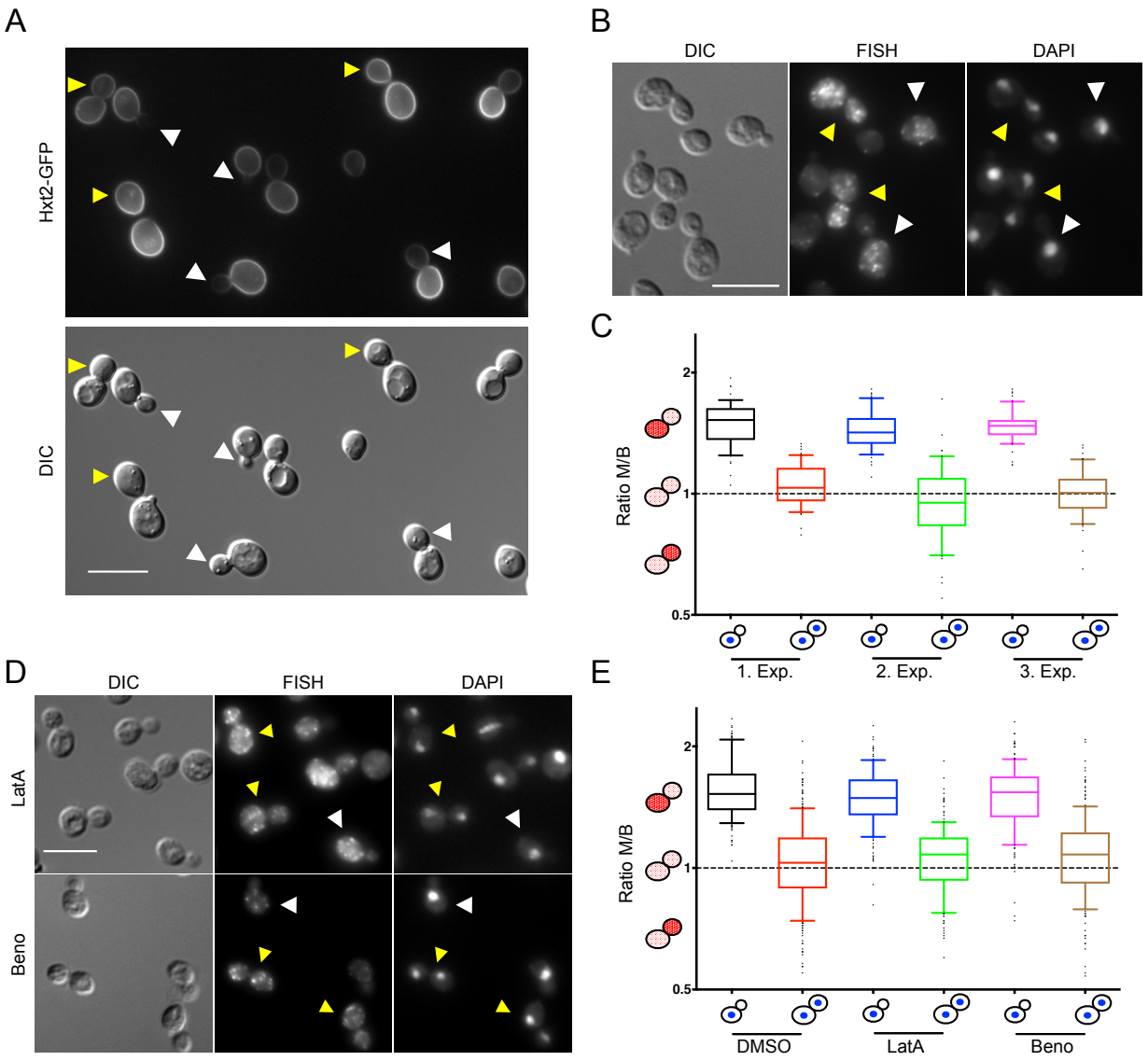

Figure 2, Stahl et al.

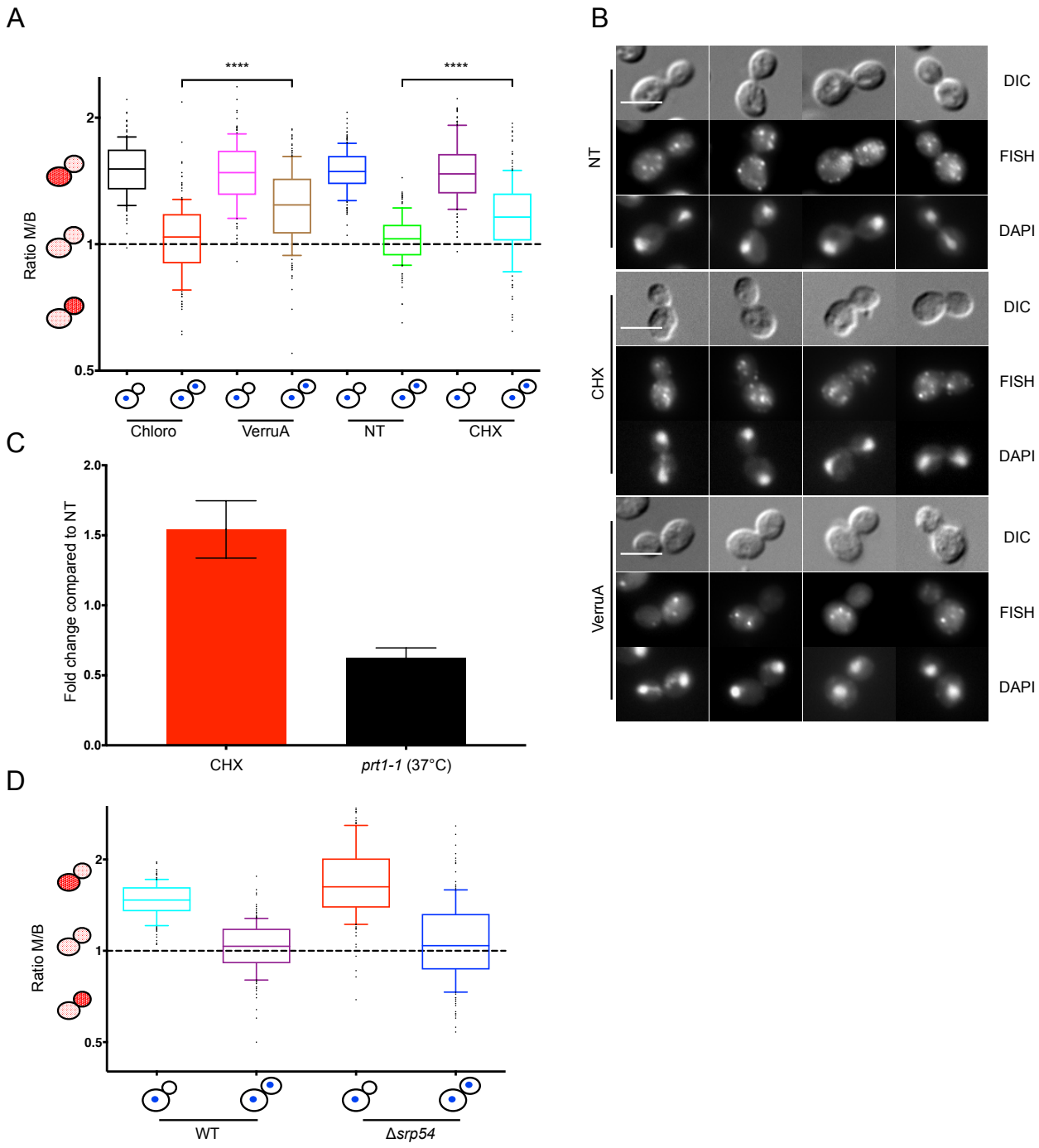

Figure 3, Stahl et al.

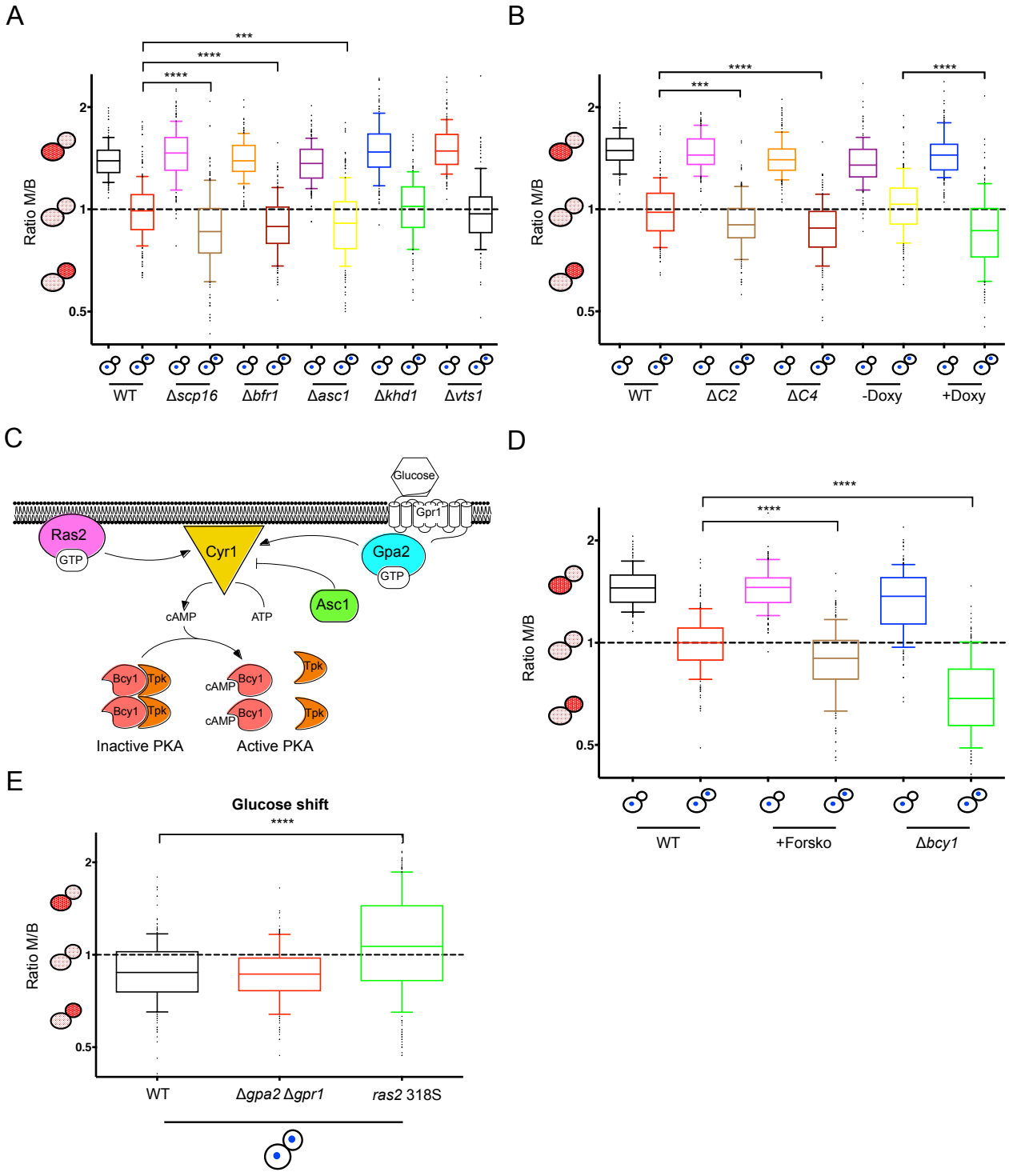

Figure 4, Stahl et al.

A

Hexose transporter	Vm	Glucose affinity
Hxt1	107 mM	low
Hxt2	1.5-2.9 mM/10-60 mM	high/moderate
Hxt3	29 mM	moderate
Hxt4	6.2 mM	high

B

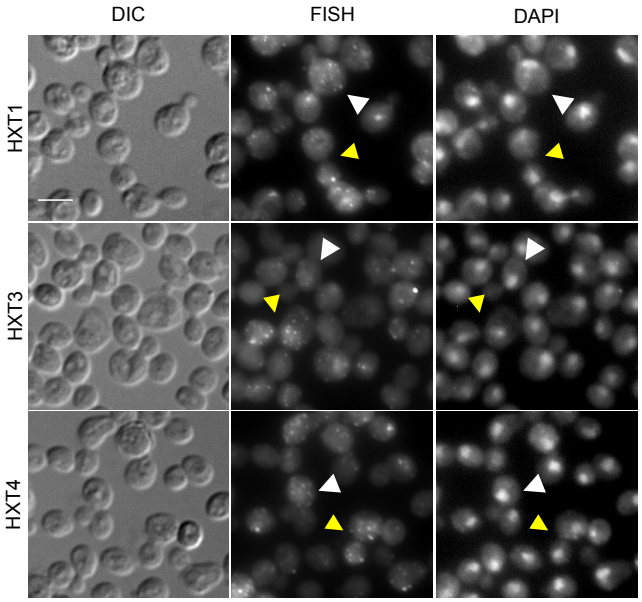

C

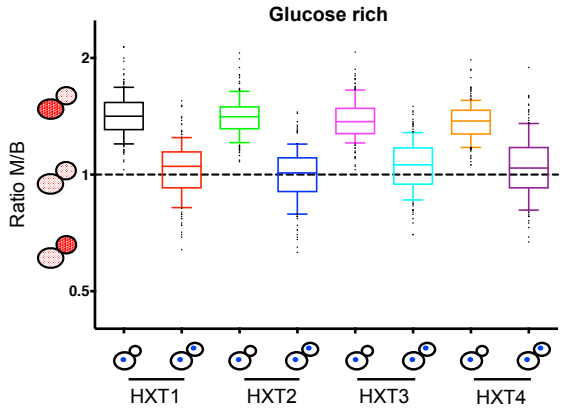

D

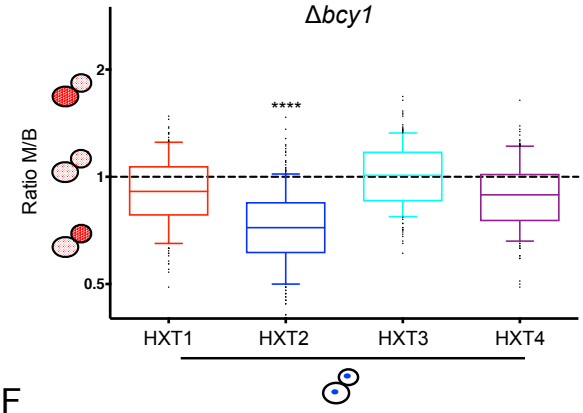

E

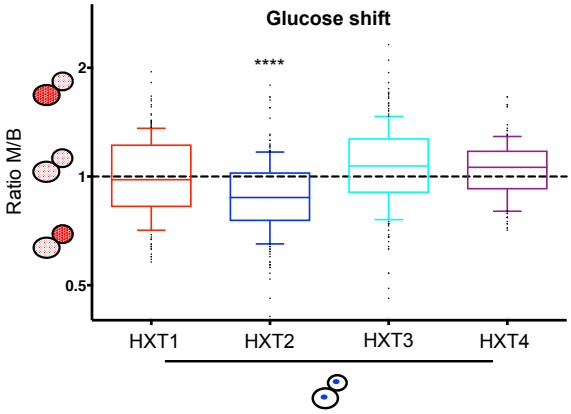

F

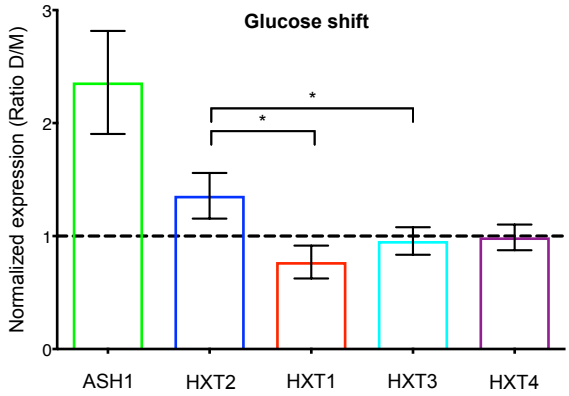

Figure 5, Stahl et al.

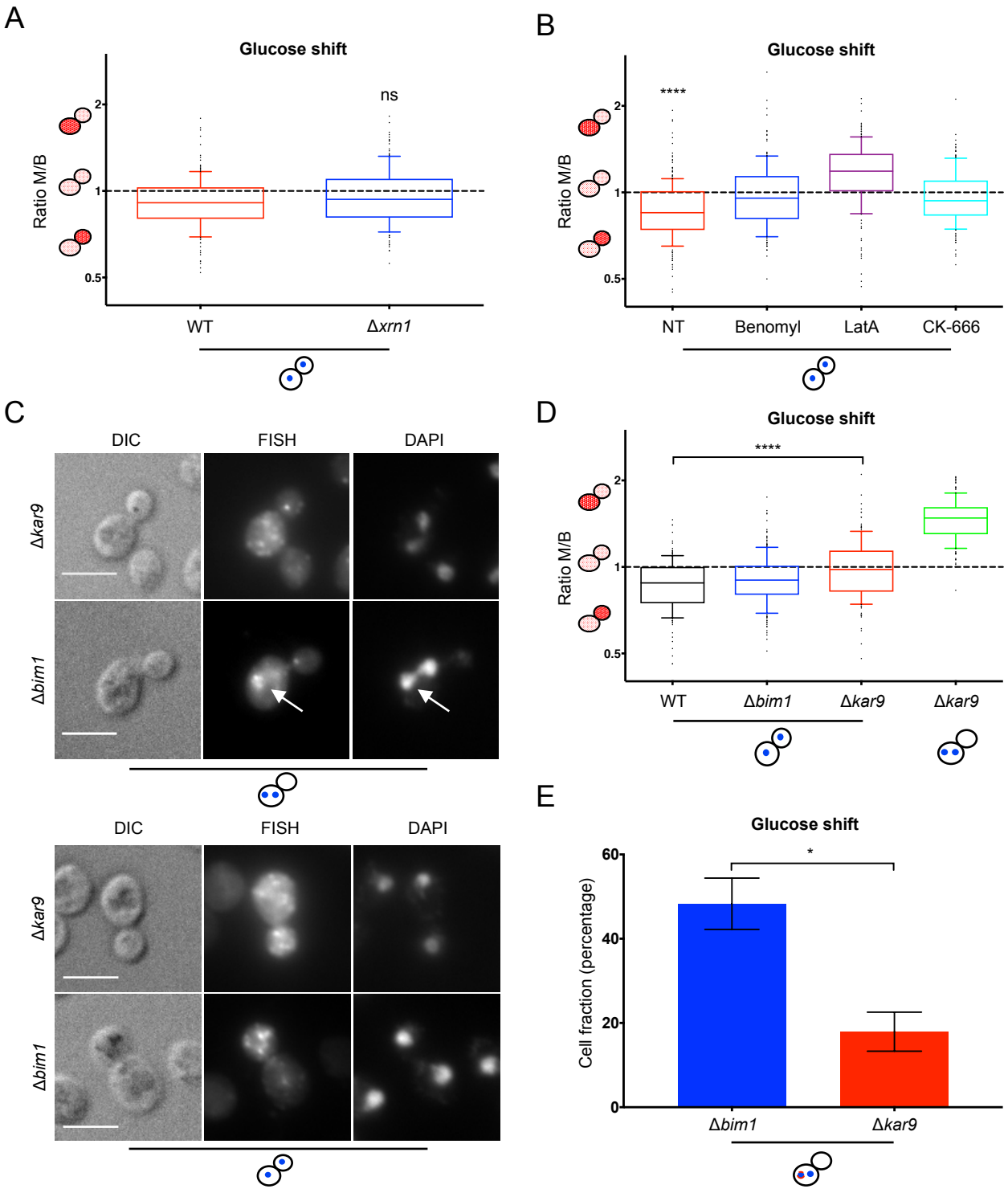

Figure 6, Stahl et al.

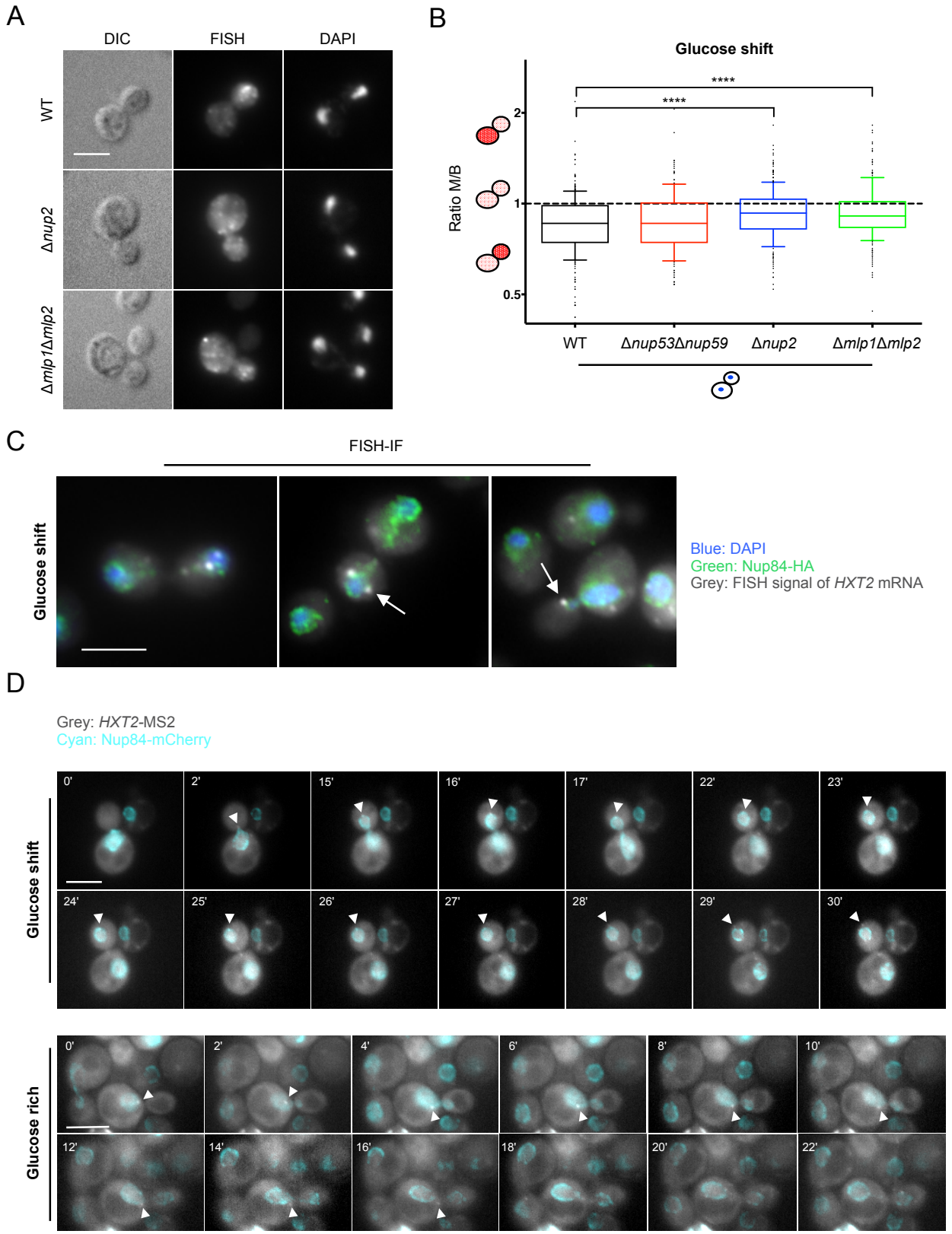

Figure 7, Stahl et al.

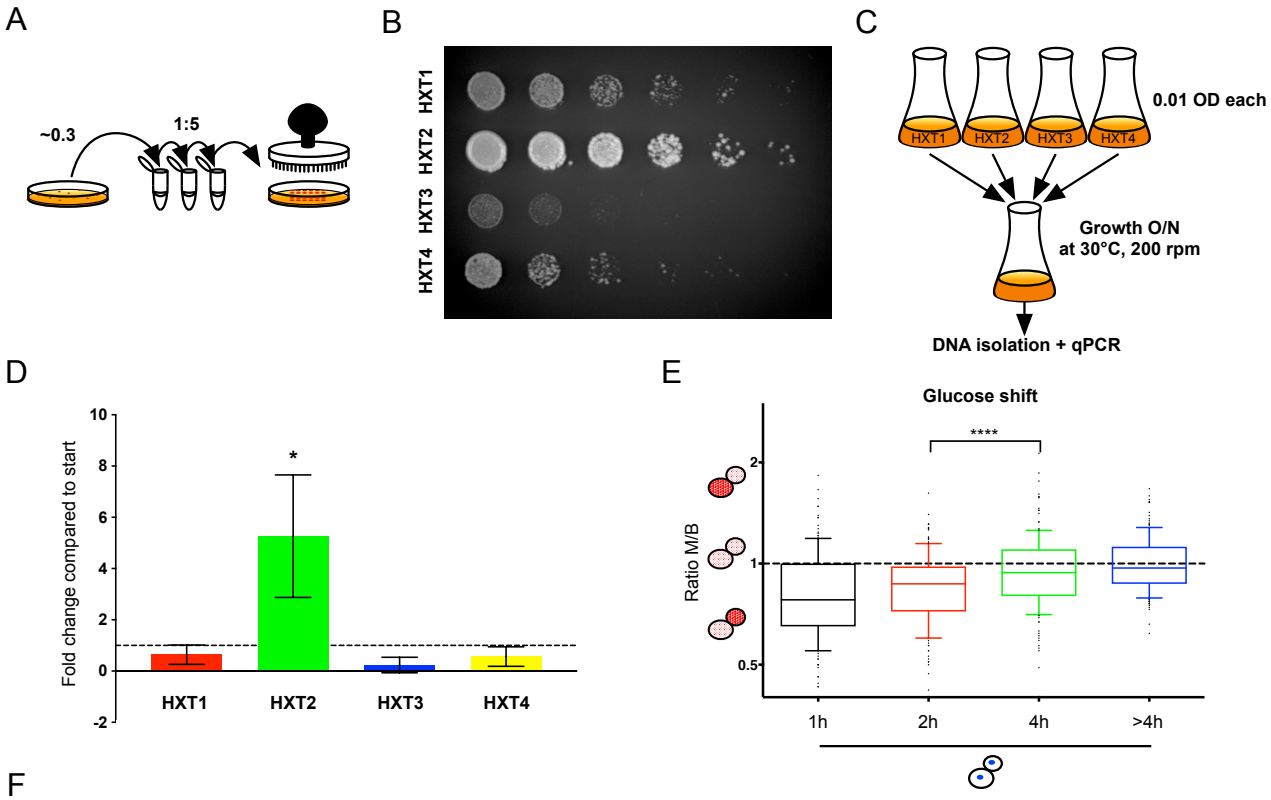

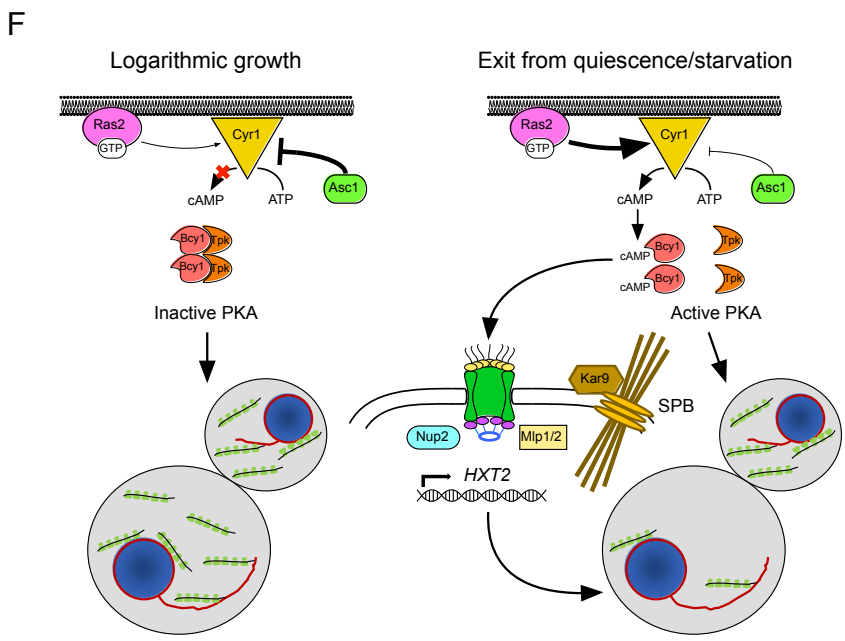

Figure S1, Stahl et al.

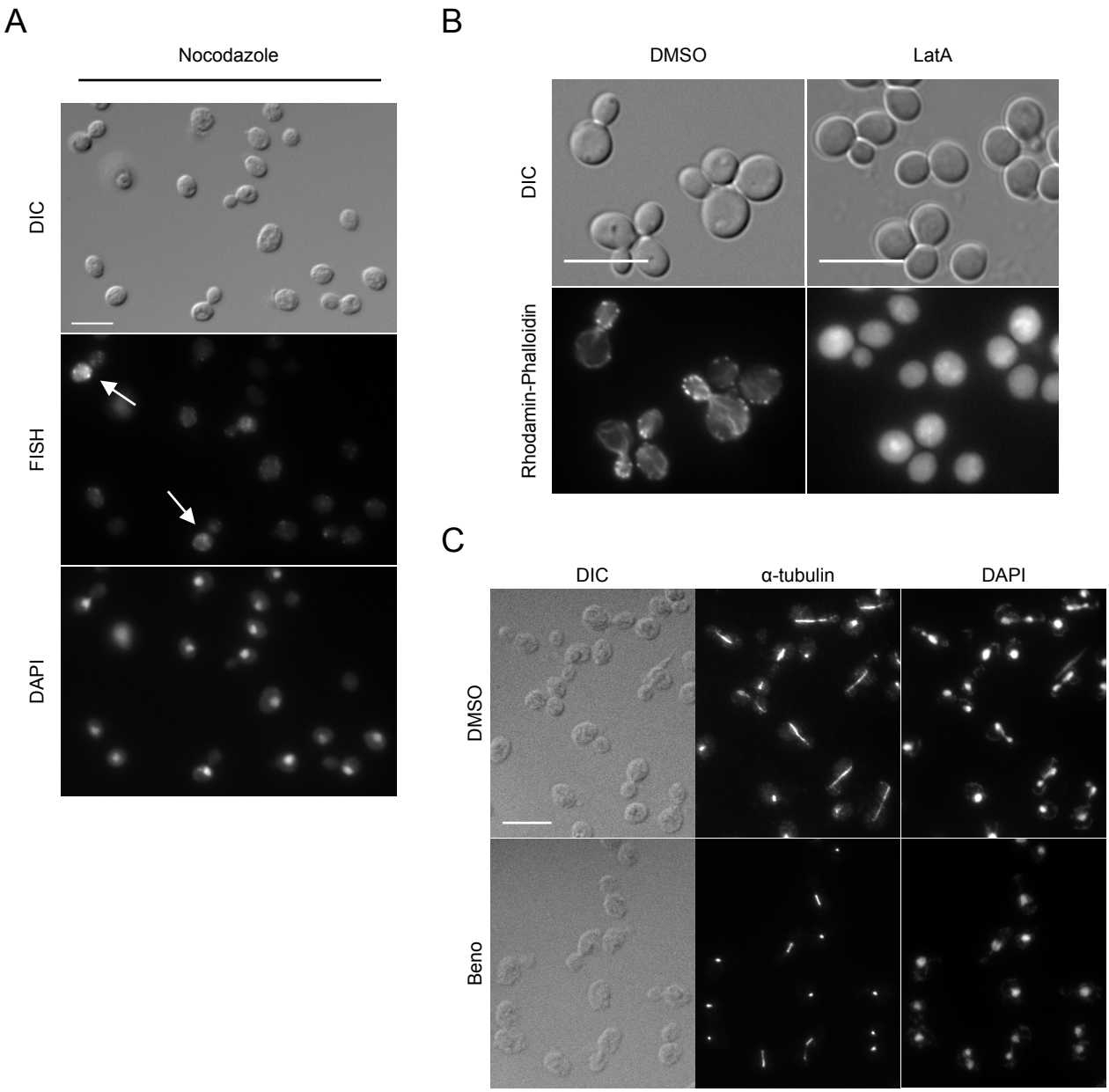

Figure S2, Stahl et al.

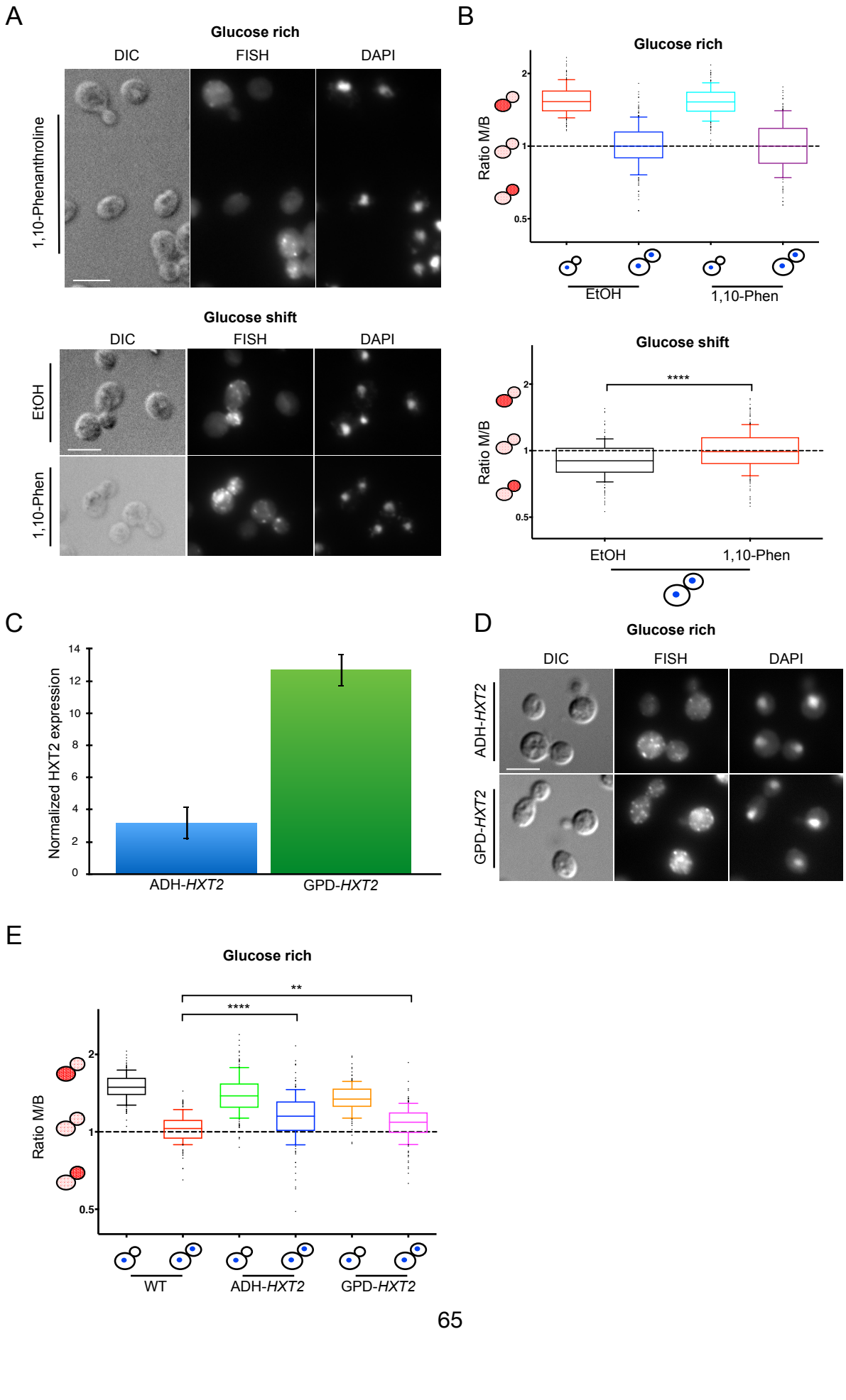

Figure S3, Stahl et al.

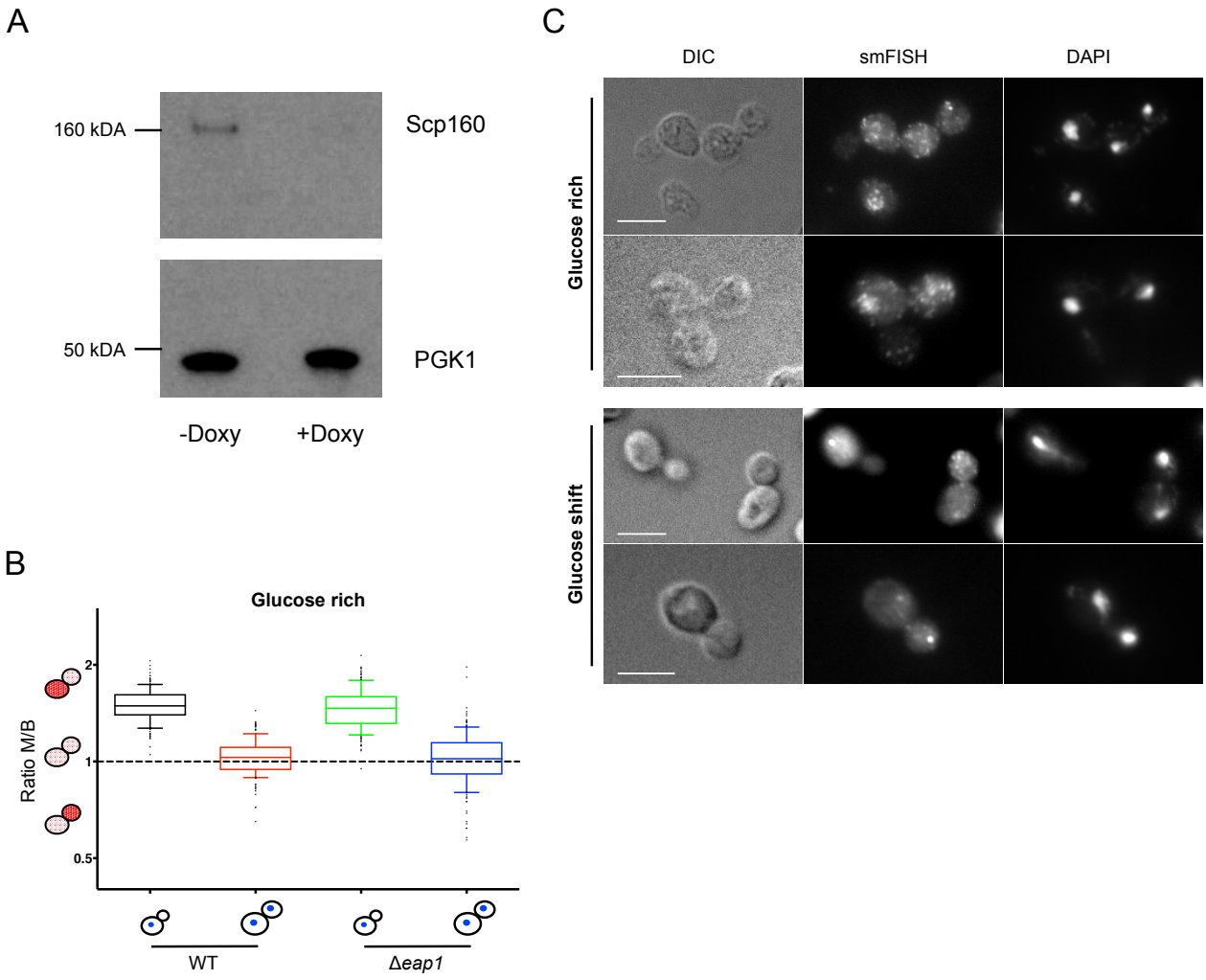

Figure S4, Stahl et al.

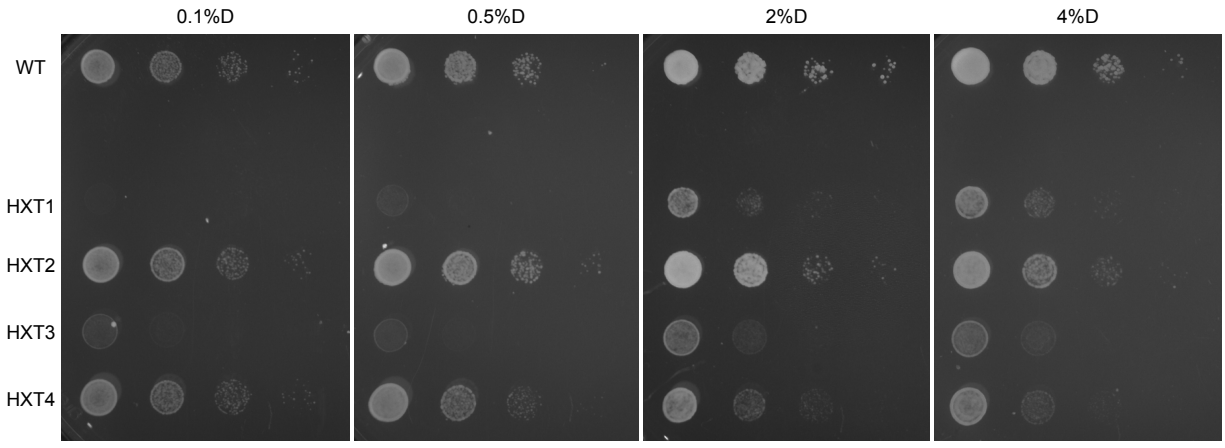

4. Additional Data

The presented data in this chapter is mainly preliminary and should be interpreted with caution. For a more detailed description see chapter ‚Further Discussion and Outlook'.

Additional Data 1

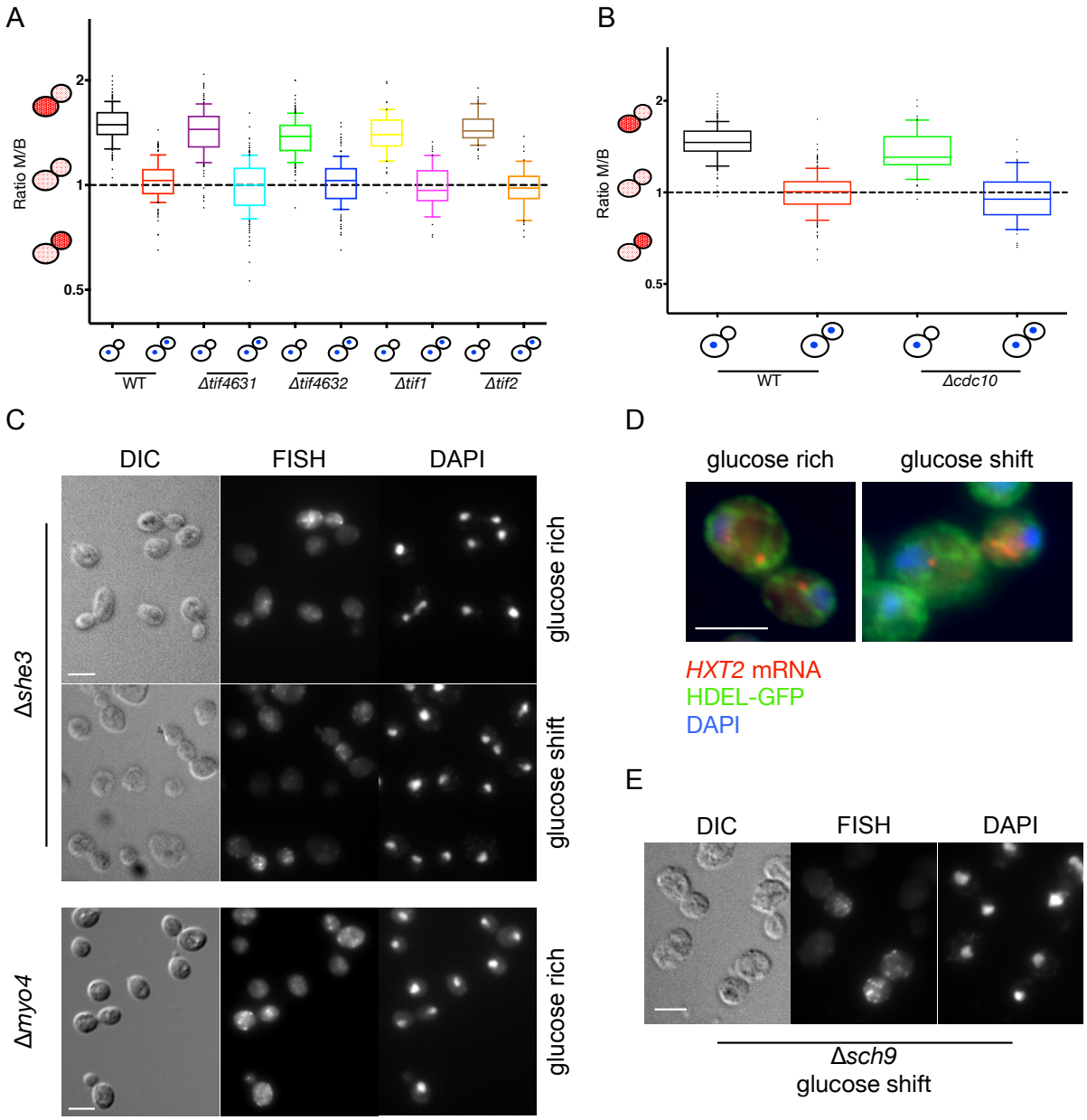

A.1: (A) Deletion of different translation initiation factors had no effect on either the retention of *HXT2* mRNA early in the cell cycle or the equal distribution late in the cell cycle. Glucose rich conditions, n = 3 for Δ*tif4631/32* and n = 2 for Δ*tif1/2* (B) Deletion of the septin ring component Cdc10 did not alter the retention or equal distribution under glucose rich conditions. n = 1. (C) FISH. ER inheritance is impaired by deleting either She3 or Myo4. We did not observe an effect on the localization of *HXT2* mRNA under glucose-rich or glucose-shift conditions in these deletion strains. (D) FISH-IF. *HXT2* mRNA and HDEL-GFP partially overlapped or were in close proximity under glucose-rich as well as glucose-shift conditions. (E) Deletion of the S6 kinase ortholog Sch9 did not impair the enrichment of *HXT2* mRNA in the bud under glucose-shift conditions.

Additional Data 2

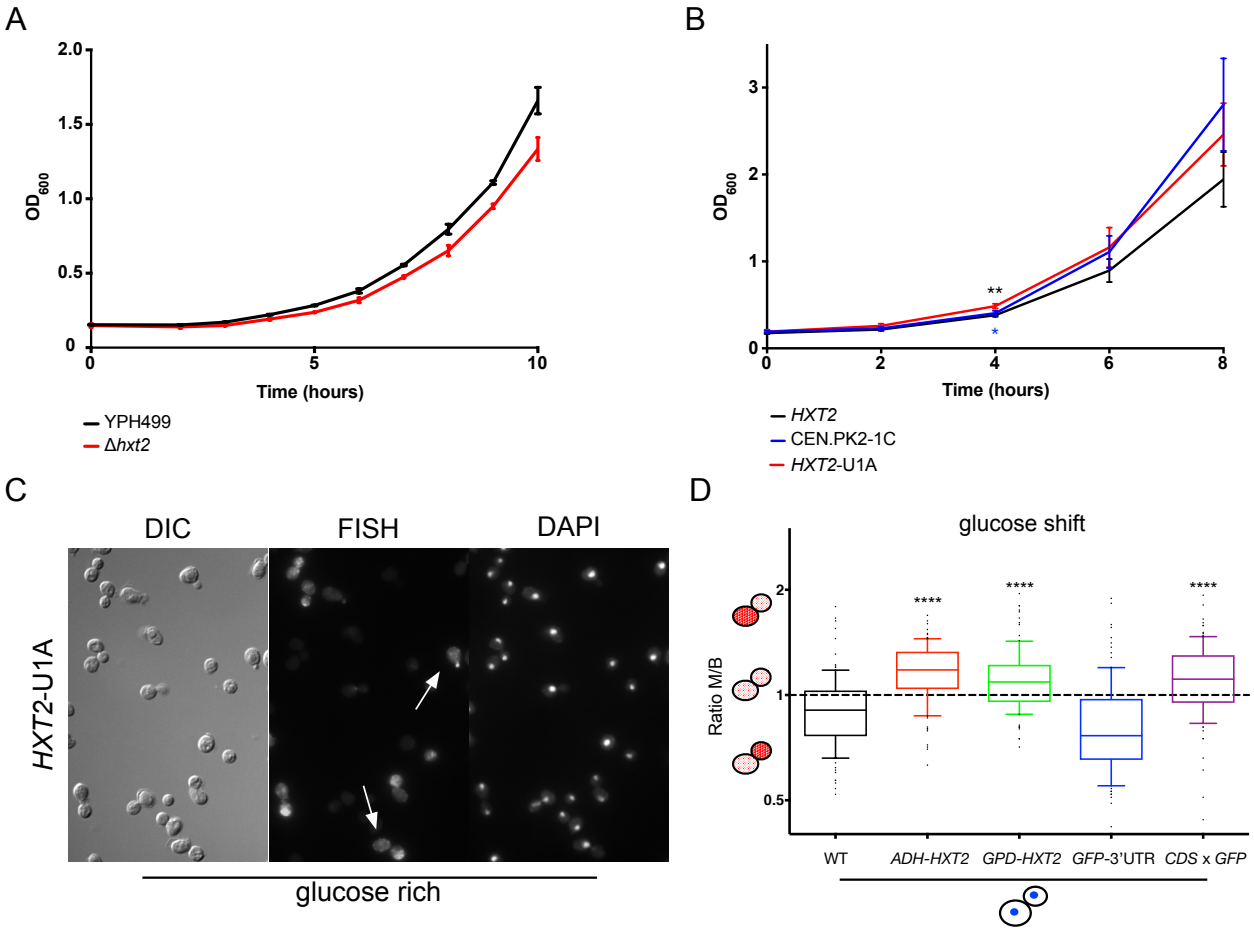

A.2: (A) Growth curves of WT (YPH499) cells and cells, where *HXT2* is deleted (Δ*hxt2).* Compared to WT, Δ*hxt2* cells show a longer lag-phase, when re-entering the cell-cycle from quiescence. Cells were scratched from YPD plates, diluted to same OD_{600} (~0.2) and grown in YPD medium at 30°C, 200 rpm. OD_{600} was measured at the indicated time points. (B) Growth curves of WT (CEN.PK2-1C) cells and cells that only express *HXT2*-U1A or *HXT2*. Compared to WT or *HXT2*-only, cells expressing *HXT2*-U1A grow slightly better in the first 4 hours, when coming out of quiescence. Experiment was carried out as described in (A). **: *HXT2* vs. *HXT2*-U1A, p = 0.0052; *: *HXT2*-U1A vs. CEN.PK2-1C, p = 0.0239. n = 3. (C) FISH with probes against *HXT2*. Introducing U1A stem loops between the CDS and the 3'UTR of *HXT2* leads to artificial enrichment in the bud, independent of the cell cycle (arrow: cells before MAT). (D) Cis-elements in the 5'UTR and the CDS of *HXT2* seem to be important for the enrichment in the bud under glucose shift conditions. Exchanging the promotor and 5'UTR of *HXT2* with either the *ADH-* or *GPD*-promotor inhibits enrichment of *HXT2* mRNA in the bud. This is also true when the CDS of *HXT2* was swapped with the CDS of GFP. The 3'UTR of HXT2 seems to be dispensable for the enrichment in the bud under glucose shift conditions. ****: $p < 0.0001$, n = 2.

5. Further Discussion and Outlook

Asymmetric cell division provides the possibility to diversify into subpopulations which in turn can increase the overall fitness of the population (Thattai and van Oudenaarden, 2004; Kussell and Leibler, 2005). This is especially true for unicellular organisms like *S. cerevisiae* which frequently face fluctuations in their environment.

Like the hexose transporter Hxt2 itself, its mRNA also localizes asymmetrically during the cell cycle and the aim of this study was to investigate the underlying mechanisms and if there are advantages or disadvantages for the cell resulting from this asymmetry. We assumed that translation could be involved linking protein and transcript localization. To this end, we globally inhibited translation and found indeed that the equal distribution late in the cell cycle was suppressed. Interestingly, it did not make a difference for the localization of *HXT2* mRNA, if we blocked either initiation or elongation of translation. In contrast, its stability was markedly reduced when the transcript was not bound to polysomes. We, therefore, postulated that the release of *HXT2* mRNA to the bud late in the cell cycle depends on active translation and that the transcript is bound to polysomes in order to be protected from degradation. We also observed this distribution pattern for the mRNA of *HXT1*, *HXT3* and *HXT4*. Although we did not test whether active translation is also important for their release, we think it is very likely that this mechanism also acts on the localization of these mRNAs.

To further elucidate which translation factors might be crucial for the localization of *HXT2* mRNA, we deleted most of them one by one. However, we did not observe a strong effect on the release of *HXT2* mRNA to the bud (A.1A). Since these factors are highly redundant and deleting more than one at a time is often lethal, we cannot exclude that translation factors are involved. Further studies with either temperature-sensitive or shut-off mutants are necessary to clarify this point.

Transmembrane proteins like hexose transporters are translated at the ER which is inherited to the daughter cell via the motor protein Myo4 and its adaptor She3. We hypothesized that retention in the mother cell, equal distribution or enrichment of *HXT2* mRNA might be linked to ER distribution during the cell cycle. To test this, we impaired cER inheritance by deleting *SHE3* or *MYO4* that carry ER tubules of the cortical ER (cER) into the bud (Estrada et al., 2003). Under these conditions, we did not see any effect on the localization of *HXT2* mRNA (A.1C). Nevertheless, several studies observed only a minor delay in cER inheritance in Δ*SHE3* or Δ*MYO4* strains (Reinke et al., 2004, Loewen et al., 2007) and we observed a partial overlap of the FISH signal with HDEL-GFP, a marker for ER (A.1D). Therefore, we cannot exclude that the cortical ER might be involved in the localization of those *HXT2* transcripts, that are not associated with the nuclear envelope. To further differentiate, whether the mRNA localizes to the membrane of the nuclear ER or to nuclear pore complexes, experiments could be performed in which nuclei are isolated and the bound mRNA fractions are tested for association with ribosomes by ribosomal profiling or with nuclear pore complexes by nuclear pore complex isolation.

During cell division in *S. cerevisiae*, a bud neck is formed which integrates many cellular inputs to regulate for example the progression from G2- to M-phase (Keaton and Lew, 2006). At the bud neck, a ring made of septins, GTP-binding proteins that assemble into filamentous structures, can act as diffusion barrier to prevent diffusion of specific proteins, e.g. cell division factors, between mother and daughter cell (Luedeke et al., 2005; Spiliotis and Nelson, 2006). We deleted the non-essential septin Cdc10, but found no effect on retention or equal distribution of *HXT2* mRNA under glucose rich conditions (A.1B). This observation argues against a diffusion barrier dependent localization mechanism.

The *S. cerevisiae* protein involved in the Control of Ploidy or Scp160 is a mRNA binding protein that is associated with translational control among other functions (Lang and Fridovich-Keil, 2000; Frey et al., 2001; Mendelsohn et al., 2003; Baum et al., 2004; Sezen et al., 2009; Hirschmann et al., 2014). Scp160 is known to bind to ribosomes, associated with Bfr1, through Asc1 (Baum et al., 2004; Lang et al., 2000). When deleting either component of the complex Scp160/Asc1/Bfr1, much to our surprise, we did not see an effect on the retention in the mother cell early in the cell cycle but rather a strong enrichment of *HXT2* mRNA in the bud late in the cell cycle. One possibility to explain this finding, would be that the complex is involved in the translocation of *HXT2* mRNA from nuclear pore complexes to polysomes at the nuclear ER. In this model, the mRNA would be stuck at the nuclear envelope until it reaches the bud late in the cell cycle. In support of our model, we could show that the enrichment of *HXT2* mRNA under glucose shift conditions is dependent on nuclear segregation and partially on components of the NPC (see below). Nevertheless, it would be interesting to see if either Scp160, Bfr1 or Asc1 is phosphorylated by PKA under glucose shift conditions and if this changes the formation of the complex or its localization to ribosomes.

When we discovered that the activation of the glucose responsiveness pathway is responsible for the enrichment of *HXT2* mRNA under glucose shift conditions, we tested which one of the two input pathways are responsible. We found that the alleged glucose receptor Gpr1 and its G-protein subunit Gpa2 are not involved. Although it is assumed that Gpr1 is a glucose receptor, there is actually only very little evidence that Gpr1 really serves as a primary mediator in the glucose responsiveness pathway, since it has only weak affinity for glucose compared to non-preferred carbon sources such as sucrose (Lemaire et al., 2004). In fact Gpr1 and Gpa2 are rather linked to nutrient sensing mediated by TORC1. It was suggested that Gpa2 acts upstream of Sch9 and that Sch9 in turn suppresses Gpa2 activity (Zaman et al., 2009). Sch9, the functional ortholog of mammalian S6 kinase, is activated by TORC1 and mediates changes in protein phosphorylation elicited by TORC1 (Urban et al., 2007). Although increased Sch9 activity was shown to phenocopy part of the transcriptional responses to glucose, the main effects of glucose addition to cells are mediated by the PKA (Zaman et al.. 2009; Broach, 2012). In agreement with this, we found that the RAS2/cAMP/PKA pathway is involved in the enrichment of *HXT2* mRNA in the bud as a response to glucose exposure, but deletion of Sch9 had no effect (A.1E).

We identified Kar9 as an important contributor to the asymmetric localization of *HXT2* mRNA under glucose shift conditions. Kar9 is involved in the asymmetric spindle pole body segregation during the cell cycle (see Introduction). Besides the known four serine residues that are phosphorylated by the mitotic kinases Cdk1/Clb4 and Dbf2/Dbf20, at least nine additional phosphorylation sites have been identified (Bodenmiller et al., 2010; Swaney et al., 2013). It seems very unlikely that all of them are involved in the regulation of the interaction of Kar9 with Bim1 (Bodenmiller et al., 2010; Swaney et al., 2013; Manatschal et al., 2016). Since deletion of Bim1 had no effect on the enrichment of *HXT2* mRNA in the bud, it is reasonable to assume that those additional phosphorylation sites could be important for Kar9's role in the asymmetric localization of *HXT2* mRNA. Although it was not yet shown that Kar9 is a target of PKA, we cannot exclude that under certain conditions, PKA phosphorylation might play a role in the asymmetric localization of Kar9 on the nuclear envelope or the interaction of Kar9 with for instance nuclear pore complexes. It would be important to test, if Kar9 mediates the enrichment of *HXT2* mRNA depending on its phosphorylation, in particular by PKA, or if Kar9 is associated with nuclear pore complexes.

As mentioned above, we could demonstrate that factors associated with the nuclear envelope, like the nuclear pore complex subunit Nup2 and the nuclear basket components Mlp1 and Mlp2, are involved in the localization of *HXT2* mRNA under glucose shift conditions. The association of Mlp1 and Mlp2 with NPCs was shown to be more dynamic than that of core Nups, which could provide the means to connect signaling with conformational changes of the nuclear basket (Strambio-de-Castillia et al., 1999; Niepel et al., 2013). The nuclear basket can serve as a binding site for mRNPs during their export (Kiseleva et al., 1996; Pante et al., 1997; Soop et al., 2005) and it is possible that upon glucose shift conditions, Mlp1 and Mlp2 preferentially associate with NPCs that localize to the bud, where they would serve as a binding site for bud directed mRNAs, like *HXT2* mRNA.

Moreover, the SPB is also connected to the nuclear basket via Mlp2 (Niepel et al., 2005; De Souza et al., 2009), which indirectly links Kar9 activity to nuclear pore complexes. Daughter cells have a higher NPC density, which consist mainly of "old" nups (Khmelinskii et al., 2012). The underlying mechanism depends on the active transport of the nuclear pore complex component Nsp1 to the bud (Colombi et al., 2013). In this model, controlled NPC inheritance rather than de novo assembly ensures daughter viability, especially when NPC assembly rates cannot keep up with rapid cell divisions (Colombi et al., 2013). Thus, this targeting of NPCs to the bud during anaphase could provide us with a mechanism of how *HXT2* mRNA is asymmetrically distributed on the nucleus during the cell cycle. However, the asymmetric distribution of NPCs allegedly depends on overcoming a diffusion barrier created by septins at the bud neck. As mentioned above, we did not find any involvement of septins in the localization of *HXT2* mRNA under glucose-rich conditions. Whether septins play a role for the enrichment of *HXT2* mRNA under glucose-shift conditions, needs to be tested. Nonetheless, it would be interesting to investigate, if NPC inheritance during anaphase influences *HXT2* mRNA localization at least under glucose shift conditions.

Our results indicate that transcription is necessary but not sufficient to promote enrichment of *HXT2* mRNA in the bud under glucose-shift conditions. Overexpression per se did not lead to enrichment and transcription played no role for the localization of *HXT2* mRNA under glucose-rich conditions. These results suggest a transient onset of transcription when cells encounter glucose again after starvation. Indeed, it was shown that *HXT2* was especially expressed during the first hours of fermentation (Luyten et al., 2005). This is particularly interesting considering that this is contradictory to the known regulation, in which expression of *HXT2* is repressed by high glucose concentrations (Özcan et al., 1995). The cell is able to bypass glucose repression somehow during lag phase and represses expression only later during growth. In contrast, *HXT3* is predominantly expressed during stationary phase and this is consistent with its capacity to maintain a high fermentation rate during starvation (Luyten et al., 2002).

Taken together, these findings support the idea that under glucose shift conditions, *HXT2* is transiently transcribed and its mRNA is distributed to the bud on the nucleus. We hypothesized that this enrichment of *HXT2* mRNA in the bud enables the daughter cell to rapidly translate Hxt2 protein, accumulate glucose and therefore quickly change from respiration to fermentation. Daughter cells that start fermenting glucose early, may outcompete those cells that are unable to mount such a response. When we compared cells that only express one hexose transporter at a time, we found that cells expressing *HXT2* indeed reinitiate growth after starvation much faster than cells expressing other hexose transporters. Consistent with this finding, *HXT2* deletion was shown to delay the start of fermentation with a corresponding increase in the lag phase (Luyten et al., 2002; A.2A).

Although our experiments suggest that expressing only *HXT2* in comparison to *HXT1* or *HXT4* has no effect on the overall survival rate (data not shown) and that the enrichment of *HXT2* mRNA happens only during the first 1-2 cell cycles after re-feeding, it is possible that the faster growth re-initiation also influences the replicative or chronological lifespan. To test this, one could seperate young daughters from either glucose-rich or glucose-shift grown cells and count the cell divisions of the individual daughter cells.

To finally prove that really the localization in the bud and not the mere expression of *HXT2* mRNA confers the growth advantage, it is important to find the essential cis-acting elements. Mutating them to prevent enrichment of the *HXT2* mRNA in the bud, would give us the opportunity to investigate whether this impairs the growth advantage of *HXT2*-only cells when released from quiescence. Surprisingly, when we introduced U1A stem loops between the CDS and the 3'UTR, we found that the *HXT2* mRNA is strongly enriched in the bud, independent of the cell cycle. We compared the growth rate of cells expressing either wildtype *HXT2* or U1A-modified *HXT2* as their sole hexose transporter. Indeed, *HXT2*-U1A expressing cells show a slightly better growth during the first hours of re-growth than those cells that express wildtype *HXT2* (A.2B). Moreover, the growth-rate of both, *HXT2*- and *HXT2*-U1A-only cells, decreases during prolonged growth compared to WT (A.2B). It is conceivable to assume that Hxt2 is especially important in the first hours after glucose addition to starved cells in order to change from respiration to

fermentation. Later, when cells head towards diauxic shift conditions, other hexose transporters like Hxt1 and Hxt3 are more important for efficient growth.

Upon exchanging the 5'-UTR of *HXT2* with either the *GPD*-or *ADH*-promotor, the equal distribution under glucose rich conditions as well as the enrichment under glucose shift conditions were impaired (Fig.S2E, A.2D). Exchanging the CDS of *HXT2* for that of GFP also prevented the enrichment in the bud under glucose shift conditions (A.2D). However, none of these experiments showed strong effects on the retention early in the cell cycle under glucose rich conditions. Taken together these results suggest that the cis-element for equal distribution lies within the 5'-UTR. We speculate that sequences around the ATG might be important, since onset of translation appears to be necessary for the equal distribution. An additional element in the CDS seems to be important for the enrichment in the bud under glucose shift conditions. Additional experiments, where the sequences of 5'-UTR and CDS of *HXT2* are mutated would allow us to further narrow down the specific sequence or structural element that functions as cis-element.

6. Appendix

6.1 Materials and Methods

Materials

Media

LB medium:	10 g Bacto-tryptone (BD)
	5 g Bacto yeast extract (BD)
	10 g NaCl (Roth)
	ad 1 l dH_2O and autoclaved
LB agar:	5 g Bacto-tryptone (BD)
	2.5 g Bacto yeast extract (BD)
	5 g NaCl (Roth)
	10 g Bacto-agar (BD)
	ad 500 ml dH_2O and autoclaved
SOC medium:	5 g yeast extract (BD)
	20 g Bacto-peptone (BD)
	20 g dextrose (Roth)
	10 mM NaCl
	2.5 mM KCl
	10 mM $MgSO_4$
	ad 1 l dH_2O and autoclaved

YP-medium:	1% Bacto yeast extract (BD) 2% Bacto-peptone (BD) ad 1l dH_2O and autoclaved
YP agar:	10 g Bacto-peptone (BD) 5 g Bacto yeast extract (BD) 10 g Bacto-agar (BD) ad 450 ml dH_2O and autoclaved 50 ml of 20% (w/v) glucose was added before plates were poured
5-FOA plates:	0.34 g Yeast Nitrogen Base without amino acids (BD) 0.05 g 5-fluoroorotic acid (Biovectra) 1 g dextrose (Roth) 5 ml 10 x HC-complete selection mixture ad 20 ml dH_2O and filter sterilized into 25 ml warm (55˚C) sterile agar (1 g in 25 ml H_2O)

10x HC-selection mixture:	0.2 mg/ml adenine hemi-sulfate 0.35 mg/ml uracil 0.8 mg/ml L-trytophan 0.2 mg/ml L-histidine-HCl 0.8 mg/ml L-leucine 1.2 mg/ml L-lysine-HCl 0.2 mg/ml L-methionine 0.6 mg/ml L-tyrosine 0.8 mg/ml L-isoleucine 0.5 mg/ml L-phenylalanine 1.0 mg/ml L-glutamic acid 2.0 mg/ml L-threonine 1.0 mg/ml L-aspartic acid 1.0 mg/ml L-valine 2.0 mg/ml L-serine 1.0 mg/ml L-arginine-HCl autoclaved without the component to select for
10x YNB:	33.5 g Yeast Nitrogen Base w/o amino acids (BD) ad 500 ml dH_2O and wrapped in aluminum foil and autoclaved

HC medium:	800 ml dH_2O 100 ml 10 x HC-XX (without the component to select for) 100 ml 10 x YNB
HC plates:	hot sterile agar (10 g Bacto-agar (BD) dissolved in 350 ml) 50 ml 20% dextrose 50 ml 10 x YNB 50 ml 10 x HC selection mixture

Commonly used solutions and buffers

Antibiotics

1000 x ampicillin	100 mg/ml in dH_2O, filter sterilized
250 x kanamycin	10 mg/ml in dH_2O, filter sterilized
100 x G418	20 mg/ml geneticin in dH_2O, filter sterilized
2000 x ClonNAT	200 mg/ml nourseotricin in dH_2O, filter sterilized
100 x hygromycin B	50 mg/ml in dH_2O, filter sterilized

Solutions

TE Buffer:	10 mM Tris/HCl pH 7.5
	1 mM EDTA
Carrier DNA:	200 mg salmon sperm DNA (Sigma)
	ad 100 ml TE buffer, sterilized
6x DNA loading buffer:	0.25% bromophenol blue
	0.25% xylene cyanol
	30% glycerol
50 x TAE-buffer:	2 M Tris/HAc pH 7.7
	5 mM EDTA
5 x Laemmli-buffer:	62.5 mM Tris/HCl pH 6.8
	5% β-mercaptoethanol
	10% glycerol
	2% SDS
	0.0025% bromophenol blue

20 x TBS:	60 g Tris/HCl pH 7.4 160 g NaCl 4 g KCl ad 1 l dH2O
TBST:	TBS with 0.1% Tween-20
20 x PBS:	46.6 g Na_2HPO_4 x 12 H2O 4.2 g KH_2PO_4 175.2 g NaCl 44.8 g KCl ad 1 l dH_2O
50 x Denhardt's reagent:	10 g Ficoll type 400 10 g BSA fraction V 10 g polyvinylpyrrolidone ad 1 l dH_2O, filter sterilized and stored at -20˚C
20 x SSC:	3 M NaCl 0.3 M Na-citrate/NaOH pH 7.0
DEPC-H2O:	1 l H_2O 1 ml DEPC, stirred for > 1 h, then autoclaved

Methods

Determination of yeast cell density

1 OD_{600} corresponds to 1.5 x 10^7 yeast cells per ml on the spectrophotometer Ultrospec 3100 pro (Amersham Biosciences). For density measurements, cells were diluted to yield an OD_{600} below 1. Unless otherwise indicated, logarithmically growing cells were harvested at an OD_{600} between 0.3 - 0.7

Preparation of yeast total cell extract

9 ml of a mid-log grown culture were taken, immediately treated with cold trichloroacetic acid (10% final concentration) and incubated on ice for at least 5 min. Yeast extracts were prepared as described (Stracka et al., 2014). Approximately 120 µl of glass beads were added. After vigorous vortexing for 5 min, samples were incubated for 5 min at 65˚C followed by an additional 1 min of vortexing. Cell debris and glass beads were sedimented (2 min at 10,000 x g), and the supernatant was transferred to a fresh reaction tube. For subsequent analysis by SDS-PAGE and immunoblotting, 5 µl of the lysate was loaded per lane. For comparison of protein expression levels, Laemmli buffer was replaced by LowDTT lysis buffer. The lysates were normalized to equal total protein concentration using the Biorad DC protein assay used according to the manufacturer's protocol. Routinely, 20 µg of total protein were loaded per lane.

6 x Laemmli buffer:

62.5 mM Tris/HCl (pH 6.8)

5%-mercaptoethanol

10% glycerol

2% SDS

0.0025% bromophenol blue

LowDTT lysis buffer:

20 mM Tris/HCl (pH 8.0)

5 mM EDTA

1 mM DTT

1 % SDS

Determination of protein concentration

Protein concentrations of detergent-free solutions were determined using the Biorad protein assay, which is based on the Bradford method (Bradford, 1976). Bovine gamma-globulin served as a protein standard. For detergent-containing solutions, the detergent-compatible Biorad DC protein assay was used, which is based on the Lowry method (Lowry et al., 1951). In this case, bovine serum albumin served as a standard. All measurements were performed according to the manufacturer's instructions.

Total RNA isolation

Total RNA was isolated from yeast essentially as described (Schmitt et al., 1990). Briefly, 10 OD_{600} of yeast cells were harvested after the different treatments. Cells were resuspended in 1 ml AE buffer, 100 µl 20% SDS and 1 ml PCI (125:24:1, pH 4.4) were added and the tube vortexed for 10 s. After incubation for 10 min at 65°C, tubes were chilled in liquid nitrogen for 30 s, thawed and then centrifuged (2 min, 20.000 x g, RT). The upper aqueous phase was transferred to a fresh tube and 1 ml PCI was again added and vortexed 10 s. After phase separation by centrifugation, the upper aqueous phase was again transferred to a fresh tube and 1/10 volume of 3 M NaCl (pH 5.2) was added. The RNA was precipitated with two volumes 100% EtOH at -80°C for at least 2 h. The precipitate was spun down (30 min., 20.000 x g, 4°C), washed with 70% EtOH and again centrifuged. The pellet was resuspended in 100 µl RNase-free water.

AE buffer:	50mM NaAc pH 5.2
	10mM EDTA

Determination of nucleic acid concentration

The concentration of nucleic acids was determined using a NanoVue (GE Healthcare). The nucleic acids were diluted in dH_2O, and the absorption at 260 nm was determined. It was assumed that a unit of absorption at 260 nm corresponds to 50 µg/ml double-stranded DNA or 40 µg/ml single-stranded RNA.

Chromosomal manipulations of yeast cells

To delete, tag or place genes under an exogenous promoter, PCR-generated cassettes were integrated into the genome as described previously (Gauss et al., 2005; Gueldener et al., 2002; Janke et al., 2004; Knop et al., 1999; Tagwerker et al., 2006). Briefly, preparative PCR was performed on template plasmids with primers bearing 45 bp 5'-overhangs homologous to the desired target site in the yeast genome. The PCR-product was transformed directly into yeast cells without further purification. Cells were selected for the corresponding auxotrophy or resistance marker and correct integration was confirmed by analytical colony PCR. If required, the chromosomal manipulation was sequenced. In this case, a fragment containing the desired manipulation was amplified

from genomic yeast DNA with the proof-reading Expand PCR system (Roche) and used as a template for sequencing.

Preparation of genomic yeast DNA

Crude yeast DNA was obtained by rapid phenol/chloroform extraction (Hoffman and Winston, 1987). For this, 5 ml of yeast culture were grown to greater than 2 OD_{600} units per ml. The cells were harvested and resuspended in 200 µl lysis buffer. Glass beads corresponding to approx. 200 µl and 200 µl PCI (25:24:1, ph 8) were added. After FastPrep treatment (20 s, 4.5 m/s, 4°C), 200 µl H_2O were added. Phase separation was accomplished by centrifugation (5 min, 10,000 x g). The aqueous phase was transferred to a fresh reaction tube and 1 ml 100% EtOH (RT) were added to precipitate the DNA, which was pelleted by centrifugation for 5 min (16,000 x g). The resulting pellet was dried at 65°C for about 5 min and resuspended in 40 µl H_2O. Routinely, 0.2 µg genomic DNA were used per PCR reaction.

Lysis buffer:

10 mM Tris/HCl pH 8.0
100 mM NaCl
1 mM EDTA
2% Triton X-100
1% SDS

Yeast transformation

Yeast cells were transformed by a highly efficient lithium acetate transformation method (Gietz et al., 1995). Cells were grown over night to early log phase. 5 OD_{600} of cells were harvested and washed once in sterile water. The cells were incubated for 5 min at 30°C in 100 mM LiAc. Subsequently, they were resuspended in 360 µl transformation mix and vortexed for 1 min. First the cells were incubated at RT for 30 min. on an over-head rotator, then a heat shock was employed for 15 min at 42°C., The cells were pelleted (30 s, 16,000 x g). and resuspended in 1 ml YPD and incubated at 30°C for up to 2 h on an over-head rotator. Afterwards cells were again pelleted, resuspended in 100 µl sterile H_2O and plated on appropriate selection plates. Sometimes, replica plating was necessary to allow for the selection of stable transformants.

Transformation mix:

240 µl 50% (w/v) PEG (AMW 3,350)
36 µl 1 M LiAc
50 µl 2 mg/ml single-stranded salmon sperm DNA
5 µg of PCR product or 100 ng plasmid DNA

ad 360 µl H_2O

Analytical PCR of yeast colonies

Analytical PCR of yeast colonies was performed to confirm chromosomal manipulations of yeast cells. Generally, a forward primer binding 100-300 bp upstream of the desired integration event was combined with a reverse primer located within the integrated cassette. A product with the correct size was only amplified, if the integration has taken place. Single yeast colonies were picked with a pipette tip and incubated in 3 µl 20 mM NaOH at 100°C for at least 10 min. Afterwards the PCR reaction mix was added. A typical reaction contained 13.4 µl H_2O, 2.5 µl 10 x reaction buffer, 2.5 µl 2 mM dNTPs, 2.5 µl $MgCl_2$, 0.5 µl of forward and reverse oligonucleotide-primer (10 µM) respectively and 0.1 µl Fire-Pol Taq DNA-polymerase. Usually, the annealing temperature was set to 53°C and 1 min/kb was allowed for elongation. Generally, 35 cycles were used for amplification. Routinely, 10 µl of the reaction were analyzed on a 1% agarose gel by electrophoresis.

Digoxigenin-labeling of RNA-antisense probes

Labeled RNA antisense probes were generated by in vitro transcription in the presence of labeled nucleotides. First, a PCR was performed on genomic DNA with primers containing a T7 promoter. Primers were chosen to yield fragments of around 800 bp. The PCR product was purified with the Pellet Paint Co-Precipitant (Novagen) and used as a template for in vitro transcription with the Ambion MEGAscript T7 kit. A ratio of 1:5.6 of Dig-11-UTP:UTP was used. The integrity of the probe was checked by formaldehyde agarose gel electrophoresis. After quantification, the probe was adjusted to working concentration (0.5 µg/ml in FISH hybridization buffer, see recipe below), divided into aliquots, and kept at –80°C. Excess probe was stored as a highly concentrated stock at 0.5 µg/µl.

Hybridization buffer:

50% formamide

5 x SSC

1 mg/ml yeast tRNA

100 µg/ml heparin

1x Denhardt's reagent

0.1% Tween-20

0.1% Triton X-100

5 mM EDTA

Transformation of E. coli

Routinely, E. coli cells were transformed chemically. Usually, 50 µl home-made chemically competent cells were thawed on ice for 5 min. and mixed with approx. 200 ng plasmid DNA or with 5 µl of a ligation reaction. The cells were heat-shocked for 30 s at 42°C and immediately placed on ice. SOC medium (240 µl) was added to the cells. The mixture was incubated on a shaker for up to 1 h at 37°C before the cells were plated out on selection plates.

Plasmid preparation from E. coli

Plasmid preparations from E. coli were performed according to the alkaline lysis method described previously (Birnboim and Doly, 1979), with minor modifications. Routinely, 1.5 ml of an overnight culture were harvested (5 min, 16,000 g, RT). Cells were carefully resuspended in 300 µl buffer P1 and 300 µl buffer P2 was added. After incubation for 5 min at RT, 300 µl of buffer P3 were added to stop the lysis. The solution was cleared by two centrifugation steps (10 min, 16,000 g, RT). The plasmid DNA in the supernatant was precipitated by addition of 600 µl isopropanol and subsequent centrifugation (10 min, 16,000 g, RT). The resulting pellet was washed with 1 ml 70% ethanol and spun again (5 min, 16,000 g, RT). The pellet was dried at 65°C for about 5 min and then dissolved in 20 µl H_20 and stored at –20°C. In cases when very pure DNA was required, the Qiagen plasmid mini kit was used according to the supplier's recommendations.

Buffer P1:	Buffer P2:	Buffer P3:
20 mM Tris/HCl pH 8.0	0.2 M NaOH	3 M KAc pH 5.5
10 mM EDTA	1% SDS	
100 µg/ml RNase		

Restriction digest of DNA

Plasmid preparations were analyzed by restriction digest and agarose gel electrophoresis. The guidelines for enzymatic digests provided by the suppliers of restriction endonucleases (NEB or Roche) were followed. For cloning purposes, restriction digests were purified with the PCR purification kit (Qiagen) and DNA fragments were eluted from agarose gels using the Gel extraction kit (Qiagen) according to the manufacturer's recommendations.

Cloning

DNA fragments for (sub-)cloning were obtained either by restriction digest of plasmid DNA or by PCR amplification from genomic yeast DNA. For protein expression in yeast, the p4XX vector series was used (Christianson et al., 1992; Mumberg et al., 1995). In case

of PCR amplification, suitable restriction sites were included in the primers. Purified vector DNA and purified DNA insert were ligated using the rapid ligation kit (Roche) following the manufacturer's recommendations. If a unique restriction site was used, the digested vector was dephosphorylated with rAPid alkaline phosphatase (Roche) to prevent re-ligation. Positive clones were identified by colony PCR or restriction digest and verified by DNA sequencing.

Polymerase chain reaction (PCR)

To produce DNA fragments for DNA cloning or homologous recombination, polymerase chain reaction was used (Mullis et al., 1986). The proof-reading Expand High Fidelity System (Roche) was used for preparative production of DNA. A typical reaction contained 40 µl H_20, 5 µl 10 x reaction buffer, 1 µl 10 mM dNTPs, 2 x 1.5 µl 10 mM oligonucleotide primer and 1 µl template DNA. Usually, 35 cycles of amplification were performed. The annealing temperature was determined for each primer pair by using the online tool from NEB (www.neb.com/). Elongation time was 45 s per 1kb fragment length.

Quantitative reverse-transcription-PCR (RT-PCR)

For qPCR, total RNA was isolated as described above. DNase treatment was carried out according to the manufacturer's protocol (Promega). In short, 2 µg RNA were treated with RQ DNase and used directly for reverse transcription using random hexamers (Promega) and oligo(dTs) (Promega) and the Transcriptor Reverse Transcriptase Kit (Roche) according to the manufacturer's protocol. 1/10 of the resulting cDNA was used for a test PCR to check for gDNA contamination. For the qPCR reaction, 50 ng of cDNA was used per well and incorporation of SyBR green (Roche) was monitored on an ABI Step One Plus qPCR machine.

Glycerol stocks

For the preparation of E. coli glycerol stocks, 750 µl of an overnight culture were mixed with 500 µl 50% glycerol and stored at –80°C. For the preparation of yeast glycerol stocks, yeast cells streaked out as a patch and grown on appropriate plates. The plates were incubated until a dense lawn of cells was obtained. The cells were transferred into 800 µl 15% glycerol with a sterile glass pipette and stored at –80°C.

Fluorescent in situ hybridization (FISH)

FISH with digoxigenin-labeled antisense probe was performed essentially as described previously (Takizawa et al., 1997). Cells were grown over night to logarithmic phase and immediately fixed or starved for 2h, further grown in 2% dextrose and then fixed. Fixation was achieved by addition of 617 µl 37% formaldehyde directly to the 5 ml culture and incubation for 1 h at RT under gentle agitation. Cells were washed twice in PBS (3 min, 1,000 g, RT) and resuspended in 1 ml 100 mM KPP (pH 7.0), 1.2 M sorbitol. 2 µl β-

mercaptoethanol were added. After incubation for 5 min. at RT, the cells were spheroplasted by addition of 4 µl zymolyase T-100 suspension (10 mg/ml) for up to 20 min at 37°C. Cells were washed three times with 100 mM KPP (pH 7.0), 1.2 M sorbitol (3 min, 1,200 g) and resuspended in 90 µl of the same buffer per slide. An aliquot (15 µl) was allowed to settle on polyethylimine treated multi-well slides for 30 min. The slides were immersed in 50% formamide/5 x SSC for 5-10 min. For prehybridization, cells were incubated with hybridization buffer in a humid chamber containing 50% formamide/5 x SSC for at least 3 h. The hybridization buffer was replaced by new buffer containing the digoxigenin-labelled antisense probe at 0.5 µg/ml and the slides incubated at 42°C over night in a humid chamber. Slides were then immersed in 0.2 x SSC for 1 h at 42°C. Blocking solution was applied for at least 30 min at RT. Fab-fragments of antibodies directed against digoxigenin and covalently coupled to alkaline phosphatase (Roche) were diluted 1:5,000 in blocking solution and applied to the cells for 1 h at 37°C. Slides were washed 3 x 5 min in washing buffer, then washed 2 x 5 min in detection buffer. The HNPP/Fast Red TR mix (Roche) was applied for up to 30 min at RT, after which slides were washed with water (1 x 10 min) and 1x 5 min. with PBS supplemented with 1 µg/ml DAPI. Approx. 5µl Citifluor AF1 were pipetted onto each well. Sildes were sealed with nail polish and stored at -80°C. Pictures were taken with Axiocam MRm on an Axioplan 2 fluorescence microscope with an eqFP611 filter using Axiovision software. Image processing was performed with Fiji.

Washing buffer:	Detection buffer:	Blocking solution:
100 mM Tris/HCl pH 7.5	100 mM Tris/HCl pH 8.0	100 mM Tris/HCl pH 7.5
150 mM NaCl	100 mM NaCl	150 mM NaCl
0.05% Tween-20	10 mM $MgCl_2$	5% horse serum

Fast Red TR solution:

25 mg/ml in H2O

always freshly made

HNPP/Fast Red TR mix:

10 µl HNPP (10 mg/ml in DMF)

10 µl Fast Red TR solution

980 µl detection buffer

prepared freshly and filtered through a 0.2 µm nylon membrane

Fluorescent in situ hybridization / immunofluorescence (FISH/IF)

If FISH was combined with immunofluorescence, the following adjustments to the protocol were made. Cells were fixed, spheroplasted, and settled on slides as described in the standard FISH protocol. Before washing the slides in 50% formamide/5 x SSC, an additional fixation step was included: Slides were first immersed in ice-cold methanol for 6 min, then transferred into ice-cold acetone for 30 s and dried at RT for 3-5 min. The prehybridization, hybridization, blocking, anti-DIG-antibody incubation and washing steps were carried out according to the standard FISH protocol. Afterwards the slides were first equilibrated with PBT (1 x 5 min), then blocked with PBTB for 10 min. Incubation with anti-GFP (Torrey Pines, 1:400) or anti-HA (1:400, sigma) was carried out for 1 h at 37°C in a humid chamber. Wells were then washed repeatedly with PBTB (6 x 5 min) and subsequently incubated with preabsorbed chicken anti-mouse-IgG-Alexa488 (Invitrogen, 1:200 in PBS) for 1 h at 37°C in a humid chamber. After repeated washing steps (3 x 5 min PBTB, 1 x 5 min PBT, 1 x 5 min PBS), the slides were equilibrated in detection buffer (2x 5 min.) and FastRed treatment, washing and sealing was carried out as described above.

PBT:

1 x PBS

0.1 % Tween-20

PBTB:

1 x PBS

0.1 % Tween-20

1 % fat free milk powder

Actin staining

Actin cytoskeleton staining was performed essentially as described previously (Adams and Pringle, 1991). Cells were grown over night to logarithmic phase and fixed directly in liquid medium by addition of 37% formaldehyde to a final concentration of 4% and incubation for 30 min at RT under gentle agitation. Cells were washed twice with PBS containing 1 mg/ml BSA (3 min, 1,000 g, RT). The cell pellet was resuspended in 25 µl PBS containing 1 mg/ml BSA and 5 µl of rhodamine-phalloidin (Molecular Probes, 300U/ 1.5 ml MeOH) were added. After incubation for 1 h at RT in the dark, cells were washed three times and resuspended in 500 µl PBS containing 1 mg/ml BSA. An aliquot was allowed to settle for 30 min. on polyethylimine-treated multi-well slides. The slides were washed briefly in PBS, Citifluor AF1 was added, and the coverslips were sealed with nail-polish. Slides were stored at -20°C. Rhodamine fluorescence was observed by epifluorescence microscopy using the Cy3 channel on an Axioplan 2 fluorescence microscope from Zeiss. Pictures were taken by Axiocam MRm using Axiovision software. Image processing was performed with Fiji.

Drop assays

Strains were grown overnight, diluted and grown to logarithmic phase. After adjusting to equal cell concentrations (OD_{600} ~ 0.3), five serial dilutions (1:5) were dropped onto YP2%D plates using a “frogger” stamp (custom-built). The plates were incubated for 2–5 days at 30°C unless indicated otherwise, and photographed for documentation.

Growth test

Colonies were scraped from YP 2%D plates (stored at 4°C) and diluted in H_2O to OD_{600} ~0.2. Cells were further grown in YP 2%D at 30°C, 200 rpm. Every 1-2 hour OD_{600} was measured.

Immunoblot

Proteins were transferred onto nitrocellulose using the wet-blot method (Towbin et al., 1979) in transfer buffer (3 h at RT), 30 V, 250 mA. After the transfer, the nitrocellulose was stained in Ponceau S solution for 1 min (optional) and rinsed with water to remove background staining. Unspecific binding sites were blocked by incubation for 1 h in 5% milk (non-fat milk powder in TBS; 0.02% NaN_3). Unless otherwise stated, the membrane was decorated with primary antibodies diluted in 5% milk for 1 h at RT or overnight at 4°C. Epitope tags and proteins were detected using the following primary antibodies: anti-myc (Sigma 1:1,000); anti-HA (Eurogentec 1:1,000); anti-Pgk1 (Invitrogen 1:1,000) and anti-Scp160p (Eurogentec 1:1,000). The membrane was briefly rinsed with water and washed in TBS-T (3 x 10 min). The secondary antibody coupled to horseradish peroxidase (HRP) was diluted in TBS-T and incubated for 1 h at RT. Goat-anti-mouse-HRP (Pierce) and goat-anti-rabbit-HRP (Pierce) were diluted 1:20,000 and 1:15,000, respectively. After repeated washes in TBS-T, the signals were detected using either the ECL or ECL Advance system (Amersham Bioscience) according to the manufacturer’s recommendations with ECL hyperfilms (GE Healthcare). Exposure times were chosen such that none of the relevant signals were outside the linear range.

6.2 Abbreviations

A_{260}	absorbance at 260 nm
Ac	acetate
AP	alkaline phosphatase
ATP	adenosine-5'-triphosphate
ATPase	ATP hydrolyzing enzyme
bp	base pair
BSA	bovine serum albumin
cDNA	complementary DNA
CHX	cycloheximide
DAPI	4',6-Diamindino-2-phenylindole dihydrochloride
DEPC	diethyl pyrocarbonate
dH_2O	distilled water
DNA	deoxyribonucleic acid
DNase	DNA-hydrolyzing enzyme
dNTPs	deoxyribonucleotide triphosphate
DTT	dithiothreitol
ECL	enhanced chemoluminescence
E. coli	*Escherichia coli*
EDTA	ethylenediaminetetraacetic acid
eqFP611	Entacmaea quadricolor fluorescence protein
ER	endoplasmic reticulum
EtOH	ethanol
FISH	fluorescence in situ hybridization
FISH/IF	FISH in combination with immunofluorescence
g	gravitational acceleration constant
GAP	GTPase-activating protein
GDP	guanosine-5'-diphosphate
GEF	guanine nucleotide exchange factor
GFP	green fluorescence protein
GTP	guanosine-5'-triphosphate
GTPase	GTP hydrolyzing enzyme
h	hour
HEPES	N-[2-Hydroxyethyl]piperazine-N'-[2-ethanesulfonic acid]
HRP	horseradish peroxidase
IF	immunofluorescence
kb	kilo base
KH	K-homology
K. lactis	Kluyveromyces lactis
LB	lysogeny broth
MeOH	methanol
Min	minutes

mRNA	messenger RNA
mRNP	messenger ribonucleoprotein
MT	microtubule
MW	molecular weight
NMD	nonsense-mediate decay
OD_{600}	optical density at 600 nm
O/N	overnight
PAGE	polyacrylamide gel electrophoresis
PBS	phosphate buffered saline
PCI	phenol:chloroform:isoamylalcohol
PCR	polymerase chain reaction
PEG	polyethylene glycol
PSMF	phenylmethylsulfonylfloride
qRT-PCR	quantitative reverse transcription followed by PCR
RBD	RNA-binding domain
RBP	RNA-binding protein
RNA	ribonucleic acid
RNA-Seq	RNA sequencing
RNase	RNA hydrolyzing enzyme
rpm	revolutions per minute
RT	room temperature
S. cerevisiae	Saccharomyces cerevisiae
SDS	sodium dodecyl sulfate
SRP	signal recognition particle
TBS	tris-buffered saline
TBST	tris-buffered saline + 0.1% tween-20
TCA	trichloro acetic acid
TEMED	N,N,N,N-tetramethylethylenediamine
tRNA	transfer RNA
ts	temperature sensitive
UTR	untranslated region
WB	westen blot
WT	wild type
w/v	weight per volume
yeGFP	yeast codon optimized GFP
YNB	yeast nitrogen base
5-FOA	5-fluoroorotic acid

6.3 References

Adames NR, Cooper JA (2000) Microtubule interactions with the cell cortex causing nuclear movements in Saccharomyces cerevisiae. J Cell Biol. 149(4): 863-74

Adams IR, Kilmartin JV (1999) Localization of core spindle pole body (SPB) components during SPB duplication in Saccharomyces cerevisiae. J Cell Biol. 145(4): 809-23

Adams IR, Kilmartin JV (2000) Spindle pole body duplication: a model for centrosome duplication? Trends Cell Biol. 10(8): 329-35

Alber F, Dokudovskaya S, Veenhoff LM, Zhang W, Kipper J, Devos D, Suprapto A, Karni-Schmidt O, Williams R, Chait BT, Sali A, Rout MP (2007) The molecular architecture of the nuclear pore complex. Nature. 450(7170): 695-701

Alberghina L, Mavelli G, Drovandi G, Palumbo P, Pessina S, Tripodi F, Coccetti P, Vanoni M (2011) Cell growth and cell cycle in Saccharomyces cerevisiae: basic regulatory design and protein-protein interaction network. Biotechnol Adv. 30(1): 52-72

Amon A (1996) Mother and daughter are doing fine: asymmetric cell division in yeast. Cell 84: 651–654

Araki Y, Lau CK, Maekawa H, Jaspersen SL, Giddings TH Jr, Schiebel E, Winey M (2006) The Saccharomyces cerevisiae spindle pole body (SPB) component Nbp1p is required for SPB membrane insertion and interacts with the integral membrane proteins Ndc1p and Mps2p. Mol Biol Cell. 17(4): 1959-70

Aronov S, Gelin-Licht R, Zipor G, Haim L, Safran E, Gerst JE (2007) mRNAs encoding polarity and exocytosis factors are cotransported with the cortical endoplasmic reticulum to the incipient bud in Saccharomyces cerevisiae. Mol. Cell. Biol. 27, 3441–3455

Asano K, Phan L, Krishnamoorthy T, Pavitt GD, Gomez E, Hannig EM, Nika J, Donahue TF, Huang HK, Hinnebusch AG (2002) Analysis and reconstitution of translation initiation in vitro. Methods Enzymol. 351: 221-47

Ashe MP, De Long SK, and Sachs AB (2000) Glucose depletion rapidly inhibits translation initiation in yeast. Mol. Biol. Cell 11: 833–848

Barral Y, Liakopoulos D (2009) Role of spindle asymmetry in cellular dynamics. Int Rev Cell Mol Biol. 278: 149-213

Bartkova J, Lukas J, Bartek J (1997) Aberrations of the G1- and G1/S-regulating genes in human cancer. Prog Cell Cycle Res. 3: 211-20

Beach D, Durkacz B, Nurse P (1982) Functionally homologous cell cycle control genes in budding and fission yeast. Nature 706-9

Besse F, Ephrussi A (2008) Translational control of localized mRNAs: restricting protein synthesis in space and time. Nat Rev Mol Cell Biol. 9(12): 971-80

Blower MD, Feric E, Weis K, Heald R (2007) Genome-wide analysis demonstrates conserved localization of messenger RNAs to mitotic microtubules. J Cell Biol. 179(7): 1365-73

Boles E and Hollenberg CP (1997) The molecular genetics of hexose transport in yeasts. FEMS Microbiol. Rev. 21: 85-111

Brauer MJ, Huttenhower C, Airoldi EM, Rosenstein R, Matese JC, Gresham D, Boer VM, Troyanskaya OG, Botstein D (2008) Coordination of growth rate, cell cycle, stress response, and metabolic activity in yeast. Mol Biol Cell. 19(1): 352-67

Broach JR (2012) Nutritional Control of Growth and Development in Yeast. Genetics 192: 73–105

Buchakjian MR, Kornbluth S (2010) The engine driving the ship: metabolic steering of cell proliferation and death. Nat Rev Mol Cell Biol. 11(10): 715-27

Burkard KT1, Butler JS (2000) A nuclear 3'-5' exonuclease involved in mRNA degradation interacts with Poly(A) polymerase and the hnRNA protein Npl3p. Mol Cell Biol. 20(2): 604-16

Busti S, Coccetti P, Alberghina L, Vanoni M (2010) Glucose signaling-mediated coordination of cell growth and cell cycle in Saccharomyces cerevisiae. Sensors (Basel) 10(6): 6195-240

Byers B, Goetsch L (1974) Duplication of spindle plaques and integration of the yeast cell cycle. Cold Spring Harb Symp Quant Biol. 38: 123-31

Byers B, Goetsch L (1975) Behavior of spindles and spindle plaques in the cell cycle and conjugation of Saccharomyces cerevisiae. J Bacteriol. 124(1): 511-23

Carminati JL, Stearns TJ (1997) Microtubules orient the mitotic spindle in yeast through dynein-dependent interactions with the cell cortex. Cell Biol. 138(3): 629-41

Chial HJ, Stemm-Wolf AJ, McBratney S, Winey M (2000) Yeast Eap1p, an eIF4E-associated protein, has a separate function involving genetic stability. Curr Biol. 10(23): 1519-22

Cody NA, Iampietro C, Lécuyer E (2013) The many functions of mRNA localization during normal development and disease: from pillar to post. Wiley Interdiscip Rev Dev Biol. 2(6): 781-96

Coller J, Parker R (2005) General translational repression by activators of mRNA decapping. Cell. 122(6): 875-86

Colombi P, Webster BM, Fröhlich F, Lusk CP (2013) The transmission of nuclear pore complexes to daughter cells requires a cytoplasmic pool of Nsp1. J Cell Biol. 203(2): 215-32

Dever TE, Feng L, Wek RC, Cigan AM, Donahue TF, Hinnebusch AG (1992) Phosphorylation of initiation factor 2 alpha by protein kinase GCN2 mediates gene-specific translational control of GCN4 in yeast. Cell. 68(3): 585-96

Di Liegro CM, Schiera G, Proia P, Saladino P, Di Liegro I (2013) Identification in the rat brain of a set of nuclear proteins interacting with H1° mRNA. Neuroscience. 229: 71-6

Donjerkovic D, Scott DW (2000) Regulation of the G1 phase of the mammalian cell cycle. Cell Res. 10(1): 1-16

Fitch I, Dahmann C, Surana U et al. (1992) Characterization of four B-type cyclin genes of the budding yeast Saccharomyces cerevisiae. Molecular Biology of the Cell 3: 805–818

Flick KM, Spielewoy N, Kalashnikova TI, Guaderrama M, Zhu Q, Chang HC, Wittenberg C (2003) Grr1-dependent inactivation of Mth1 mediates glucose-induced dissociation of Rgt1 from HXT gene promoters. Mol Biol Cell. 14(8): 3230-41

Forrest KM1, Gavis ER (2003) Live imaging of endogenous RNA reveals a diffusion and entrapment mechanism for nanos mRNA localization in Drosophila. Curr Biol. 13(14): 1159-68

Franks TM, Lykke-Andersen J (2008) The control of mRNA decapping and P-body formation. Mol Cell. 32(5): 605-15

Gimeno CJ, Ljungdahl PO, Styles CA, Fink GR (1992) Unipolar cell divisions in the yeast S. cerevisiae lead to filamentous growth: regulation by starvation and RAS. Cell 68: 1077–1090

Gingras AC, Raught B, Sonenberg N (1999) eIF4 initiation factors: effectors of mRNA recruitment to ribosomes and regulators of translation. Annu Rev Biochem. 68: 913-63

Grava S, Schaerer F, Faty M, Philippsen P, Barral Y (2000) Asymmetric recruitment of dynein to spindle poles and microtubules promotes proper spindle orientation in yeast. Dev Cell. 10(4): 425-39

Guo M, Aston C, Burchett SA, Dyke C, Fields S, Rajarao SJR, Uetz P, Wang Y, Young K and Dohlman HG (2003) The yeast G protein α subunit Gpa1 transmits a signal through an RNA binding effector protein Scp160. Molecular Cell 12: 517–524

Halbeisen RE, Galgano A, Scherrer T, Gerber AP (2008) Post-transcriptional gene regulation: from genome-wide studies to principles. Cell Mol Life Sci. 65(5): 798-813

Hartwell LH, Unger MW (1977) Unequal division in Saccharomyces cerevisiae and its implications for the control of cell division. J Cell Biol. 75(2 Pt 1): 422-35

Hildebrandt ER, Hoyt MA (2000) Mitotic motors in Saccharomyces cerevisiae. Biochim. Biophys. Acta 1496: 99–116

Hinnebusch AG (1984) Evidence for translational regulation of the activator of general amino acid control in yeast. Proc Natl Acad Sci U S A. 81(20): 6442-6

Holt CE, Bullock SL (2009) Subcellular mRNA localization in animal cells and why it matters. Science 326: 1212– 1216

Jansen RP (2001) mRNA localization: message on the move. Nat Rev Mol Cell Biol. 2(4): 247-56

Jansen RP, Niessing D (2012) Assembly of mRNA-protein complexes for directional mRNA transport in eukaryotes-an overview. Curr Protein Pept Sci. 13(4): 284-93

Jaspersen SL, Winey M (2004) The budding yeast spindle pole body: structure, duplication, and function. Annu Rev Cell Dev Biol. 20: 1-28

Johnson A, Skotheim JM (2013) Start and the restriction point. Curr Opin Cell Biol. 25(6): 717-23

Johnston GC, Singer RA, McFarlane S (1977) Growth and cell division during nitrogen starvation of the yeast Saccharomyces cerevisiae. J Bacteriol. 132(2): 723-30

Johnston M, and Carlson M (1993) Regulation of carbon and phosphate utilization, p. 193–281. In Broach J, Jones EW, and Pringle J (ed.), The biology of the yeast Saccharomyces, vol. 2. Cold Spring Harbor Laboratory Press, Cold Spring Harbor, N.Y.

Johnston M, Kim JH (2005) Glucose as a hormone: receptor-mediated glucose sensing in the yeast Saccharomyces cerevisiae. Biochem Soc Trans. 33(Pt 1): 247-52

Kaniak A, Xue Z, Macool D, Kim JH, Johnston M (2004) Regulatory network connecting two glucose signal transduction pathways in Saccharomyces cerevisiae. Eukaryot Cell. 3(1): 221-31

Khmelinskii A, Keller PJ, Bartosik A, Meurer M, Barry JD, Mardin BR, Kaufmann A, Trautmann S, Wachsmuth M, Pereira G, Huber W, Schiebel E, Knop M (2012) Tandem fluorescent protein timers for in vivo analysis of protein dynamics. Nat Biotechnol. 30(7): 708-14

Kilchert C, Weidner J, Prescianotto-Baschong C, Spang A (2010) Defects in the secretory pathway and high Ca2+ induce multiple P-bodies. Mol Biol Cell. 21(15): 2624-38

Kim JH, Brachet V, Moriya H, Johnston M (2006) Integration of transcriptional and posttranslational regulation in a glucose signal transduction pathway in Saccharomyces cerevisiae. Eukaryot Cell. 5(1): 167-73

Kim JH, Johnston M (2006) Two glucose-sensing pathways converge on Rgt1 to regulate expression of glucose transporter genes in Saccharomyces cerevisiae. J Biol Chem. 281(36): 26144-9

Kiseleva E, Goldberg MW, Daneholt B, Allen TD (1996) RNP export is mediated by structural reorganization of the nuclear pore basket. J Mol Biol. 260(3): 304-11

Kölling R, Nguyen T, Chen EY, Botstein D (1993) A new yeast gene with a myosin-like heptad repeat structure. Mol Gen Genet. 237(3): 359-69

Korinek WS, Copeland MJ, Chaudhuri A, Chant J (2000) Molecular linkage underlying microtubule orientation toward cortical sites in yeast. Science. 287(5461): 2257-9

Kruckeberg AL (1996) The hexose transporter family of Saccharomyces cerevisiae. Arch Microbiol. 166(5): 283-92

Kühne C and Linder P (1993) A new pair of B-type cyclins from Saccharomyces cerevisiae that function early in the cell cycle. EMBO J. 12(9): 3437-47

Kusch J, Meyer A, Snyder MP, Barral Y (2002) Microtubule capture by the cleavage apparatus is required for proper spindle positioning in yeast. Genes Dev. 16: 1627–39

Lakshmanan J, Mosley AL, Ozcan S (2003) Repression of transcription by Rgt1 in the absence of glucose requires Std1 and Mth1. Curr Genet. 44(1): 19-25

Lasko P (2009) Translational control during early development. Prog Mol Biol Transl Sci 90: 211-254

Lau CK, Giddings TH Jr, Winey M (2004) A novel allele of Saccharomyces cerevisiae NDC1 reveals a potential role for the spindle pole body component Ndc1p in nuclear pore assembly. Eukaryot Cell. 3(2): 447-58

Lécuyer E1, Yoshida H, Parthasarathy N, Alm C, Babak T, Cerovina T, Hughes TR, Tomancak P, Krause HM (2007) Global analysis of mRNA localization reveals a prominent role in organizing cellular architecture and function. Cell. 131(1): 174-87

Lee L, Tirnauer JS, Li J, Schuyler SC, Liu JY, Pellman D (2000) Positioning of the mitotic spindle by a cortical-microtubule capture mechanism. Science 287: 2260–62

Lemaire K, Van de Velde S, Van Dijck P, Thevelein JM (2004) Glucose and sucrose act as agonist and mannose as antagonist ligands of the G protein-coupled receptor Gpr1 in the yeast Saccharomyces cerevisiae. Mol Cell. 16(2): 293-9

Lew DJ and Reed SI (1995) A cell cycle checkpoint monitors cell morphogenesis in budding yeast. J Cell Biol. 129(3): 739-49

Liakopoulos D, Kusch J, Grava S, Vogel J, Barral Y (2003) Asymmetric loading of Kar9 onto spindle poles and microtubules ensures proper spindle alignment. Cell. 112(4): 561-74

Liang H, Ko CH, Herman T, Gaber RF (1998) Trinucleotide insertions, deletions, and point mutations in glucose transporters confer K+ uptake in Saccharomyces cerevisiae. Mol Cell Biol. 18(2): 926-35

Liu G, Grant WM, Persky D, Latham VM Jr, Singer RH, Condeelis J (2002) Interactions of elongation factor 1alpha with F-actin and β-actin mRNA: implications for anchoring mRNA in cell protrusions

Luedeke C, Frei SB, Sbalzarini I, Schwarz H, Spang A, Barral Y (2005) Septin-dependent compartmentalization of the endoplasmic reticulum during yeast polarized growth. J Cell Biol. 169(6): 897-908

Luyten K, Riou C and Blondin B (2002) The hexose transporters of Saccharomyces cerevisiae play different roles during enological fermentation. Yeast 19: 1–15

Madrid AS, Mancuso J, Cande WZ, Weis K (2006) The role of the integral membrane nucleoporins Ndc1p and Pom152p in nuclear pore complex assembly and function. J Cell Biol. 173(3): 361-71

Maier A, Völker B, Boles E, and Fuhrmann GF (2002) Characterisation of glucose transport in Saccharomyces cerevisiae with plasma membrane vesicles (countertransport) and intact cells (initial uptake) with single Hxt1, Hxt2, Hxt3, Hxt4, Hxt6, Hxt7 or Gal2 transporters. FEMS Yeast Research 2: 539–550

Marc P, Margeot A, Devaux F, Blugeon C, Corral-Debrinski M, Jacq C (2002) Genome-wide analysis of mRNAs targeted to yeast mitochondria. EMBO Rep. 3(2): 159-64

Marger MD, Saier MH Jr. (1993) A major superfamily of transmembrane facilitators that catalyse uniport, symport and antiport. Trends Biochem Sci. 18(1): 13-20

Medioni C, Mowry K, Besse F (2012) Principles and roles of mRNA localization in animal development. Development. 139(18): 3263-76

Meignin C, Davis I (2010) Transmitting the message: intracellular mRNA localization. Curr Opin Cell Biol. 22(1): 112-9

Mili S, Moissoglu K, Macara IG (2008) Genome-wide screen reveals APC-associated RNAs enriched in cell protrusion. Nature. 453(7191): 115-9

Miller RK, Matheos D, Rose MD (1999) The cortical localization of the microtubule orientation protein, Kar9p, is dependent upon actin and proteins required for polarization. J Cell Biol. 144(5): 963-75

Miller RK, Rose MD (1998) Kar9p is a novel cortical protein required for cytoplasmic microtubule orientation in yeast. J. Cell Biol. 140: 377–90

Mingle LA, Okuhama NN, Shi J, Singer RH, Condeelis J, Liu G (2005) Localization of all seven messenger RNAs for the actin-polymerization nucleator Arp2/3 complex in the protrusions of fibroblasts. J Cell Sci. 118(Pt 11): 2425-33

Mosley AL, Lakshmanan J, Aryal BK, Ozcan S (2003) Glucose-mediated phosphorylation converts the transcription factor Rgt1 from a repressor to an activator. J Biol Chem. 278(12): 10322-7

Müller D, Exler S, Aguilera-Vázquez L, Guerrero-Martín E, Reuss M (2003) Cyclic AMP mediates the cell cycle dynamics of energy metabolism in Saccharomyces cerevisiae. Yeast. 20(4): 351-67

Niepel M, Molloy KR, Williams R, Farr JC, Meinema AC, Vecchietti N, Cristea IM, Chait BT, Rout MP, Strambio-De-Castillia C (2013) The nuclear basket proteins Mlp1p and Mlp2p are part of a dynamic interactome including Esc1p and the proteasome. Mol Biol Cell. 24(24): 3920-38

Onischenko E, Stanton LH, Madrid AS, Kieselbach T, Weis K (2009) Role of the Ndc1 interaction network in yeast nuclear pore complex assembly and maintenance. J Cell Biol. 185(3): 475-91

Özcan S and Johnston M (1995) Three different regulatory mechanisms enable yeast hexose transporter (HXT) genes to be induced by different levels of glucose. Molecular and Cellular Biology 15: 1564–1572

Özcan S and Johnston M (1999) Function and regulation of yeast hexose transporters. Microbiol. Mol. Biol. Rev. 63: 554-569

Panté N, Jarmolowski A, Izaurralde E, Sauder U, Baschong W, Mattaj IW (1997) Visualizing nuclear export of different classes of RNA by electron microscopy. RNA. 3(5): 498-513

Paalman JW, Verwaal R, Slofstra SH, Verkleij AJ, Boonstra J, Verrips CT (2003) Trehalose and glycogen accumulation is related to the duration of the G1 phase of Saccharomyces cerevisiae. FEMS Yeast Res. 3(3):261-8

Palmer RE, Sullivan DS, Huffaker T, Koshland D (1992) Role of astral microtubules and actin in spindle orientation and migration in the budding yeast, Saccharomyces cerevisiae. J. Cell Biol. 119: 583–93

Palomino A, Herrero P, Moreno F (2006) Tpk3 and Snf1 protein kinases regulate Rgt1 association with Saccharomyces cerevisiae HXK2 promoter. Nucleic Acids Res. 34(5): 1427-38

Paquin N, Ménade M, Poirier G, Donato D, Drouet E, Chartrand P (2007) Local activation of yeast ASH1 mRNA translation through phosphorylation of Khd1p by the casein kinase Yck1p. Mol Cell. 26(6): 795-809

Parker R, Sheth U (2007) P bodies and the control of mRNA translation and degradation. Mol Cell. 25(5): 635-46

Pasula S, Chakraborty S, Choi JH, Kim JH (2010) Role of casein kinase 1 in the glucose sensor-mediated signaling pathway in yeast. BMC Cell Biol. 11: 17

Peeters K, Van Leemputte F, Fischer B, Bonini BM, Quezada H, Tsytlonok M, Haesen D, Vanthienen W, Bernardes N, Gonzalez-Blas CB et al. (2017) Fructose-1,6-bisphosphate couples glycolytic flux to activation of Ras. Nature Communications 8: 922

Pereira G, Schiebel E (2001) The role of the yeast spindle pole body and the mammalian centrosome in regulating late mitotic events. Curr Opin Cell Biol. 13(6): 762-9

Perez M, Luyten K, Michel R, Riou C, Blondin B (2005) Analysis of Saccharomyces cerevisiae hexose carrier expression during wine fermentation: both low- and high-affinity Hxt transporters are expressed. FEMS Yeast Res. 5(4-5): 351-61

Perez WB, Kinzy TG (2014) Translation elongation factor 1A mutants with altered actin bundling activity show reduced aminoacyl-tRNA binding and alter initiation via eIF2α phosphorylation. J Biol Chem. 289(30): 20928-38

Pichon X, Wilson LA, Stoneley M, Bastide A, King HA, Somers J, Willis AE (2012) RNA binding protein/RNA element interactions and the control of translation. Curr Protein Pept Sci. 13(4): 294-304

Pratt CA, and Mowry KL (2013) Taking a cellular road-trip: mRNA transport and anchoring. Curr. Opin. Cell Biol. 25: 99–106

Pruyne D, Legesse-Miller A, Gao L, Dong Y, and Bretscher A (2004) Mechanisms of polarized growth and organelle segregation in yeast. Annu. Rev. Cell Dev. Biol. 20: 559–591

Ptacek J, Devgan G, Michaud G, Zhu H, Zhu X, Fasolo J, Guo H, Jona G, Breitkreutz A, Sopko R, McCartney RR, Schmidt MC, Rachidi N, Lee SJ, Mah AS, Meng L, Stark MJ, Stern DF, De Virgilio C, Tyers M, Andrews B, Gerstein M, Schweitzer B, Predki PF, Snyder M (2005) Global analysis of protein phosphorylation in yeast. Nature. 438(7068): 679-84

Rolfes RJ, Hinnebusch AG (1993) Translation of the yeast transcriptional activator GCN4 is stimulated by purine limitation: implications for activation of the protein kinase GCN2. Mol Cell Biol. 13(8): 5099-111

Rolland F, Winderickx J & Thevelein JM (2002) Glucose-sensing and-signalling mechanisms in yeast. FEMS yeast research 2: 183–201

Roy A, Jouandot D 2nd, Cho KH, Kim JH (2014) Understanding the mechanism of glucose-induced relief of Rgt1-mediated repression in yeast. FEBS Open Bio. 4: 105-11

Rüthnick D, Schiebel E (2018) Duplication and Nuclear Envelope Insertion of the Yeast Microtubule Organizing Centre, the Spindle Pole Body. Cells. 7(5). pii: E42

Sabina J, Johnston M (2009) Asymmetric signal transduction through paralogs that comprise a genetic switch for sugar sensing in Saccharomyces cerevisiae. J Biol Chem. 284(43): 29635-43

Saint-Georges Y, Garcia M, Delaveau T, Jourdren L, Le Crom S, Lemoine S, Tanty V, Devaux F, Jacq C (2008) Yeast mitochondrial biogenesis: a role for the PUF RNA-binding protein Puf3p in mRNA localization. PLoS One. 3(6): e2293

Schramm C, Elliott S, Shevchenko A, Schiebel E (2000) The Bbp1p-Mps2p complex connects the SPB to the nuclear envelope and is essential for SPB duplication. EMBO J. 19(3): 421-33

Schwartz K, Richards K, Botstein D (1997) BIM1 encodes a microtubule-binding protein in yeast. Mol. Biol. Cell 8: 2677–91

Schweiggert J, Stevermann L, Panigada D, Kammerer D, Liakopoulos D (2016) Regulation of a Spindle Positioning Factor at Kinetochores by SUMO-Targeted Ubiquitin Ligases. Dev Cell. 36(4): 415-27

Schwob E and Nasmyth K (1993) CLB5 and CLB6, a new pair of B cyclins involved in DNA replication in Saccharomyces cerevisiae. Genes Dev. 7(7A): 1160-75

Sezen B, Seedorf M, Schiebel E (2009) The SESA network links duplication of the yeast centrosome with the protein translation machinery. Genes Dev. 23(13): 1559-70

Shepard KA, Gerber AP, Jambhekar A, Takizawa PA, Brown PO, Herschlag D, DeRisi JL, Vale RD (2003) Widespread cytoplasmic mRNA transport in yeast: identification of 22 bud-localized transcripts using DNA microarray analysis. Proc Natl Acad Sci U S A. 100(20): 11429-34

Shestakova EA1, Singer RH, Condeelis J (2001) The physiological significance of beta - actin mRNA localization in determining cell polarity and directional motility. Proc Natl Acad Sci U S A. 98(13): 7045-50

Siller KH, Doe CQ (2009) Spindle orientation during asymmetric cell division. Nat Cell Biol. 11(4): 365-74

Silljé HH, ter Schure EG, Rommens AJ, Huls PG, Woldringh CL, Verkleij AJ, Boonstra J, Verrips CT (1997) Effects of different carbon fluxes on G1 phase duration, cyclin expression, and reserve carbohydrate metabolism in Saccharomyces cerevisiae. J Bacteriol. 179(21): 6560-5

Soop T, Ivarsson B, Björkroth B, Fomproix N, Masich S, Cordes VC, Daneholt B (2005) Nup153 affects entry of messenger and ribosomal ribonucleoproteins into the nuclear basket during export. Mol Biol Cell. 16(12): 5610-20

Spielewoy N, Flick K, Kalashnikova TI, Walker JR, Wittenberg C (2004) Regulation and recognition of SCFGrr1 targets in the glucose and amino acid signaling pathways. Mol Cell Biol. 24(20): 8994-9005

Spiliotis ET, Nelson WJ Here come the septins: novel polymers that coordinate intracellular functions and organization. (2006) J Cell Sci. 119(Pt 1): 4-10

Stavru F, Hülsmann BB, Spang A, Hartmann E, Cordes VC, Görlich D (2006) NDC1: a crucial membrane-integral nucleoporin of metazoan nuclear pore complexes. J Cell Biol. 173(4): 509-19

Steward O, Schuman EM (2003) Compartmentalized synthesis and degradation of proteins in neurons. Neuron. 40(2): 347-59

Strambio-de-Castillia C, Blobel G, Rout MP (1999) Proteins connecting the nuclear pore complex with the nuclear interior. J Cell Biol. 144(5): 839-55

Sullivan M, Morgan DO (2007) Finishing mitosis, one step at a time. Nat Rev Mol Cell Biol. 11: 894-903.

Takizawa PA, Sil A, Swedlow JR, Herskowitz I, Vale RD (1997) Actin-dependent localization of an RNA encoding a cell-fate determinant in yeast. Nature. 389(6646): 90-3

Thattai M, van Oudenaarden A (2004) Stochastic gene expression in fluctuating environments. Genetics 167: 523–530

Theesfeld CL, Irazoqui JE, Bloom K, Lew DJ (1999) The role of actin in spindle orientation changes during the Saccharomyces cerevisiae cell cycle. J. Cell Biol. 146: 1019– 32

Tirnauer JS, O'Toole E, Berrueta L, Bierer BE, Pellman D (1999) Yeast Bim1p promotes the G1-specific dynamics of microtubules. J. Cell Biol. 145: 993–1007

Toda T, Cameron S, Sass P, Zoller M, Wigler M (1987) Three different genes in S. cerevisiae encode the catalytic subunits of the cAMP-dependent protein kinase. Cell. 50(2): 277-87

Torchet C, Bousquet-Antonelli C, Milligan L, Thompson E, Kufel J, Tollervey D (2002) Processing of 3'-extended read-through transcripts by the exosome can generate functional mRNAs. Mol Cell. 9(6): 1285-96

Turner JJ, Ewald JC, Skotheim JM (2012) Cell size control in yeast. Curr Biol. 22(9): R350-9

Tzamarias D, Roussou I, Thireos G (1989) Coupling of GCN4 mRNA translational activation with decreased rates of polypeptide chain initiation.Cell. 57(6): 947-54

Urban J, Soulard A, Huber A, Lippman S, Mukhopadhyay D, Deloche O, Wanke V, Anrather D, Ammerer G, Riezman H, Broach JR, De Virgilio C, Hall MN, Loewith R (2007) Sch9 is a major target of TORC1 in Saccharomyces cerevisiae. Mol Cell. 26(5): 663-74

van Oevelen CJC, van Teeffelen HAAM, van Werven FJ, Timmers HTM (2006) Snf1p-dependent Spt-Ada-Gcn5-acetyltransferase (SAGA) Recruitment and Chromatin Remodeling Activities on the HXT2 and HXT4 Promoters. Journal of Biological Chemistry 281: 4523–4531

Vander Heiden MG, Cantley LC, Thompson CB (2009) Understanding the Warburg effect: the metabolic requirements of cell proliferation. Science. 324(5930): 1029-33

Wang X, Proud CG (2009) Nutrient control of TORC1, a cell-cycle regulator. Trends Cell Biol. 19(6): 260-7

Weidner J, Wang C, Prescianotto-Baschong C, Estrada AF, Spang A (2014) The polysome-associated proteins Scp160 and Bfr1 prevent P body formation under normal growth conditions. J Cell Sci. 127(Pt 9): 1992-2004

Winey M, Bloom K (2012) Mitotic spindle form and function. Genetics. 190(4): 1197-224

Winey M, Goetsch L, Baum P, Byers B (1991) MPS1 and MPS2: novel yeast genes defining distinct steps of spindle pole body duplication. J Cell Biol. 114(4): 745-54

Yin H, Pruyne D, Huffaker TC, Bretscher A (2000) Myosin V orientates the mitotic spindle in yeast. Nature. 406(6799): 1013-5

Yoder TJ, Pearson CG, Bloom K, Davis TN (2003) The Saccharomyces cerevisiae spindle pole body is a dynamic structure. Mol Biol Cell. 14(8): 3494-505

Youk H and van Oudenaarden A (2009) Growth landscape formed by perception and import of glucose in yeast. Nature 462: 875–879

Zaman S, Lippman SI, Zhao X, Broach JR (2008) How Saccharomyces responds to nutrients. Annu Rev Genet. 42: 27-81

Zeller CE, Parnell SC, and Dohlman HG (2007) The RACK1 Ortholog Asc1 Functions as a G-protein beta Subunit Coupled to Glucose Responsiveness in Yeast. Journal of Biological Chemistry 282: 25168–25176

Zipor G, Haim-Vilmovsky L, Gelin-Licht R, Gadir N, Brocard C, Gerst JE (2009) Localization of mRNAs coding for peroxisomal proteins in the yeast, Saccharomyces cerevisiae. Proc Natl Acad Sci U S A. 106(47): 19848-53

6.4 Acknowledgments

A very big THANK YOU to the following people:

Anne Spang, for giving me the opportunity to work in her lab, for her supervision and her tireless support and commitment to teach valuable lessons. She always kept an open door and ear for questions, problems or theories, despite her being responsible for so many diverse and difficult projects. I was always given the freedom to envision new strategies and experiments to tackle scientific problems. Moreover, she taught me how to find the central theme in sometimes rather confusing data, put everything into a great story and finally present it, in the most convincing and coherent way.

My thesis committee, Prof. Sabine Rospert and Dr. Jeffrey Chao, for their time, support and important advice.

Stefan Hümmer for introducing me to RNA, FISH and all things yeast.

All present and past members of the Spang lab (in no particular order): Carla Cadena del Castillo, Alejandra Fernandez Belmonte, Alejandro Fernandez-Estrada, Alicja Drozdowska-Ritz, Thomas Gross, Congwei Wang, Martina Huranova, Gopinath Muruganandam, Maria Podinovskaya, Jachen Solinger, Julia Stevens, Claudia Stohrer, Diego Stohrer, Kiril Tishinov, Harun-Or Rashid, Sheuli Begun, Jonas Fürst, Mihaela Anitei , Emmanouil Kyriakakis, E-ming Rau, Pascal Ankli, Cedrine Küng

Brigitte Olufsen, for always being a big help, not only when it came to administrative matters.

Last but not least, my family and friends for having my back and dealing with my moods. Without them I would not have been able to accomplish any of this.